PB-230 727

STUDIES OF OXYGEN REDUCTION AT A ROTATING DISK ELECTRODE

California University

PREPARED FOR
Office of Saline Water

March 1974

SELECTED WATER
RESOURCES ABSTRACTS

INPUT TRANSACTION FORM INT-056-ROPS-74-935

PB 230 727

W

Studies of Oxygen Reduction at a Rotating [redacted] Electrode (RDE)

March 1974

Melvin Forbes and Scott Lynn

University of California, Berkeley
Berkeley, California

Grant 14-01-0001-1461

Office of Saline Water

155 pages, 15 tables, 41 figures, 60 references, 2 appendices

The kinetics and mechanism of oxygen reduction at platinum were investigated by means of the RDE. A kinetic expression for the current for oxygen reduction was developed, taking into account both direct 4-electron reduction of OH^- or H_2O, and electrochemical reduction via hydrogen peroxide. Possible catalytic decomposition of hydrogen peroxide and loss of H_2O_2 by diffusion were considered. This expression was used to demonstrate that, in impure neutral saline solutions, oxygen reduction generally proceeds via the peroxide intermediate.

The mechanism of activation and deactivation of a platinum surface with respect to oxygen reduction was investigated. It was found that, under the experimental conditions of this study, the surface was deactivated by a mixed process of poisoning and desorption of a catalytic layer which had been formed during anodic activation.

A miniature version of the Winkler oxygen analysis was developed for use in this study. This technique permitted an accuracy of ±1% when measuring oxygen concentrations of 6-7 ppm. An accuracy of ±5% was sometimes obtained at the 0.1 ppm level, but there was a tendency for larger errors to occur because of shortcomings in the sampling procedure.

*Desalination, Electrodes, *Electrochemistry, *Ion Transport, *Oxidation, *Reduction

*Rotating Disk Electrode, *Platinum Electrode, *Silver Electrode, *Gold Electrode, *Rate Constants, *Kinetics, Winkler Oxygen Analyses

Research and Development Progress Report No. 935 March 1974

STUDIES OF OXYGEN REDUCTION AT A ROTATING DISK ELECTRODE

By: Melvin Forbes and Scott Lynn, University of California at Berkeley, Berkeley, California for the Office of Saline Water, J. W. O'Meara, Director, W. Sherman Gillam, Assistant Director, Research, S. Johnson, Chief, Applied Science Division

Grant No. 14-01-0001-1641

IWT-OSW-RDPR-74-935

United States Department of the Interior Rogers C. B. Morton, Secretary
Jack O. Horton, Assistant Secretary for Land and Water Resources

TABLE OF CONTENTS

ABSTRACT

The reduction of oxygen, in neutral saline solution and in seawater, was studied with a rotating disk electrode (RDE). Platinum, gold, silver, and copper electrodes were used to measure polarization curves for oxygen reduction at concentrations between 0.07 ppm and 7.2 ppm. The purpose of these measurements was to test the applicability of the RDE as a primary reference standard for the measurement of oxygen concentrations below 0.1 ppm in seawater.

It was found that an activated platinum electrode could be used to determine oxygen concentrations as low as 0.07 ppm in neutral saline solution with ±2% accuracy, but gave results which were about 20% high in seawater at the same oxygen level.

The lower limit of applicability of the gold electrode to oxygen measurement in seawater was found to be about 1 ppm. The copper and silver electrodes corroded too rapidly to be of use in this study.

The kinetics and mechanism of oxygen reduction at platinum were investigated by means of an RDE. A kinetic expression for the current for oxygen reduction was developed, taking into account both direct 4-electron reduction to OH^- or H_2O, and electrochemical reduction via hydrogen peroxide. Possible catalytic decomposition of hydrogen peroxide and loss of H_2O_2 by diffusion were

considered. This expression was used to demonstrate that, in impure neutral saline solutions, oxygen reduction generally proceeds via the peroxide intermediate.

The rate constant for hydrogen peroxide reduction in 3.5% NaCl solution and seawater was measured. The dependence of this rate constant on electrode potential was found to agree quite well with that measured by two other investigators.

The mechanism of activation and deactivation of a platinum surface with respect to oxygen reduction was investigated. It was found that, under the experimental conditions of this study, the surface was deactivated by a mixed process of poisoning and desorption of a catalytic layer which had been formed during anodic activation.

A miniaturized version of the Winkler oxygen analysis was developed for use in this study. This technique permitted an accuracy of $\pm$1% when measuring oxygen concentrations of 6-7 ppm. An accuracy of $\pm$5% was sometimes obtained at the 0.1 ppm level, but there was a tendency for larger errors to occur because of shortcomings in the sampling procedure.

LIST OF TABLES

LIST OF FIGURES

ACKNOWLEDGEMENT

I am grateful to the following people:

Dr. Scott Lynn, for his guidance, wisdom, restraint, very gentle prodding, subtle humor, grammatical precision, and above all, patience.

Drs. Rolf Muller and Israel Cornet, for reviewing this work.

Howard Wood, for teaching me machine shop technique and common sense in matters mechanical.

Steve Willett, for teaching me darkroom technique, and for unselfish donation of his time and resources.

The gentlemen of the Chemistry Glassblowing shop, and Morley Corbett of the Physics Glassblowing shop, for introducing me to the pleasures of glassblowing, and for many happy hours of glassplay.

The staff of the Chemistry Machine Shop, for their assistance in construction of equipment.

Nancy Wurschmidt, Susan Clark, Linda Betters, and Ann Harrington, for prompt typing.

My office-mates, David, Stuart, Derk, and Joe, for friendship, reliability, and tolerance.

My wife, Valerie, for inspiration, distraction, love, companionship, fine food, forbearance, and devotion.

This work was supported by Grant # 14-01-0001-1641 of the U.S. Dept. of the Interior, Office of Saline Water.

This thesis is dedicated to the memory of my father,

Jack Forbes

CHAPTER 1: INTRODUCTION

1.1 Primary Objective of This Study

In seawater desalination plants, and in other installations where large quantities of water are heated in boilers, corrosion of the boilers can be minimized by maintaining a low oxygen concentration in the boiler feed. Seawater near the surface of the ocean usually has an oxygen concentration of 6-7 ppm at 20°C. This is reduced to 0.01-0.1 ppm before the seawater is fed to the boilers of a desalination plant. Some type of oxygen sensor with a fast response is required as a check on the performance of the deoxygenation apparatus. The primary objective of this study was to investigate the applicability of a rotating disk electrode for use as such a sensor.

1.2 Existing Oxygen Sensors

The two main techniques for measuring oxygen concentration in solution are the Winkler titration, and oxygen-specific electrochemical devices. The former is capable of high accuracy (Behrens, 1970; Edgington and Roberts, 1969) when performed under strictly controlled conditions. It will be discussed in detail in Chapter 6. Because the Winkler titration requires discrete samples, and analyses can take up to an hour to be completed, it is not suitable for use in on-line continuous oxygen monitoring.

The large number of electrochemical oxygen sensors available commercially can be divided into three main categories: galvanic, gas phase, and polarographic.

1) The galvanic type comprises two dissimilar metal electrodes (e.g. an Ag cathode and an Fe - Zn anode*) immersed in the sample, which acts as an electrolyte. Oxygen in the sample is reduced at the cathode, metal dissolution occurs at the anode, and a current proportional to the oxygen concentration flows in the external circuit.

An electrode of this type was found to give accurate results (Behrens, 1970) in deaerated raw seawater. However, in acidified seawater such as is typically found in a desalination plant, the sensor gave readings which were high, apparently responding to H^+ ions in the sample. This somewhat limits the suitability of such an instrument for use in desalination applications.

2) Sensors designed to measure oxygen in the gas phase may be used to measure dissolved oxygen by equilibrating nitrogen with a liquid sample. However, cells of this type were found by Behrens (1970) to display poor stability towards temperature fluctuations

*Mays Corp. Model 625 Dissolved Oxygen Analyzer.

and electrical noise, and nonlinearity between oxygen concentration and output signal.

3) The polarographic sensor comprises two metal electrodes (e.g. an Ag anode and an Au cathode) between which a potential is maintained. The cell containing the electrodes is made of a plastic such as PVC, filled with an electrolyte, and sealed at one end with a membrane. This membrane is permeable to oxygen, but not to other reducible species present in the solution being analyzed. Oxygen diffuses through the membrane from the sample, is reduced at the cathode, and a current flows. Sensors of this type show the best resistance to interference by ions in solution, and good temperature stability, as well as high accuracy in the 0-100 ppb range. However, changes in pH have been observed to result in altered oxygen concentration readings (Behrens, 1970). Moreover, this cell is sensitive to the partial pressure of the oxygen in the sample rather than to the weight fraction of dissolved oxygen, even though the readout is in ppb or ppm O_2. The Henry's Law constant for oxygen in seawater is dependent on salinity (e.g. Truesdale, et al., 1955) so the indicated oxygen concentration should be corrected for salinity variations if high accuracy is required.

Because it is not possible to calculate the instrument readings as a function of oxygen concentration, all commercial oxygen sensors must be calibrated against

known concentration standards. This can be inconvenient and time-consuming. Moreover, the electrical output of these cells at a given oxygen concentration can vary with time, so they must be recalibrated periodically.

An electrode for which a calibration would not be required is the rotating disk electrode (RDE); the current corresponding to a given set of operating conditions and solution parameters can be predicted theoretically if certain restrictions of electrode kinetics are obeyed. These will be explained fully in section 1.3. It was for this reason that the use of an RDE in measuring oxygen concentrations in seawater was investigated.

In the next sections, the theory of the RDE and its application to practical systems are described. An introduction to the mechanism of oxygen reduction follows, and the chapter ends with a description of techniques used to analyze the reaction mechanism.

1.3 Theory of the Rotating Disk Electrode

The rotating disk electrode (Fig. 1.1) consists ideally of an infinite horizontal lamina immersed in a fluid of infinite extent and rotating with angular velocity ω about the vertical axis, $r = 0$. At the under-surface of the disk the velocity of the fluid relative to the disk is zero, and the fluid moves with the disk. Just below the disk surface the fluid velocity acquires a tangential component and is thus

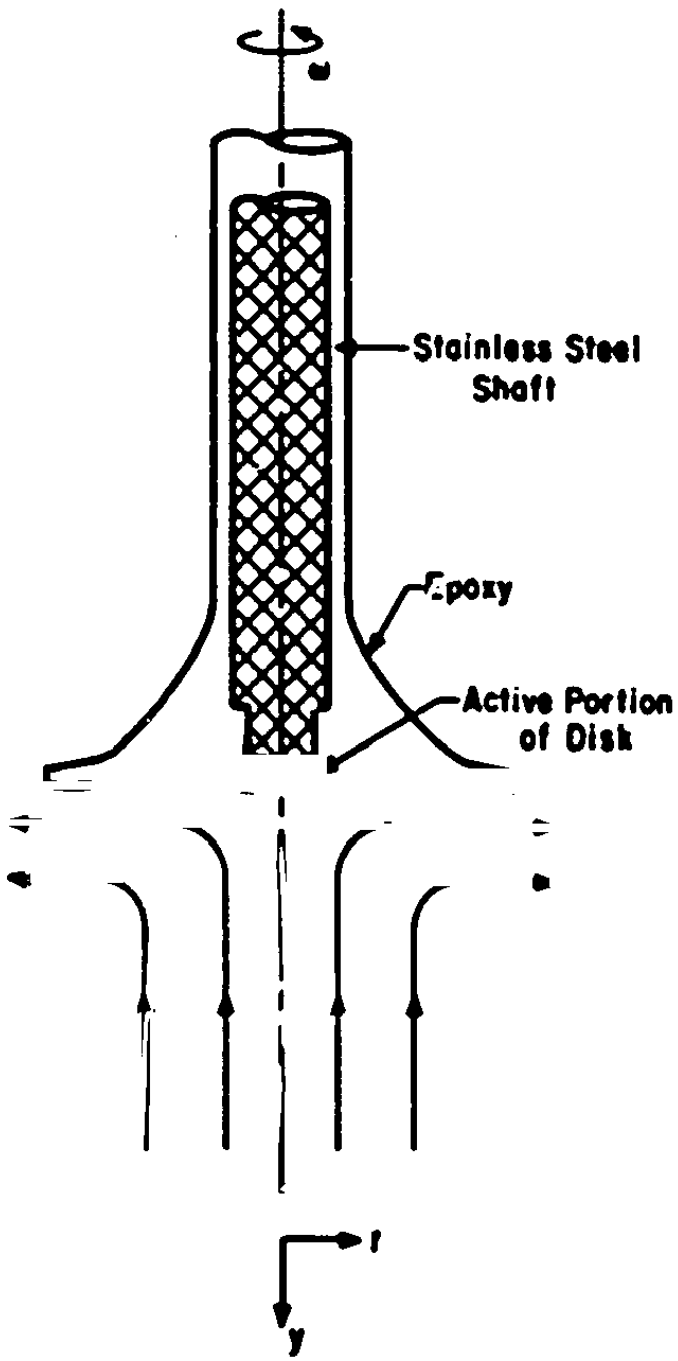

Figure 1.1. The Rotating Disk Electrode: Flow pattern and details of construction.

thrown horizontally outward. To balance this flow, fluid must simultaneously flow upward in the y-direction, and the flow pattern illustrated in Fig. 1.1 is established.

If a species in a solution in which a rotating disk is immersed reacts at the surface of the disk, the mass flux of this species to the surface is jointly determined by its diffusivity and by the hydrodynamic characteristics of the system. In order to determine this mass flux, it is first necessary to evaluate the velocity profile by means of the Navier-Stokes equation,

$$\frac{d\bar{v}}{dt} = -\text{grad}\,\frac{p}{\rho} + \nu\,\text{div grad}\,\bar{v} + \frac{\bar{g}}{\rho} \qquad (1.1)$$

and the equation of continuity,

$$\text{div}\,\bar{v} = 0 \qquad (1.2)$$

where

$\bar{v}$ is the velocity vector,

p is the pressure,

ρ is the density,

ν is the kinematic viscosity,

$\bar{g}$ is the gravitational force.

Because the system possesses cylindrical symmetry, equations (1.1) and (1.2) are conveniently expressed in cylindrical coördinates r, ϕ and y. In addition, the following assumptions are made:

The flow is laminar,

The flow is in steady state, so that $\frac{d\bar{v}}{dt} = 0$,

The component of $\bar{v}$ in the y-direction, v_y, is assumed to be independent of r,

Since the fluid is assumed to be incompressible and the rotating disk is horizontal, p is a function of y only.

Because forced convection predominates over natural convection the gravitational term is ignored. Also, because of the cylindrical symmetry all derivatives with respect to ϕ disappear.

Equation (1.1) becomes (Riddiford, 1966):

$$v_r \frac{\partial v_r}{\partial r} + v_y \frac{\partial v_r}{\partial y} - \frac{v_\phi^2}{r} = \nu \left| \frac{\partial^2 v_r}{\partial r^2} + \frac{\partial}{\partial r}\left(\frac{v_r}{r}\right) + \frac{\partial^2 v_r}{\partial y^2} \right| \quad (1.3)$$

$$v_r \frac{\partial v_\phi}{\partial r} + v_y \frac{\partial v_\phi}{\partial y} + \frac{v_r v_\phi}{r} = \nu \left| \frac{\partial^2 v_\phi}{\partial r^2} + \frac{\partial}{\partial r}\left(\frac{v_\phi}{r}\right) + \frac{\partial^2 v_\phi}{\partial y^2} \right| \quad (1.4)$$

$$v_y \frac{\partial v_y}{\partial y} = -\frac{1}{\rho}\frac{\partial p}{\partial y} + \nu \frac{\partial^2 v_y}{\partial y^2} . \quad (1.5)$$

Equation (1.2) becomes:

$$\frac{\partial v_r}{\partial r} + \frac{v_r}{r} + \frac{\partial v_y}{\partial y} = 0 . \quad (1.6)$$

The boundary conditions are:

$$v_r = 0 \ , \ v_\phi = \omega r \ , \ v_y = 0 \ , \text{ at } \ y = 0 \qquad (1.7)$$

$$v_r = 0 \ , \ v_\phi = 0 \ , \ v_y = -x \ , \text{ at } \ y = \infty \ . \qquad (1.8)$$

Details of the solution of these equations may be found in Riddiford (1966).

The hydrodynamic boundary layer can be defined as the distance in which the fluid motion changes substantially from that of the rotating disk to that observed in the bulk of the solution. Riddiford finds its thickness, δ_H to be:

$$\delta_H = 2.8 \left(\frac{\nu}{\omega}\right)^{1/2} \ . \qquad (1.9)$$

Note that δ_H is independent of r.

The equation for steady state transport of an uncharged species 'i' in solution is, in cylindrical coördinates,

$$D_i\left(\frac{\partial^2 c_i}{\partial r^2} + \frac{1}{r}\frac{\partial c_i}{\partial r} + \frac{1}{r^2}\frac{\partial^2 c_i}{\partial \phi^2} + \frac{\partial^2 c_i}{\partial y^2}\right) = v_r \frac{\partial c_i}{\partial r} + \frac{v_\phi}{r}\frac{\partial c_i}{\partial \phi} + v_y \frac{\partial c_i}{\partial y} \qquad (1.10)$$

where c_i is the concentration of species 'i' in solution,

D_i is the diffusivity of species 'i', and is assumed to be independent of concentration. As before, from considerations of symmetry, c_i is independent of ϕ.

It is also assumed that c_i is independent of r, since the convective flow which is responsible for bringing fresh reactant to the surface depends only on y. Equation (1.10) therefore becomes:

$$D_i \frac{d^2 c_i}{dy^2} = v_y \frac{dc_i}{dy} \tag{1.11}$$

with the following boundary conditions:

$$\begin{aligned} c_i &= c_i(0) \quad \text{at} \quad y = 0 \\ c_i &= c_i(\infty) \quad \text{at} \quad y = \infty \, . \end{aligned} \tag{1.12}$$

The concentration profile is obtained by substituting for the velocity in eqn. (1.11) and integrating twice. The mass flux of species 'i' at the rotating disk is then given by:

$$J = -D_i \left(\frac{dc_i}{dy}\right)_{y=0} \tag{1.13}$$

which leads to the result:

$$J = \frac{D_i}{\delta} \frac{[c_i(\infty) - c_i(0)]}{\int_0^\infty \exp\left[-\xi^3 + 0.885(Sc)^{-1/3}\xi^4 - 0.394\, Sc^{-2/3}\xi^5 + ..\right] d\xi} \tag{1.14}$$

where: Sc is the Schmidt number, $\frac{\nu}{D}$, a dimensionless parameter,

$\delta = 1.80\ Sc^{-1/3}\left(\frac{\nu}{\omega}\right)^{1/2}$, and is introduced for convenience in solving eqn. (1.13).

Levich, who obtained the first solution to this mass transfer problem, assumed that at large Schmidt numbers, of the order of 1000, only the first term in the exponential expression in eqn. (1.14) was of importance, and obtained the result:

$$J = 0.6205\ Sc^{-2/3}(\omega\nu)^{1/2}[c_i(\infty) - c_i(0)] \quad . \quad (1.15)$$

Gregory and Riddiford (in Riddiford, 1966) evaluated the denominator in eqn. (1.14) numerically, and by fitting the result to a function of Sc, obtained the expression:

$$J = \frac{0.554}{0.8934 + 0.316\ Sc^{-0.36}}\ Sc^{-2/3}(\omega\nu)^{1/2}[c_i(\infty) - c_i(0)] \quad . \quad (1.16)$$

Newman (1966) expanded the exponential term in eqn. (1.14) and integrated the denominator analytically, to obtain:

$$J = \frac{0.62048}{1 + 0.2980\ Sc^{-1/3} + 0.14514\ Sc^{-2/3}}\ Sc^{-2/3}(\omega\nu)^{1/2} \cdot [c_i(\infty) - c_i(0)] \quad . \quad (1.17)$$

At Sc = 500, which corresponds to the diffusion of oxygen in seawater, equation (1.17) deviates from the "exact" solution obtained by numerical integration of

eqn. (1.14) with Sc set equal to 500, by 0.15%. The solution of Gregory and Riddiford deviates by 0.18%, and that of Levich by 4.00% (Newman, 1966). Hence the Newman solution is the most accurate one available, and was used to calculate all the numerical mass-flux values used in this study.

The mass-transport boundary layer is analogous to the hydrodynamic boundary layer which was introduced earlier. Riddiford (1966) defined the thickness δ_M of the former, as the distance over which the concentration of the diffusing species changes from its value at the RDE surface to its value in the bulk of the solution. He found that

$$\delta_M \sim 3.2(Sc)^{-1/3}\left(\frac{\nu}{\omega}\right)^{1/2} \qquad (1.18)$$

Note that δ_M is smaller than δ_H (eqn. 1.9) by a factor of approximately $Sc^{1/3}$ and is independent of r.

The current due to the electrochemical reaction of species 'i' at a conducting RDE can now be found, using (1.17). By Faraday's law,

$$i = nFJ \qquad (1.19)$$

where: n is the number of electrons transferred when one molecule of 'i' reacts,

F is the Faraday, 96450 coulombs/mole,

and i is the current density.

Substitution from eqn. (1.17) into eqn. (1.19) gives

$$i = \frac{0.6205}{1 + 0.298\,Sc^{-1/3} + 0.14514\,Sc^{-2/3}}\, Sc^{-2/3}(\omega\nu)^{1/2} \cdot nF[c_i(\infty) - c_i(0)] \quad (1.20)$$

The corresponding expression based on the Levich solution (1.15) for the mass flux, is similar to eqn. (1.20), differing from it only by the factor $1 + 0.298\,Sc^{-1/3} + 0.14514\,Sc^{-2/3}$. Therefore, eqn. (1.20) will be referred to as the "Levich equation" in this study, so as to acknowledge the fact that Levich played a major rôle in solving the RDE mass-transfer equation.

When species 'i' reacts at the surface of the RDE as quickly as it arrives by convection and diffusion, $c_i(0) = 0$ and the current reaches its maximum value. This is known as the diffusion-limited current density i_{lim}, or more simply, as the limiting current density. Here the appeal of the RDE as an analytical tool becomes apparent, since with a knowledge of the transport properties of a system, and the rotational speed ω, the current density can be accurately predicted if the concentration of the electroactive species in the bulk of the solution is known, and if the electrode reaction is effectively instantaneous and proceeds to completion.

1.4 The Polarization Curve

Consider an RDE immersed in a solution containing an electroactive species 'i'. If no external potential is imposed on the electrode, the oxidized and reduced forms of species 'i' will assume equilibrium concentrations. Charge will be transferred briefly between the electrode and the solution, and the electrode will assume a potential known as the rest potential, whose magnitude is characteristic of the solvent, the concentrations, and the electrochemical nature of species 'i'.

If the electrode is now made more cathodic by means of an external power source, species 'i' will be reduced at the RDE surface and a current will flow. Fresh material will be brought to the surface at a rate given by the Levich equation. The current will increase as the cathodic potential of the electrode is increased, until the current becomes limited by diffusion, at which point a "limiting current plateau" will be observed, as shown in Fig. 3.2* The potential of the electrode can then be increased with no further increase in current, until the potential is reached at which an additional electrode reaction can occur. In the case of Fig. 3.2 this reaction is the reduction of hydrogen ions to molecular hydrogen.

* Upper curve.

1.5 Practical Rotating Disk Systems

The following constraints apply to the design of a practical RDE (Riddiford, 1966):

1) The diameter should be sufficiently large that forced convection predominates over free convection, but not so large that turbulence develops at the edge of the electrode. The Reynolds number $\left(Re = \frac{r_o^2 \omega}{\nu}\right.$, where r_o is the radius of the electrode$\left.\right)$ for the onset of turbulence has been variously estimated (Riddiford, 1966) as being between 1.8×10^5 and 2.4×10^5. The minimum Reynolds number necessary to ensure forced convection is 2×10^2.

2) The diameter should be considerably greater than the thickness of the mass-transfer boundary layer, so as to justify the assumption that the RDE is of infinite extent.

3) Edge effects can be avoided if the active portion of the disk, i.e., the portion where an electrochemical reaction occurs, occupies only the central region of the RDE.

4) The assumption that the fluid is of infinite extent is justified if the bounding surfaces of the cell containing the RDE are at least 0.5 cm away from the electrode.

5) The rugosity of the under-side of the RDE should be negligible compared to the mass-transfer boundary layer thickness, so as not to inhibit its formation.

6) It is important that the flow above the plane of the RDE not interfere with the flow below it. Riddiford suggests that this can be achieved by making the thickness of the disk less than 4% of its diameter, and the diameter of the RDE shaft less than 30% of the disk diameter.

7) From a study of results obtained with twelve different electrode shapes, Riddiford concludes that a bell-shaped electrode best conforms to the requirements of RDE theory. However, Prater and Adams (1966) compared the performance of cylindrical and bell-shaped RDE's over a Reynolds number range of 16-640. They measured limiting currents for the reduction of $Fe(CN)_6^{-4}$ at carbon surfaces, and calculated $i/\omega^{1/2}$ for each electrode at a given speed. The results for each electrode shape agreed within 1%, with a small deviation for the cylindrical electrode at Re < 32. In view of the greater ease of construction of the cylindrical electrode, its use seems preferable for many applications.

8) Eccentricity of the electrode should be avoided in order to satisfy the boundary condition of equation (1.7). Bardin and Dikusar (1970) studied the effect of eccentricity on the limiting currents at micro-electrodes with active portions of about 1 mm. diameter. They found that no deviation greater than 3% of theoretically predicted currents occurred until the

active portion was displaced a distance approximately equal to half its radius from the center of rotation. Bardin and Dikusar did not, however, study the effect of "wobble," wherein the shaft of the RDE does not rotate completely on-center; this must be restricted to a minimum.

1.6 Previous Research

Peters (1970) measured polarization curves for the reduction of oxygen at a platinum RDE in 3.5% NaCl solution. Because of the complexity of seawater, there was a possibility that side reactions would occur and obscure the effects of oxygen reduction. The 3.5% NaCl solution was used instead in this preliminary study because it was relatively pure, and its salinity and electrical conductivity were similar to those of seawater.

Peters found that, at oxygen concentrations of 6.8 and 32.1 ppm, the limiting current for oxygen reduction at an activated electrode was within 1% of that predicted by the Levich equation. This indicated that a platinum RDE could be used as an instrument for measuring oxygen concentrations of that order of magnitude. An objective of this study was to extend the work of Peters to far lower oxygen concentrations, similar to those occurring in process streams in a desalination plant. It was also to be determined whether the Levich equation accurately predicts limiting

currents in seawater at these low oxygen concentrations. If a platinum RDE was not suitable for this application, the use of other materials was to be investigated.

Peters found that at any given electrode potential the oxygen reduction current at a platinum RDE decreased with time, down to a steady value. The current could be restored to its former value by making the electrode anodic for a short time, after which a decline in cathodic current would again occur. This effect has been noted by some investigators while others have either not observed it or have neglected to mention it.

It is evident that the rate of reduction of oxygen on platinum is related to the catalytic nature of the platinum surface, and this in turn is a function of electrode potential, its history, and several other factors. Chapter 4 is devoted to a discussion of the conflicting opinions expressed in the literature on this subject, as well as to some experiments which were performed in this study to provide additional information.

1.7 Mechanism and Kinetics of Oxygen Reduction

Fuel cell development and corrosion studies have, in the last decade or so, greatly stimulated interest in the reduction of oxygen on a wide variety of electrode materials. The reader is particularly referred to a systematic study (Khomutov and Zakhodyakina, 1970) of oxygen reduction on 38 different metals.

The overall reduction reaction is (Gnanamuthu and Petrocelli, 1967):

$$O_2 + 4H^+ + 4e^- = 2H_2O \text{ , in acid solution}$$

and (1.21)

$$O_2 + 2H_2O + 4e^- = 4OH^- \text{ , in basic solution .}$$

The reaction proceeds via a series of electron transfer and elementary reaction steps, the exact details of which are the subject of much disagreement among electrochemists, and vary according to the electrode material and the pH. At least sixteen different reaction paths have been proposed (Gnanamuthu and Petrocelli, 1967), all with supporting evidence. In all reaction paths the electrode surface participates in each step of the reaction. Gnanamuthu and Petrocelli (1967) derived a precise expression for the Tafel slope for oxygen reduction in terms of basic reaction parameters, but were still unable to restrict the number of possible paths for the oxygen reduction mechanism to less than six.

Nevertheless, since hydrogen peroxide can be detected whenever oxygen is reduced (Hoare, 1968), the reaction must proceed via the formation of H_2O_2, irrespective of the sequence of elementary steps involved, and H_2O_2 is regarded as a stable reaction intermediate.

An expanded reaction scheme for oxygen reduction, taking hydrogen peroxide formation into account, can be represented as follows (Bagotskĭ, et al., 1968;

Tarasevich, 1968; Luk'yanycheva, et al., 1971):

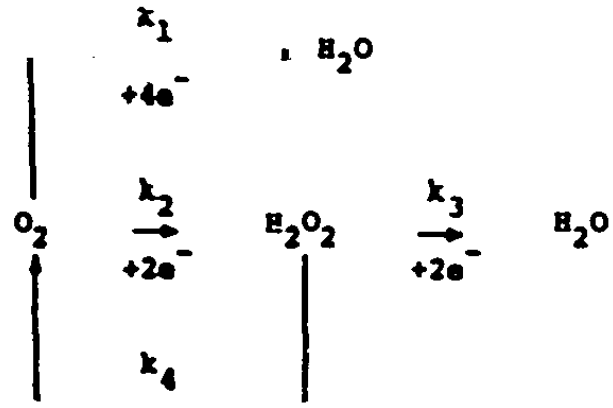

(1.22)

Note that this reaction model only considers 2- or 4-electron steps, rather than single-electron steps. It possesses the advantage, however, that it deals in terms of stable, identifiable species. Oxygen can be reduced directly to water by a 4-electron reaction, or to H_2O_2 via a 2-electron reaction. The H_2O_2 can then be reduced electrochemically to H_2O, or decompose catalytically to H_2O and O_2, or diffuse away from the electrode surface.

If loss by diffusion occurs to any appreciable extent, the number of electrons transferred per molecule of oxygen being reduced, instead of being equal to four, will be between two and four. The values of the reaction rate constants k_1 - k_4 will depend on the nature of the surface at which the oxygen is reduced as well as on the pH of the solution.

The Levich equation predicts a linear relationship between the limiting current and the square root of the rotational speed ω in the ideal case. Peters (1970) obtained a non-linear relationship, asymptotic at low

$\omega^{1/2}$ to the straight line predicted by the Levich equation, with an increasing deviation from this line with increasing $\omega^{1/2}$.

He explained this behavior by means of the simplified reaction mechanism shown below.

$$O_2 \xrightarrow[+2e^-]{k_2} H_2O_2 \xrightarrow[+2e^-]{k_3} H_2O \; . \qquad (1.22A)$$

This can be seen to be equivalent to (1.22), with $k_1 = k_4 = 0$. In addition Peters assumed that $k_2 >> k_3$. In such a case H_2O_2 exists transiently as a stable reaction intermediate. The effect of increasing the rotational speed was to increase the proportion of H_2O_2 leaving the vicinity of the RDE by convection before being reduced to H_2O. The increasing deviation of the i vs. $\omega^{1/2}$ curve from linearity with increasing $\omega^{1/2}$ can only be explained by assuming that the rate of H_2O_2 reduction is considerably less than the rate of O_2 reduction. Making the above assumptions, Peters derived the expression:

$$i_{lim} = 2FK_{O_2} c^{\circ}_{O_2} \omega^{1/2} \left(1 + \frac{1}{1 + \frac{K_{H_2O_2} \omega^{1/2}}{k_3}} \right) \qquad (1.23)$$

where K_{O_2} and $K_{H_2O_2}$ are equal to the expression

$\frac{0.6205}{1 + 0.298\ Sc^{-1/3} + 0.14514\ Sc^{-2/3}}\ Sc^{-2/3}\nu^{1/2}$ evaluated for Sc_{O_2} and $Sc_{H_2O_2}$, respectively. Peters calculated k_3 from sets of experimental i_{lim} and $\omega^{1/2}$ values. His calculated results exhibited a systematic decrease in k_3 as $\omega^{1/2}$ increased, instead of being independent of $\omega^{1/2}$.

As will be discussed in a later chapter, the mechanism of oxygen reduction varies according to the medium, the pH, electrode material, and oxygen concentration. The simple reaction model was tested further in this study to determine whether it applied under certain experimental conditions. It also provided a convenient means of calculating very approximate values of k_3 for comparison under a variety of experimental conditions.

1.8 Derivation of an Expanded Expression for the Current at an RDE in a Solution Containing Both O_2 and H_2O_2

The RDE can be used to elucidate the mechanism of O_2 reduction, as mentioned in the previous section. In this section an expression is derived for the limiting current due to O_2 reduction, using the expanded reaction model (eqn. 1.22). It is later shown, in Section 3.5.3, how this expression can be used to differentiate between the simplified and expanded reaction mechanisms by measuring the dependence of i_{lim} on $\omega^{1/2}$ with the RDE. The expression derived can be applied to solutions containing appreciable concentrations of both O_2 and H_2O_2.

The following assumptions are made:

1) All reactions involved are first-order. (Damjanovic, et al., 1967b; Tarasevich, 1968)
2) Both 4-electron and 2-electron O_2 reduction are very fast compared to H_2O_2 reduction.
3) The rate of O_2 reduction corresponds to the limiting-current situation, so that $c^s_{O_2} = 0$.

Let the fraction of O_2 undergoing 2-electron reduction to H_2O_2 be f; a fraction (1 - f) thus undergoes 4-electron reduction. Note that $f = k_2/(k_1 + k_2)$. The convective flux of oxygen to the RDE is $K_{O_2} c^b_{O_2} \omega^{1/2}$. The rate of formation of O_2 by catalytic decomposition of H_2O_2 at the RDE is $\frac{1}{2} k_4 c^s_{H_2O_2}$, where $c^s_{H_2O_2}$ is the H_2O_2 concentration at the surface of the RDE. The total rate of arrival of O_2 at the RDE is therefore

$$N_{O_2} = K_{O_2} c^b_{O_2} \omega^{1/2} + \tfrac{1}{2} k_4 c^s_{H_2O_2} . \qquad (1.24)$$

The current due to 2-electron O_2 reduction is $2FfN_{O_2}$, whereas that due to 4-electron O_2 reduction is $4F(1 - f)N_{O_2}$. The total current due to O_2 reduction is therefore

$$i_{O_2} = [2Ff + 4F(1 - f)]\left[K_{O_2} c^b_{O_2} \omega^{1/2} + \tfrac{1}{2} k_4 c^s_{H_2O_2}\right] . \qquad (1.25)$$

The current due to H_2O_2 reduction is

$$i_{H_2O_2} = 2Fk_3c^s_{H_2O_2} \cdot \qquad (1.26)$$

The total current is the sum of (1.25) and (1.26),

$$i = 2(2 - f)F\left(K_{O_2}c^b_{O_2}\omega^{1/2} + \tfrac{1}{2}k_4c^s_{H_2O_2}\right) + 2Fk_3c^s_{H_2O_2} \cdot \qquad (1.27)$$

Rearranging,

$$i = 2F\left[(2 - f)K_{O_2}c^b_{O_2}\omega^{1/2} + c^s_{H_2O_2}\left(k_4\left[\tfrac{2-f}{2}\right] + k_3\right)\right] . \qquad (1.28)$$

The surface concentration of H_2O_2 is found from a H_2O_2 material balance, as follows:

The rate of appearance of H_2O_2 by 2-electron reduction of O_2 is

$$R_{formation} = f\left(K_{O_2}c^b_{O_2}\omega^{1/2} + \tfrac{1}{2}k_4c^s_{H_2O_2}\right) . \qquad (1.29)$$

The rate of disappearance of H_2O_2 by reduction is

$$R_{red} = k_3c^s_{H_2O_2} \cdot \qquad (1.30)$$

The rate of disappearance of H_2O_2 by catalytic decomposition is

$$R_{decomp} = k_4c^s_{H_2O_2} \cdot \qquad (1.31)$$

The rate of loss of H_2O_2 by diffusion is

$$N_{H_2O_2} = K_{H_2O_2}\left(c^s_{H_2O_2} - c^b_{H_2O_2}\right)\omega^{1/2} . \qquad (1.32)$$

At steady state,

$$R_{formation} = R_{red} + R_{decomp} + N_{H_2O_2} . \qquad (1.33)$$

So,

$$f\left(K_{O_2}c^b_{O_2}\omega^{1/2} + \tfrac{1}{2}k_4c^s_{H_2O_2}\right) = k_3c^s_{H_2O_2} + k_4c^s_{H_2O_2} + K_{H_2O_2}\left(c^s_{H_2O_2} - c^b_{H_2O_2}\right)\omega^{1/2} . \qquad (1.34)$$

Solving (1.34) for $c^s_{H_2O_2}$, one obtains

$$c^s_{H_2O_2} = \frac{\left(fK_{O_2}c^b_{O_2} + K_{H_2O_2}c^b_{H_2O_2}\right)\omega^{1/2}}{k_3 + k_4\left(1 - \frac{f}{2}\right) + K_{H_2O_2}\omega^{1/2}} . \qquad (1.35)$$

Substituting for $c^s_{H_2O_2}$ from (1.35) in (1.28), the expression for the current is obtained.

$$i = 2F\left\{(2 - f)K_{O_2}c^b_{O_2}\omega^{1/2} + \frac{\left(fK_{O_2}c^b_{O_2} + K_{H_2O_2}c^b_{H_2O_2}\right)\omega^{1/2}\left[k_4\left(1 - \frac{f}{2}\right) + k_3\right]}{k_3 + k_4\left(1 - \frac{f}{2}\right) + K_{H_2O_2}\omega^{1/2}}\right\} . \qquad (1.36)$$

After rearranging, (1.36) becomes

$$i = 2F\omega^{1/2}\left\{(2 - f)K_{O_2}c^b_{O_2} + \frac{fK_{O_2}c^b_{O_2} + K_{H_2O_2}c^b_{H_2O_2}}{1 + \dfrac{K_{H_2O_2}\omega^{1/2}}{k_3 + k_4\left(1 - \frac{f}{2}\right)}}\right\} . \quad (1.37)$$

We can now derive simplified expressions for some special cases. Let us first neglect 4-electron O_2 reduction and catalytic H_2O_2 decomposition, i.e., assume $f = 1$ and $k_4 = 0$. Equation (1.37) reduces to

$$i = 2F\omega^{1/2}K_{O_2}c^b_{O_2}\left[\frac{1 + \dfrac{K_{H_2O_2}c^b_{H_2O_2}}{K_{O_2}c^b_{O_2}}}{1 + \dfrac{K_{H_2O_2}\omega^{1/2}}{k_3}}\right] . \quad (1.38)$$

This equation was used to calculate approximate values for k_3 when using solutions containing both O_2 and H_2O_2.

When the H_2O_2 concentration is negligible compared to that of O_2 equation (1.38) becomes

$$i = 2FK_{O_2}c^b_{O_2}\omega^{1/2}\left(1 + \frac{1}{1 + \dfrac{K_{H_2O_2}\omega^{1/2}}{k_3}}\right) . \quad (1.39)$$

This is identical to the expression derived by Peters (1970), equation (1.23).

When the O_2 concentration is negligible compared to that of H_2O_2 equation (1.38) becomes

$$i = \frac{2FK_{H_2O_2}c^b_{H_2O_2}\omega^{1/2}}{1 + \frac{K_{H_2O_2}\omega^{1/2}}{k_3}} \quad . \qquad (1.40)$$

This equation was used to calculate approximate values of k_3 in H_2O_2 solutions containing negligible amounts of O_2. Note that eqns. (1.39) and (1.40), based on the simplified reaction model, contain only one unknown, k_3, which can thus be calculated using a single i vs. $\omega^{1/2}$ data point.

An interesting consequence of this derivation is obtained for the case of very rapid catalytic decomposition of H_2O_2. Let us take a solution containing O_2 but with a negligible amount of H_2O_2 in the bulk. Equation (1.37) becomes

$$i = 2F\omega^{1/2}\left\{(2 - f)K_{O_2}c^b_{O_2} + \frac{fK_{O_2}c^b_{O_2}}{1 + \frac{K_{H_2O_2}\omega^{1/2}}{k_3 + k_4\left(1 - \frac{f}{2}\right)}}\right\} . \qquad (1.41)$$

If catalytic decomposition is very rapid compared to the rate of diffusion of H_2O_2 from the surface of the RDE the term $\frac{K_{H_2O_2}\omega^{1/2}}{k_3 + k_4\left(1 - \frac{f}{2}\right)}$ will approach zero, and

equation (1.41) can be written as follows:

$$i = 4F\omega^{1/2}K_{O_2}c^{b}_{O_2} \quad . \qquad (1.42)$$

Such a case would thus be completely equivalent to 4-electron reduction of O_2 and a plot of i_{lim} vs. $\omega^{1/2}$ would not enable one to distinguish between them. This point is discussed further in Section 3.5.

1.9 The Ring-Disk Electrode

The use of a rotating ring-disk electrode (RRDE) to study reactions such as (1.22), where a stable intermediate is produced, was first suggested by Frumkin and Nekrasov (Tarasevich, 1968) and later developed in more detail by Damjanovic, et al., (1966), Tarasevich (1968) and Bagotskii, et al., (1968).

The RRDE is essentially an RDE with a narrow, coplanar, concentric ring set close to the active portion of the disk. A full theoretical treatment of the hydrodynamics and mass transport characteristics of the RRDE may be found in the papers by Albery and Bruckenstein (1966), and Smyrl and Newman (1972).

Damjanovic, et al., (1966) developed a diagnostic technique for determining whether a reaction such as (1.22) proceeds via single or parallel paths, whether intermediates are formed, and whether they react further. The limiting current at the disk, I_D, and the corresponding current at the ring, I_R, are measured at a series of

rotational speeds, ω. The ratio $\frac{I_D}{I_R}$ is then plotted against $\omega^{-1/2}$, resulting in a curve characteristic of the reaction mechanism. This treatment does not take catalytic H_2O_2 decomposition into account, and thus can lead to erroneous conclusions when such a reaction is present to a significant extent, as was shown in the previous section. (e.g., eqn. (1.41))

The methods developed by Tarasevich (1968) and Bagotskii, et al., (1968), do take catalytic H_2O_2 decomposition into account, and permit evaluation of the four reaction rate constants, $k_1 - k_4$, of reaction (1.22). The former derived a set of simultaneous nonlinear equations for the ring and disk currents in terms of $k_1 - k_4$, necessitating data of at least ±0.5% precision in order to obtain accurate solutions for the rate constants. The latter, however, were able to derive a set of linear equations which they claimed permitted accurate evaluation of the rate constants without requiring data of especially high precision. The conclusions reached by the authors mentioned in this section will be discussed in a later chapter.

In studies on oxygen reduction kinetics, experimental results are quoted only for work performed with strongly acidic or alkaline solutions which are of high purity. By contrast, the present project was concerned with oxygen reduction in seawater, which is high in organic impurities and has a pH close to 7. The kinetic data

obtained with this system thus supplement the results obtained by other researchers.

1.10 Choice of Electrode Material

The material used as the active portion of the RDE had to satisfy the following criteria:

(a) Be a good catalyst for oxygen reduction, so that polarization curves would exhibit a definite limiting current plateau.

(b) Give reproducible reduction kinetics over the potential range investigated.

(c) Be inert in 3.5% NaCl and seawater.

Although there exists an extensive literature on oxygen reduction at various electrode materials it is difficult to choose an electrode material on the basis of published experimental data. This is so because, firstly, all results quoted in the literature were obtained with very pure electrolytes, at pH values close to either 1 or 14. By contrast the investigations made in this study involved neutral solutions which were not purified, in order to simulate the actual operating conditions in a desalination plant as closely as possible. It has been demonstrated that the oxygen reduction mechanism depends strongly on pH (Bonnemay, et al., 1970, Damjanovic, et al., 1966b) and electrolyte purity (Damjanovic, et al., 1967a). Second, over half the papers surveyed were concerned solely with the mechanism of oxygen reduction and described polarization

only at currents an order of magnitude below the limiting value. In such cases the more active metal was taken to be the one where a higher current density for oxygen reduction occurred at a given potential.

Khomutov and Zakhodyakina (1970) measured polarization curves for oxygen reduction on RDE's made of 38 different metals, under identical experimental conditions. They plotted the half-wave potential, $E_{1/2}$, for each metal vs. its atomic number. The half-wave potential is the potential at the inflection point on the polarization curve, and is one measure of the ease of reduction of oxygen at a given metal. The most favorable values of $E_{1/2}$ were observed for Cu, Ru, Rh, Pd, Pt, and Au. Additional electrode materials which will be discussed below, because of their frequency of appearance in the literature, are Ag and graphite.

Copper and Silver

Copper oxidizes relatively rapidly in air; silver oxidizes much more slowly. If these metals were used as electrodes in seawater, corrosion due to both anodic dissolution, and local cell currents might be expected. Nevertheless, since a copper RDE was available and a silver RDE could be quickly made, they were briefly tested to assess their rate of corrosion.

Platinum

More is known about oxygen reduction on Pt than on any other metal (e.g., Hoare, 1968). Well-defined

limiting current plateaux corresponding to the overall reaction:

$$O_2 + 2H_2O + 4e^- \rightarrow 4OH^- \qquad (1.21)$$

were obtained by Müller and Nekrassow (1964), Oshe, et al., (1965), Peters (1970), and Yuzhanina, et al., (1970). Many other authors have observed an apparent number of less than 4-electrons transferred per mole of oxygen in the above reaction. Damjanovic, et al., (1966b) ascertained that the following reactions:

$$O_2 + 2H^+ + 2e^- \rightarrow H_2O_2 \qquad (1.43)$$

$$H_2O_2 + 2H^+ + 2e^- \xrightarrow{slow} 2H_2O \qquad (1.44)$$

occurred as parallel reactions to the 4-electron reduction. The extent to which either reaction path predominated was dependent on the experimental conditions and the electrode material. Since the H_2O_2 reduction is known to be comparatively slow under certain conditions, the number of electrons passed per mole of O_2 reduced will be less than 4 if:

(i) Direct 4-electron reduction (1.21) is absent, and the H_2O_2 reduction step (1.43) occurs slowly, or

(ii) Direct 4-electron reduction is present, and H_2O_2 reduction is either slow or does not occur.

Since 4-electron stoichiometry had been observed on platinum in a neutral solution (Peters, 1970) and it satisfied the criteria for an electrode material, a platinum RDE was used in this study.

Gold

Ganshaw, et al., (1967a) and Tarasevich, et al., (1970) observed a limiting current due to 2-electron reduction at a gold electrode. At more cathodic potentials, using the same electrode, a limiting current corresponding to 4-electron reduction also occurred. Giner, et al., (1969) observed only 2-electron reduction in alkaline solution. It was felt that even if kinetic factors prevented the measurement of a limiting current for 4-electron reduction, it might still be possible to measure a '2-electron' limiting current. Moreover gold is used in many commercial oxygen sensors and is therefore of special interest, so it too was investigated in this study.

Palladium

According to Hoare (1965) Pd is a poorer H_2O_2 decomposition catalyst than Pt. This indicates that in the limiting current region, kinetic limitations would result in a poor limiting current plateau at a Pd electrode.

Damjanovic and Brusić (1967) investigated O_2 reduction at Pt, Pd, and Au electrodes and found that the activity of Pt was almost an order of magnitude

greater than that of Pd, in the current density range 10^{-7} - 10^{-3} A/cm^2. These authors also concluded that the oxygen reduction mechanism was the same at Pt and Pd. It was decided that, since the RDE envisaged in this present study would ultimately be used in applications where the current density would be below 10^{-5} A/cm^2, no advantage would be gained with a Pd electrode.

Ruthenium

Nekrasov and Khrushcheva (1967) measured polarization curves for oxygen reduction at Ru and found that the low rate of H_2O_2 reduction obscured the limiting current plateau. Ruthenium was therefore not considered for further study.

Rhodium

Khrushcheva, et al., (1967) found that the limiting current for O_2 reduction at Rh in 1 N H_2SO_4 was equal to the current predicted by the Levich equation. Radyushkina, et al., (1970) found the same to be true in highly alkaline solutions, although Nekrasov, et al., (1966) obtained limiting currents equal to only 85% of the theoretical current in 0.1 N KOH. They found that the rate of reduction of H_2O_2 on Rh was only 10% of that at a Pt electrode.

Genshaw, et al., (1967b) investigated O_2 reduction in 0.1 N H_2SO_4 and 0.1 N KOH, both purified and unpurified, or "impure". They found that only in very

pure solutions was 4-electron reduction observed at the limiting current. In impure acid solutions the current dropped quickly when the electrode was polarized, and in impure alkaline solution slow H_2O_2 reduction limited the current. The authors concluded that the mechanism of O_2 reduction on Rh was similar to that observed with Pt. In view of this, and the fact that this study was concerned only with unpurified solutions, it seemed inappropriate to conduct any experiments with an Rh electrode.

Graphite

Tarasevich, et al., (1968) and Yeager, et al., (1964) obtained limiting current plateaux for 2-electron reduction at pyrolytic graphite in alkaline solutions. The former found that, as the pH was decreased to about 12, the plateau became less distinct and finally disappeared. Morcos and Yeager (1970) found that kinetic limitations led to an apparent number of less than 2 electrons discharged per mole of O_2 reduced, in 1 M KOH with P_{O_2} = 0.97 atm, at high-pressure annealed pyrolytic graphite as well as at cleavage-surface and ordinary pyrographite.

Sabirov, et al., (1970) obtained a plateau for 2-electron O_2 reduction at pyrolytic graphite in 1 N H_2SO_4, but no plateau was observed when P_{O_2} was lowered from 0.97 to 0.23 atm. Sabirov and Tarasevich (1969) found the O_2 reduction rate to be lower on

vitreocarbon than on pyrolytic graphite. It can be surmised, then, that in a neutral solution with $P_{O_2} < 0.01$ atm a limiting current plateau would not be expected to occur at a graphite electrode. Accordingly no experiments were conducted with a graphite RDE.

CHAPTER 2: APPARATUS AND PROCEDURE

2.1 Experimental Apparatus

The RDE cell (Plate 1) was made from a Kimax tempered-glass reduction fitting, 7.6 cm. I.D. at the base, 5.1 cm. I.D. at the top, and 13 cm. long. It was flange-mounted on a polypropylene base 2.5 cm. thick. The cell was made airtight by means of a flange-mounted clear plastic lid with an O-ring seal.

Several RDE's were used: one of these is shown in Plate 2. Each electrode had a stainless steel shaft 32 cm. long and 1.3 cm. in diameter, machined to 0.6 cm. diameter for the lower 1 cm. of its length. The material to be used as the active portion of the electrode was soldered to the end of this reduced portion of the shaft, and machined concentric with the shaft. The lower 10 cm of the shaft was set in Cargille "Araldite 6005" epoxy resin, which was machined to the smooth bell shape shown in Fig. 2.1.

The average diameter of the disks used was 4.7 cm.; the average thickness was 0.15 cm. The active portions averaged 0.6 cm. in diameter. The ratios:
(i) disc diameter / diameter of active portion,
(ii) disc diameter / shaft diameter, and
(iii) disc thickness / disc diameter
satisfied the criteria summarized by Riddiford (1966).

The flat under-surface of each electrode was

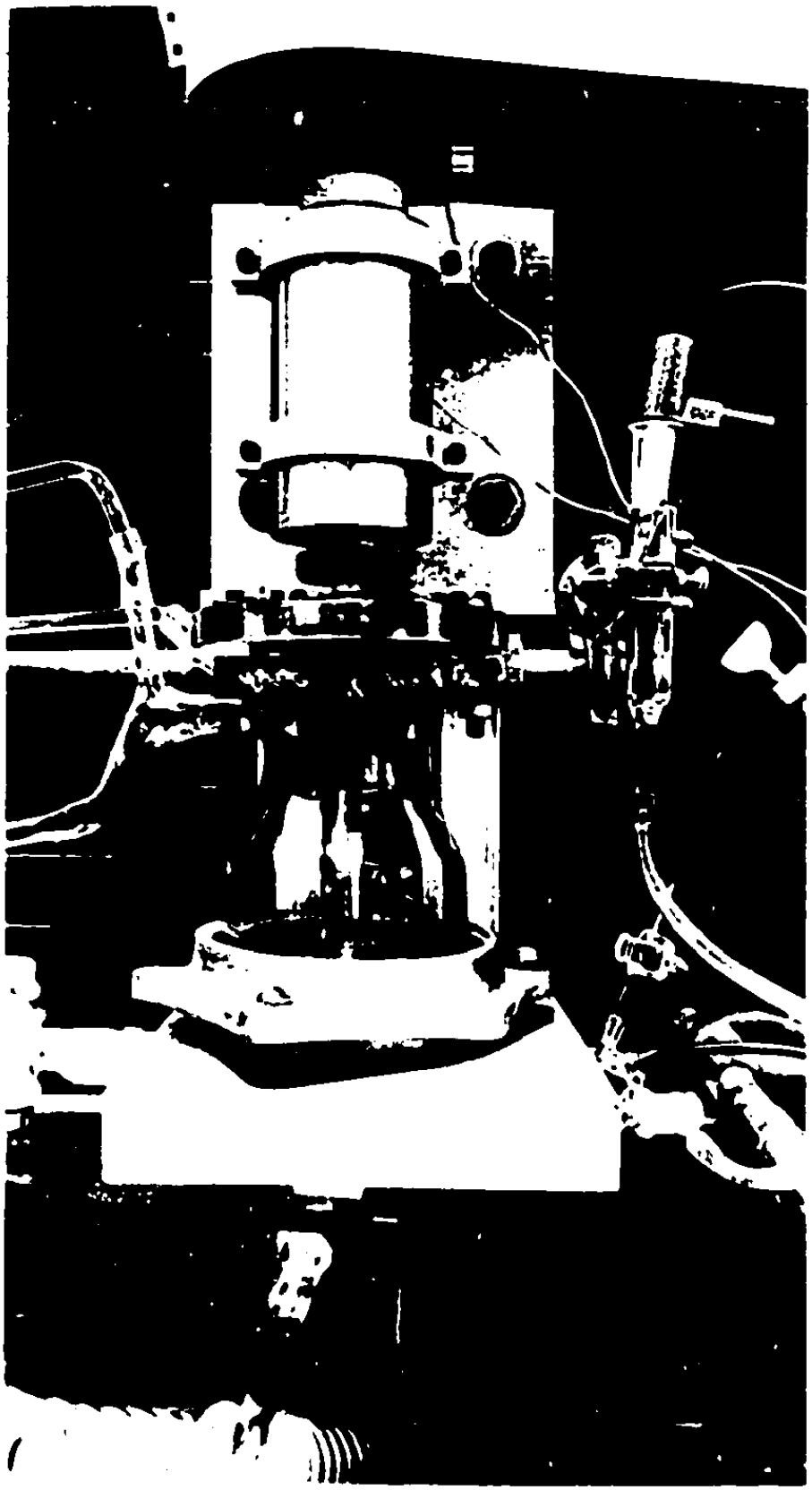

Plate 1. The RDE Cell.

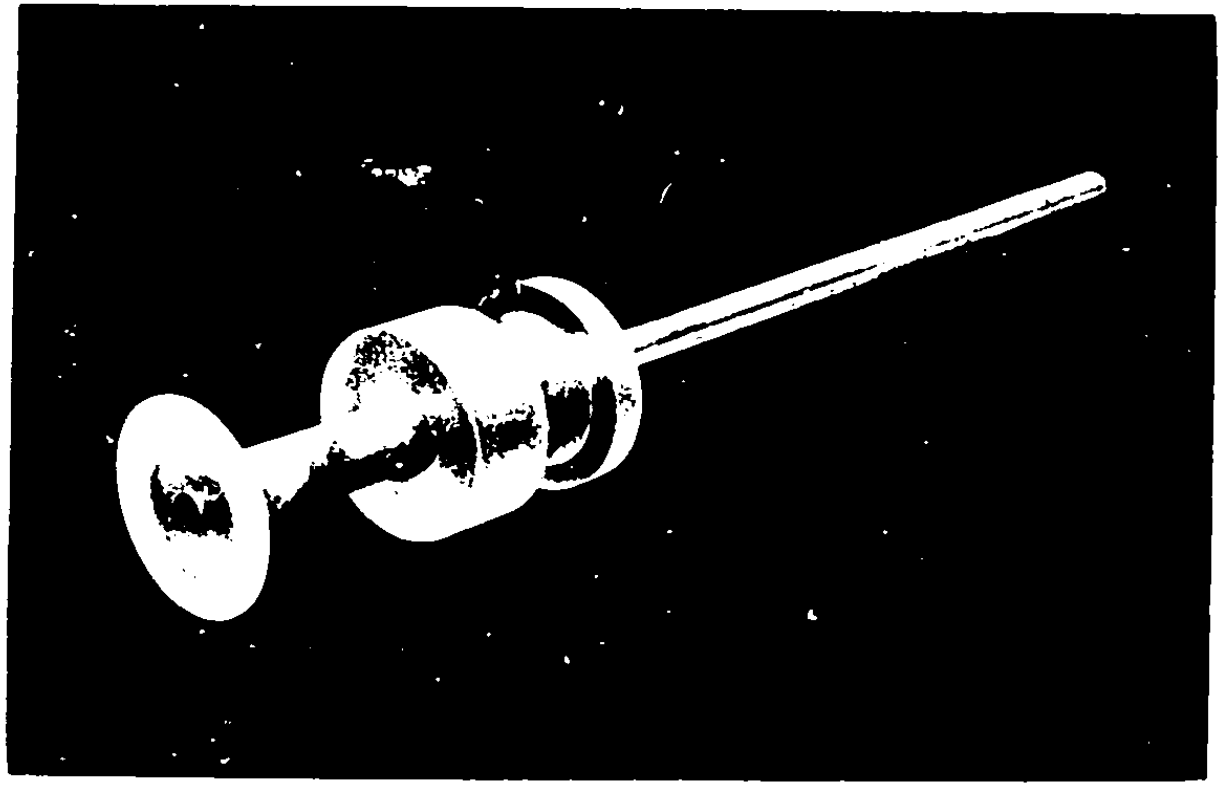

Plate 2. Rotating Disk Electrode.

polished using increasingly fine abrasive papers or powders. Final polishing was done using Buehler Ltd. "Metadi" 1 μ diamond polishing compound, which resulted in a mirror-like finish. The rugosity of the polished disks was an order of magnitude lower than the smallest boundary layer thickness (approx. 25 μ) encountered, so no boundary layer disruption was envisaged.

A C/R rubber oil seal prevented air from leaking into the cell where the electrode shaft passed through the cell lid. The shaft was held in two bearings mounted in an aluminum casing. It was driven by a 1/8 H.P. Servo-Tek STE-230T-1A, variable speed D.C. motor with a range of 0 to 3600 RPM, via a notched rubber belt, with a 1:1 gear ratio. The selected motor speed was held constant by a Servo-Tek ST-579-1 controller/rectifier. The rotational speed was measured with a General Radio Corp. "Strobotac," Type 631-B, stroboscope.

Electrical contact with the electrode was maintained by means of carbon commutators in contact with a copper sleeve placed over the upper end of the shaft.

The counter-electrode was a circular piece of platinum foil with an area of about 4 cm^2., placed at the bottom of the cell about 2 cm. from the RDE. A platinum wire spot-welded to the counter-electrode passed through the base of the cell to facilitate electrical contact with the electrode.

A Corning saturated calomel electrode (SCE) was placed in a 1.5 cm. diameter open cell, which was connected by "Tygon" tubing to a Luggin capillary protruding through the base of the RDE cell. The end of the capillary was about 2.5 cm. from the active portion of the RDE. This distance was sufficient to ensure that the capillary would not disrupt the hydrodynamic situation near the RDE. The potential drop in the solution between the RDE and the reference electrode was negligible, due to the high electrical conductivity of the test solution.

The potential of the RDE relative to that of the SCE was controlled by a McKee-Pedersen MP1026 potentiostat. The current in the external circuit was measured as a potential drop across a 160Ω precision resistor, using a Sargent SRG millivolt recorder.

The potential selector of the potentiostat was modified slightly in order to permit rapid switching of the RDE between anodic and cathodic potentials for electrode pretreatment. A modification was also made to allow the potentiostat to warm up without putting an electrical signal through the RDE circuit. These modifications are shown diagramatically in Fig. 2.2.

The saturator (Fig.2.1.) was an all-glass vessel in which a test solution was brought to a desired oxygen concentration before being pumped to the RDE cell. Oxygen, air, or a known mixture of N_2 and O_2,

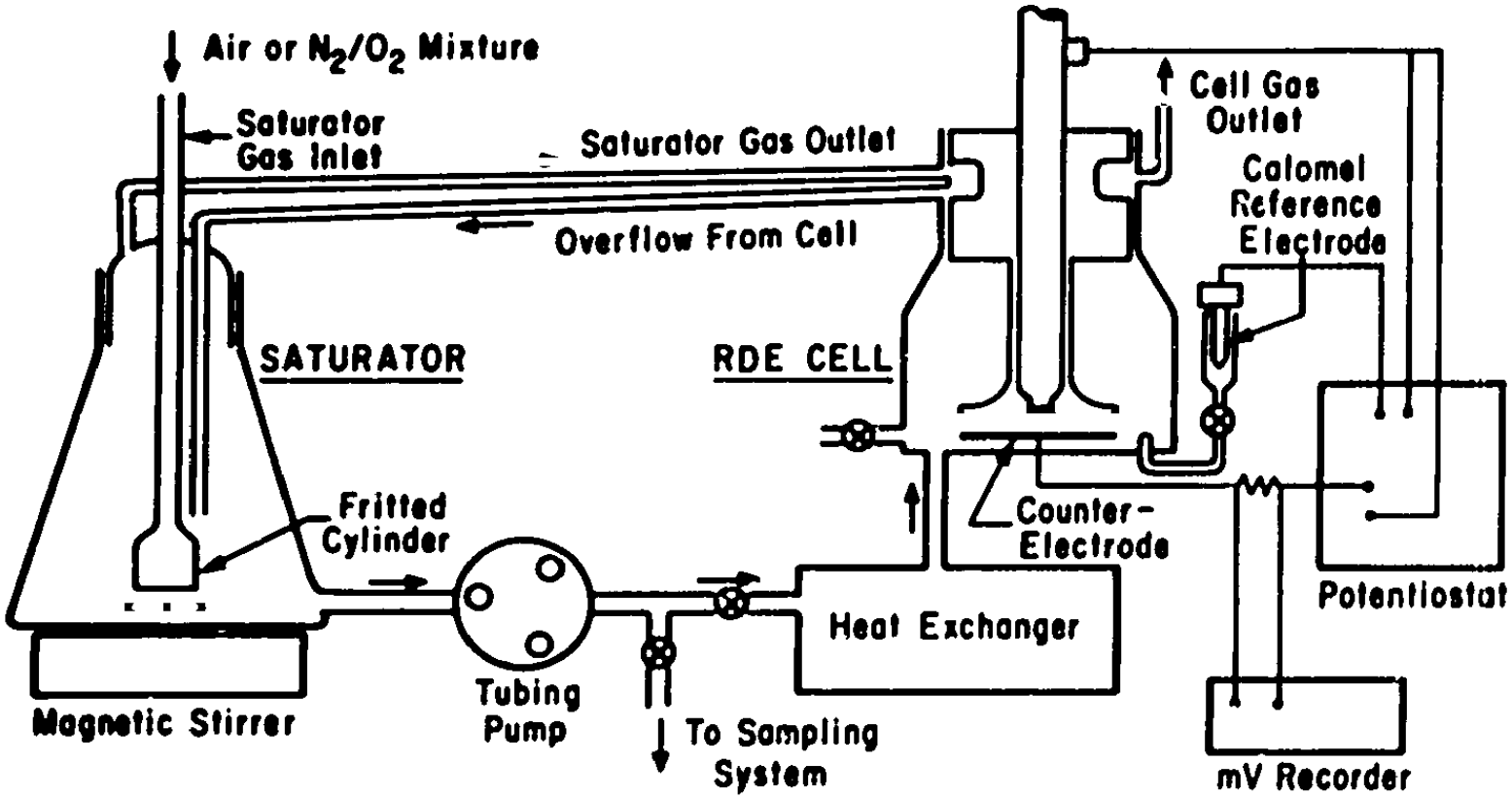

Figure 2.1. Experimental Apparatus.

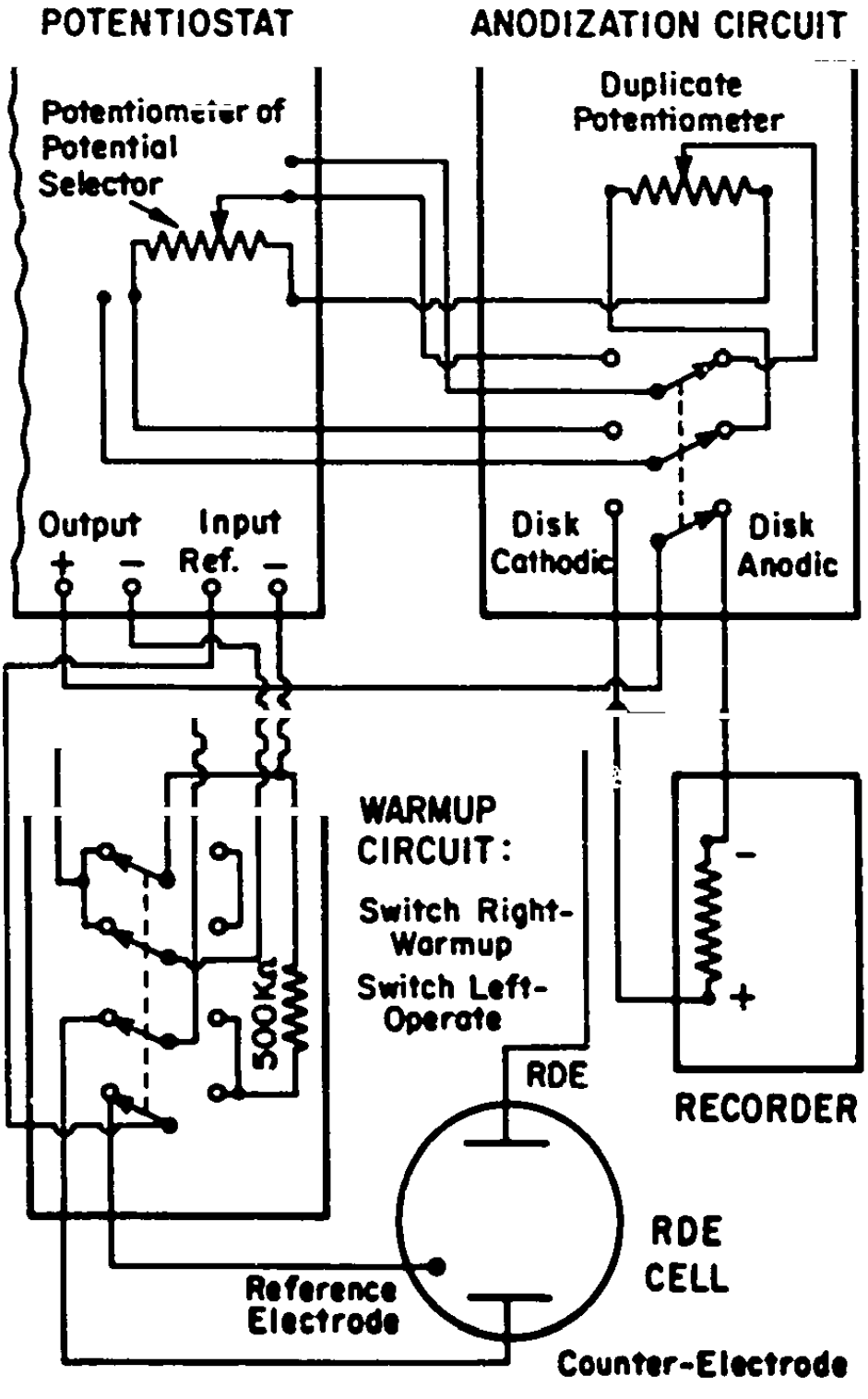

Figure 2.2. Potentiostat Modifications.

was bubbled through the solution via a fritted cylinder. A glass thermowell which accomodated a standard thermometer extended almost to the bottom of the saturator. Stirring was done by a Teflon-coated stirrer bar and an air-driven magnet. A rubber septum could be attached to a port at the base of the saturator by means of a ball joint whose male connector had been ground down by about 2 mm. Samples could be withdrawn, or reagents added, via this septum using a hypodermic syringe.

Test solution was pumped from the saturator, through a heat exchanger, to the bottom of the RDE cell using a Masterflex 7020V-14 tubing pump, capable of pumping rates between 7.5 and 150 ml./min. Solution flowed upward through the cell past the RDE. Varying the pumping rate from its minimum to its maximum value was found to have no effect on the rate of mass transfer to the RDE. The heat exchanger consisted of glass coils with a total length of 290 cm., immersed in a constant temperature bath. The cell inlet was about 5 cm. from the bath, so it could be assumed that the temperature of the solution entering the cell was effectively equal to that of the solution leaving the heat exchanger.

The bath temperature was controlled within 0.5°C. Stricter temperature control was not necessary in this study for the following reason:

The Henry's law constant for oxygen in a saline medium decreases with increasing temperature, while the term $\frac{0.6205\ Sc^{-2/3}\nu^{1/2}}{1 + 0.298\ Sc^{-1/3} + 0.1451\ Sc^{-2/3}}$, from the Levich equation, increases. The product of the two terms is affected very little by changes in temperature. Table 2.1 shows that the theoretical limiting current density for oxygen reduction in a 3.5% NaCl solution, for example, increases by an average of only 0.3% for each 1 C° rise in temperature over the range 20°C-30°C.

TABLE 2.1

Variation of $i/\omega^{1/2}$ with Temperature

T(°C)	$i/\omega^{1/2}$ (mA.sec$^{1/2}$/cm.^{2})	T(°C)	$i/\omega^{1/2}$ (mA.sec$^{1/2}$/cm.^{2})
20	0.07670	26	0.07825
21	0.07692	27	0.07851
22	0.07714	28	0.07878
23	0.07734	29	0.07890
24	0.07769	30	0.07930
25	0.07795		

An overflow tube was located 2 cm. from the top of the RDE cell. Solution leaving the cell returned by gravity to the saturator.

Gas leaving the saturator after bubbling through the test solution was brought into the top of the RDE cell. It circulated as a gas blanket above the over-

flowing solution, left via an outlet on the opposite side of the cell, and was released to the atmosphere through a bubbler with a head of about 6 cm. H_2O. As mentioned earlier, liquid samples could be withdrawn from the saturator. They could also be pumped into the sampler described in Chapter 6 by diverting the flow downstream of the pump.

All tubing in the system, with the exception of the pump tubing, was of glass. Most connections were made with 12/5 ball joints. Wherever "Tygon" tubing was used in connections for the sake of flexibility, its length was kept to a minimum. Gas cylinders were connected to the system using 1/4" copper tubing and Swagelock fittings.

2.2 Electrolytes and Their Preparation

In many experiments a 3.5 weight % NaCl solution was used as the electrolyte. Reasons for its use are discussed in Section 1.6. The solution was made using Mallinckrodt "Analytical Reagent" grade 99.96% pure NaCl, and distilled water which was piped to the laboratory. It was stored in a refrigerator to inhibit the growth of microorganisms.

Seawater from Bodega Bay, California was used in all other experiments. Seawater in its natural state contains an abundance of microorganisms which may multiply rapidly during storage and have an adverse

effect on electrolytic experiments. To prevent this the following procedure was adopted when collecting and storing seawater samples.

The seawater was pumped via a polypropylene line from a point one-half mile offshore. The line was flushed for 10-15 minutes before samples were collected in thoroughly washed and dried bottles. Within 24 hours of being collected the seawater was filtered through Millipore HAWP 142-00 filters with a pore size of 0.45μ, using a sterilized Buchner funnel. The filtrate was stored in sterilized vessels, in a refrigerator.

2.3 Blending and Analysis of N_2/O_2 Mixtures

Initially, the N_2/O_2 ratio was controlled by mixing separately metered flows of N_2 and O_2 at a point 70-80 cm. upstream of the saturator. When working with gas mixtures containing less than 0.5 vol. % O_2 the N_2/O_2 ratio was so large that either a very high N_2 flowrate or a very low O_2 flowrate was required. The former wasted N_2, while the latter was difficult to control.

This problem was circumvented by blending N_2 and O_2 mixtures, by forcing high-pressure O_2 into a cylinder of N_2 which was at a lower pressure. The O_2 concentrations of the gas mixtures were checked by analyzing 2 ml. samples with a Varian Aerograph A-90-P gas chromatograph. The instrument incorporated an

0.6 mm. diameter column 3.3 meters long, filled with "5A" molecular sieves and held at 125°C. The nickel filaments of the thermal-conductivity detector were held at 160 °C. The carrier gas was helium, flowing at 80 ml./min.; the reference gas flowrate was 8 ml./min.

The air used to saturate solutions in some experiments was taken from an outlet in the laboratory and contained a very small amount of oil. Before entering the saturator the air was cleaned by passing it through a wash bottle packed with glass wool.

2.4 Procedure

The experimental work can be divided into two broad categories: that in which the test solution was saturated with air, and that in which an N_2/O_2 mixture containing less than 20 vol. % O_2 was used. In the former case no special precautions were taken to exclude atmospheric O_2 from the system, and the O_2 content of the test solution was determined by means of solubility tables (e.g., Truesdale, et al., 1955). In the latter case the flow system was purged prior to the experiment with the same gas as was used in the saturator.

The test solution was added to the saturator; refrigerated solutions were first warmed to room temperature to prevent gas bubbles from coming out of solution in the cell.

The onset of equilibrium between the test solution and the gas was sometimes hastened by removing most of the dissolved oxygen from the solution before feeding it into the flow system. Approximately one liter of solution was boiled in a 2-liter round-bottomed flask for 1/2-1 hour while N_2 was bubbled through the solution. The solution was cooled to room temperature, whereupon it was pumped by N_2 pressure into the flow system. This treatment was only used for NaCl solutions, not for seawater.

A gas flow of about 200 ml./min. was maintained in the saturator while the test solution was pumped around the flow system. If H_2O_2 solution was to be used in an experiment the H_2O_2 was injected into the circulating NaCl solution through the septum on the saturator. The potentiostat and recorder were warmed up for about thirty minutes before measurements were made. The approach to steady-state O_2 concentration in the system was checked occasionally by measuring the O_2 reduction current at a potential in the limiting current region. When two identical current readings were obtained half an hour apart the solution was considered to be in equilibrium with the gas in the saturator, and data could then be taken.

Polarization data were taken by recording the current flowing between the RDE and the counter-electrode as a function of RDE potential. The

potential was made cathodic in 100 mV steps, beginning at or near the rest potential, and ending when the current increased rapidly at the onset of H_2 evolution. The same procedure was often repeated in the opposite direction. These polarization data were taken with the electrode rotating at a known rate between 600 and 800 RPM. The rotational speed was then increased in steps; the current at a fixed RDE potential in the limiting current region was recorded at each step. The maximum speed of rotation was limited by the formation of a vortex which gradually extended under the RDE.

Samples of the test solution were withdrawn and analyzed for O_2 or H_2O_2 by means of the Winkler titration, or a modification thereof, respectively. The analytical technique is described fully in Chapter 6.

After each experiment the flow system was dismantled. The cell, saturator, and heat exchanger coils were cleaned with detergent and water, rinsed in tap water and then with distilled water. The saturator was occasionally soaked in chromic cleanser overnight. This was followed by rinsing with tap water, soaking in distilled water with detergent, and finally, rinsing with distilled water. The RDE was soaked briefly in 2N HNO_3, then rinsed with distilled water.

3. Polarization and Kinetic Data Obtained With a Platinum RDE

3.1. Scope of this Chapter

The first section of this chapter is devoted to a discussion of the transient nature of the current for O_2 reduction at a platinum electrode in air-saturated 3.5% NaCl solution. The techniques used to activate the electrode and measure polarization curves are described. Polarization curves measured in 3.5% NaCl solution and seawater at oxygen levels between 0.1 and 7 ppm, are shown.

The rate constant for electrochemical H_2O_2 reduction is calculated using a simplified reaction model, and is compared with values published in the literature. The shortcomings of this simplified reaction model are discussed with the aid of the expanded reaction model derived in Chapter 1. Finally, the values of the H_2O_2 reduction rate constant obtained in this study are plotted against electrode potential, and the resulting correlation is compared with one given in the literature.

3.2. Transience of the Oxygen Reduction Current, and Electrode Activation Technique

The current due to O_2 reduction at an RDE held at a constant cathodic potential was found to decrease with time to a steady-state value. This behavior was also observed by Peters (1970), as well as by a number

of other investigators (see Section 4.2). Some typical current decay curves are shown in Fig. 3.1.

The rate and extent of current decay were found to depend on both the oxygen concentration and the electrolyte used. In all cases the rate of decay was initially high, then decreased after about 5 sec. Peters noted that the current steadied out for about 2 minutes after this initial transient before slowly decaying again. Such behavior was observed in this study only at oxygen concentrations of above 7 ppm in 3.5% NaCl. At all other times a continuous current decay was observed. In the potential region of the limiting current, however, the decay curve was much flatter than at potentials below those of the limiting current.

The current could be restored to its initial value by holding the RDE at an anodic potential for several seconds. The electrode was then said to be in an "activated" state. The potential and duration of anodization had only a minor effect on the subsequent behavior of the electrode. This topic will be explored in more detail in Chapter 4.

It was observed, as in Peters' work, that shortly after the initial transient, about 0.2 min. after electrode activation, the current was within 1% of that predicted by the Levich equation. The

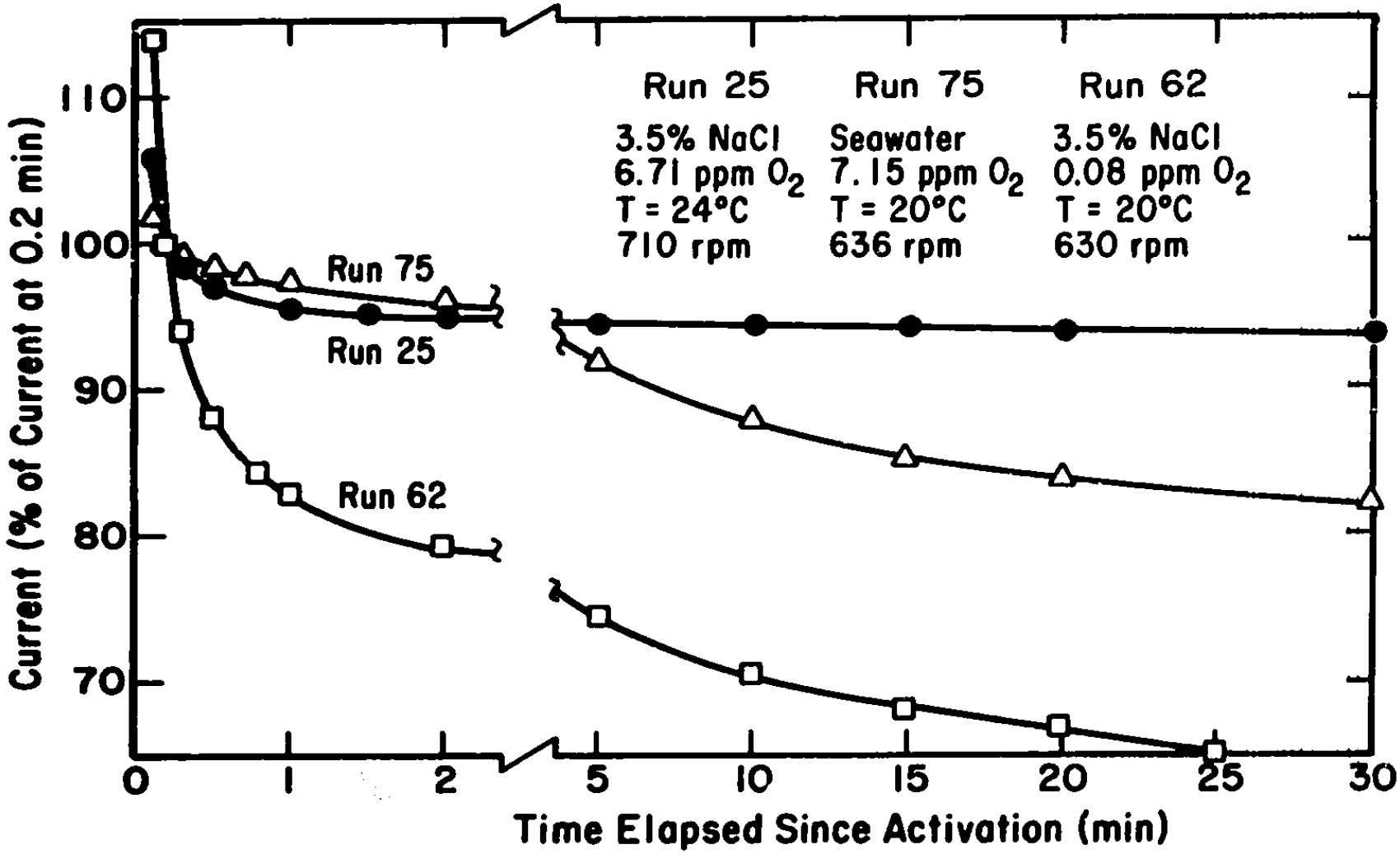

Figure 3.1. Decay of the Current for Oxygen Reduction at a Platinum RDE.

following procedure was therefore used to measure each point on the polarization curves: After anodization at 0.5-1.0 volts vs. SCE for several seconds the potential was made cathodic and the current was recorded continuously. The current at 0.2 min. after the switch from anodic to cathodic polarization was plotted against the potential. This procedure was repeated for each stepwise increase in the cathodic potential.

Fig. 3.2 shows a polarization curve measured by this technique. The limiting current plateau is well-defined and the current at the plateau is equal to the theoretical limiting current. The lower curve in Fig. 3.2 is a plot of the steady-state, or "declined", current vs. potential. It shows no evidence of a limiting current plateau.

It appears that, under conditions identical to those of Run 86, the platinum RDE could be used as an instrument for measuring O_2 concentration. The limiting current would be found from a polarization curve using the technique outlined above, and the Levich equation (1.20) would then be used to calculate the O_2 concentration. It must be pointed out that this method is not entirely based on theory. The time at which to measure the current after activation of the

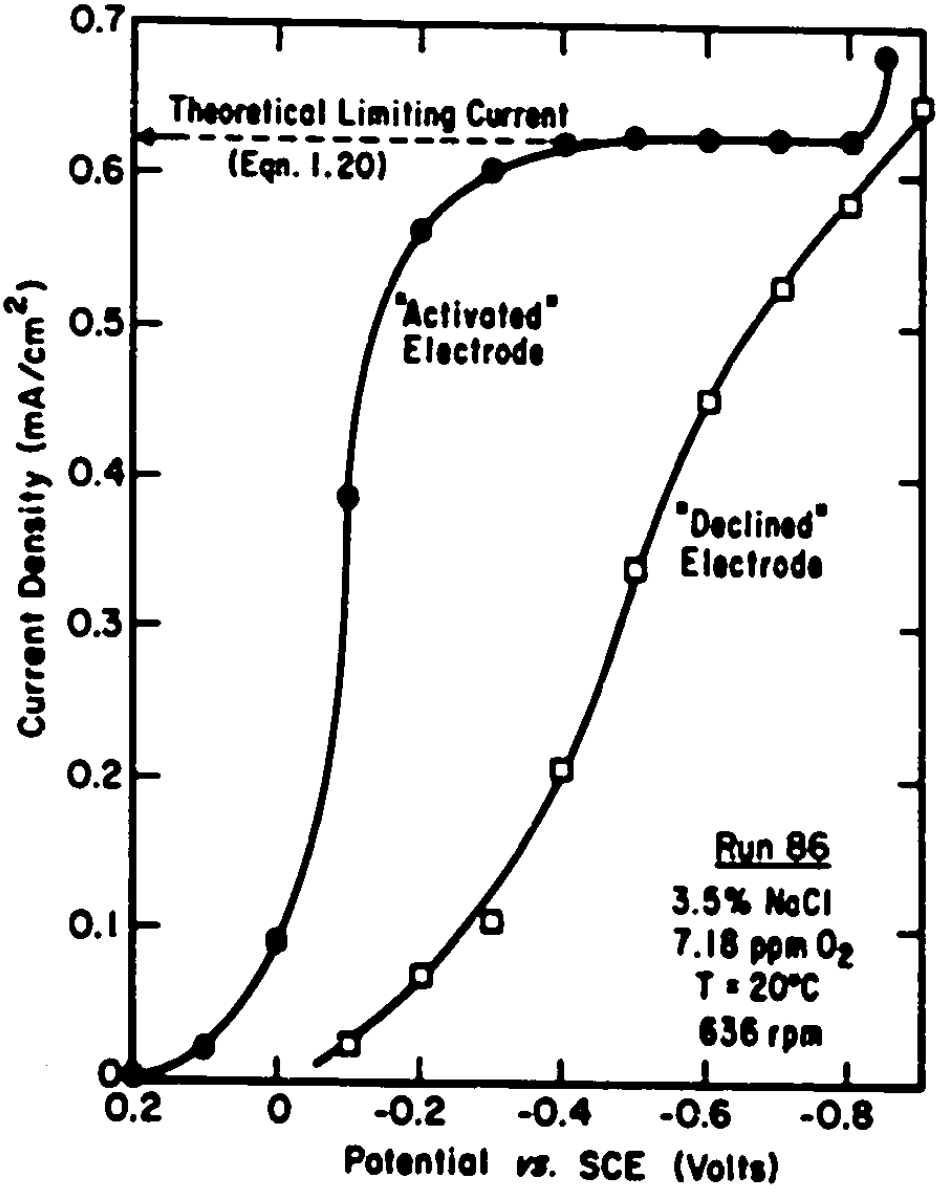

Figure 3.2. Polarization Curve for Oxygen Reduction at an Activated Platinum RDE in Air-saturated NaCl Solution.

electrode was determined empirically.

This time factor is hard to justify either on the basis of known electrode surface phenomena or on the characteristics of the electronic equipment used. The time required for the formation of the mass transfer boundary layer is generally considered to be on the order of 0.1 sec. The response time of the potentiostat to a step change in potential is approximately 100 mV/μsec. A step change from a potential of +1.0V to -0.8V would therefore take 18μsec. The full-range travel time of the recorder is less than 1 sec. The sum of all these terms is only about 1.1 sec.

The initial and subsequent transients may be caused by adsorption or desorption of impurities present in the solution, as well as reduction or desorption of oxygen species adsorbed at the surface of the electrode during activation. These and other possibilities are discussed in detail in Chapter 4.

The best justification for the use of the empirical time factor is the fact that it gives very good results. Fig. 3.3 shows sets of polarization curves measured by reading the current at each electrode potential at various times after activation. For a time of 0.1 min. the plateau (or inflection point, at lower O_2 concentrations) occurs at a current

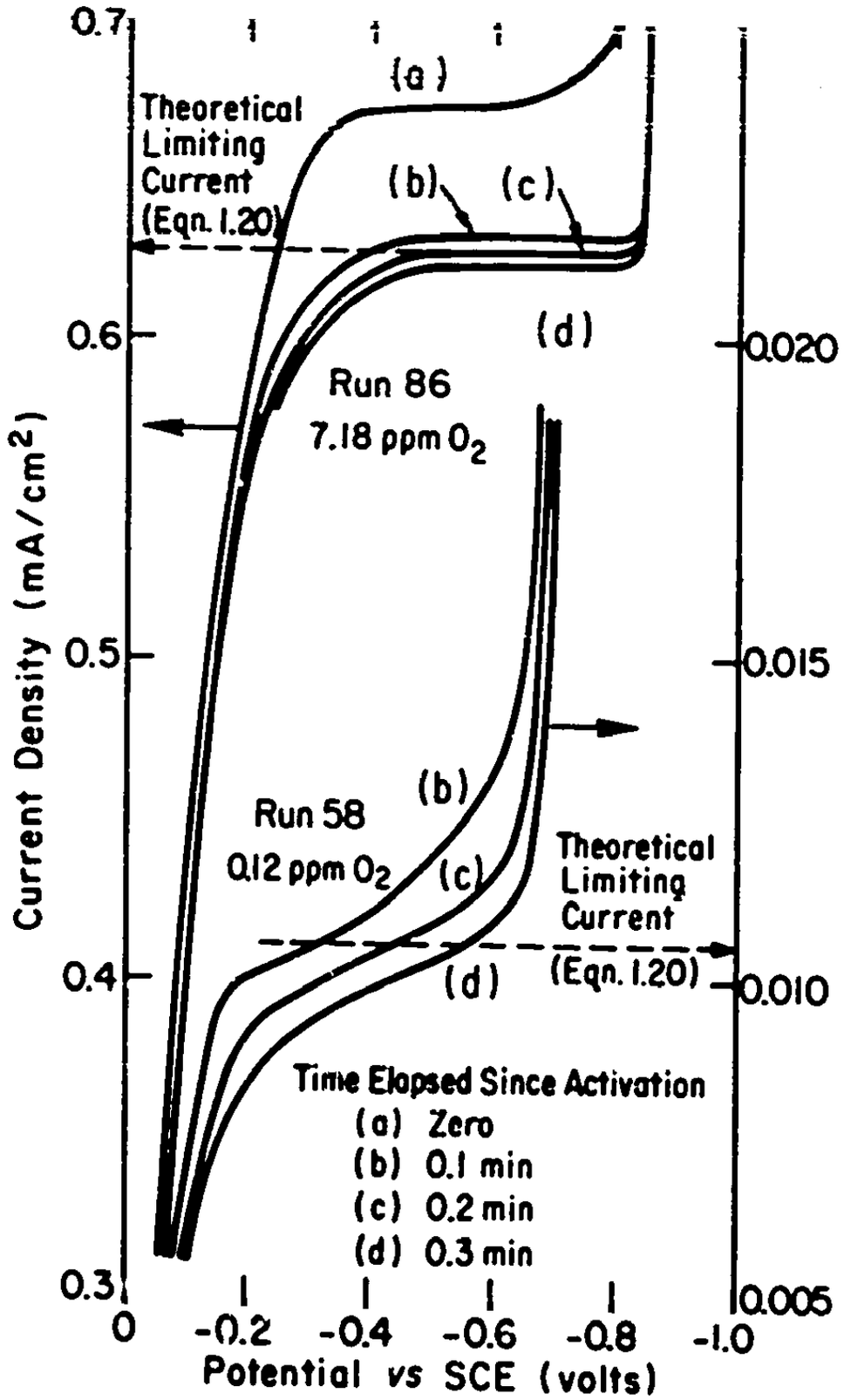

Figure 3.3. Variation in Shape of Polarization Curve with Time Elapsed Since Activation.

above the theoretical value.

Using a time of 0.3 min. the plateau occurs at too low a current. This latter effect is of less importance at a "high" O_2 concentration of 7 ppm than at the lower, 0.12 ppm, level. The optimum time at which to read the current is seen to be at, or very close to, 0.2 min. for a wide range of O_2 concentrations.

An empirical means of "correcting" the current decay curve to eliminate the initial transient, was investigated. When the electrode was held at the rest potential the current decayed from a non-zero value to a steady-state value of zero within about 0.2 min. It was thought that if this rest-potential transient were subtracted from the current decay curves obtained at more cathodic potentials these latter curves might be flattened to such an extent that the corrected current immediately after anodization would be equal to the theoretical limiting current. Fig. 3.4 shows some corrected decay curves. They are somewhat flattened, but not to the necessary extent.

The question of what happens at a platinum electrode during anodic activation, and the extent to which various factors contribute to the subsequent decay in current, are very complex. They will be discussed more fully in Chapter 4. The remainder of this chapter will be devoted to polarization and kinetic

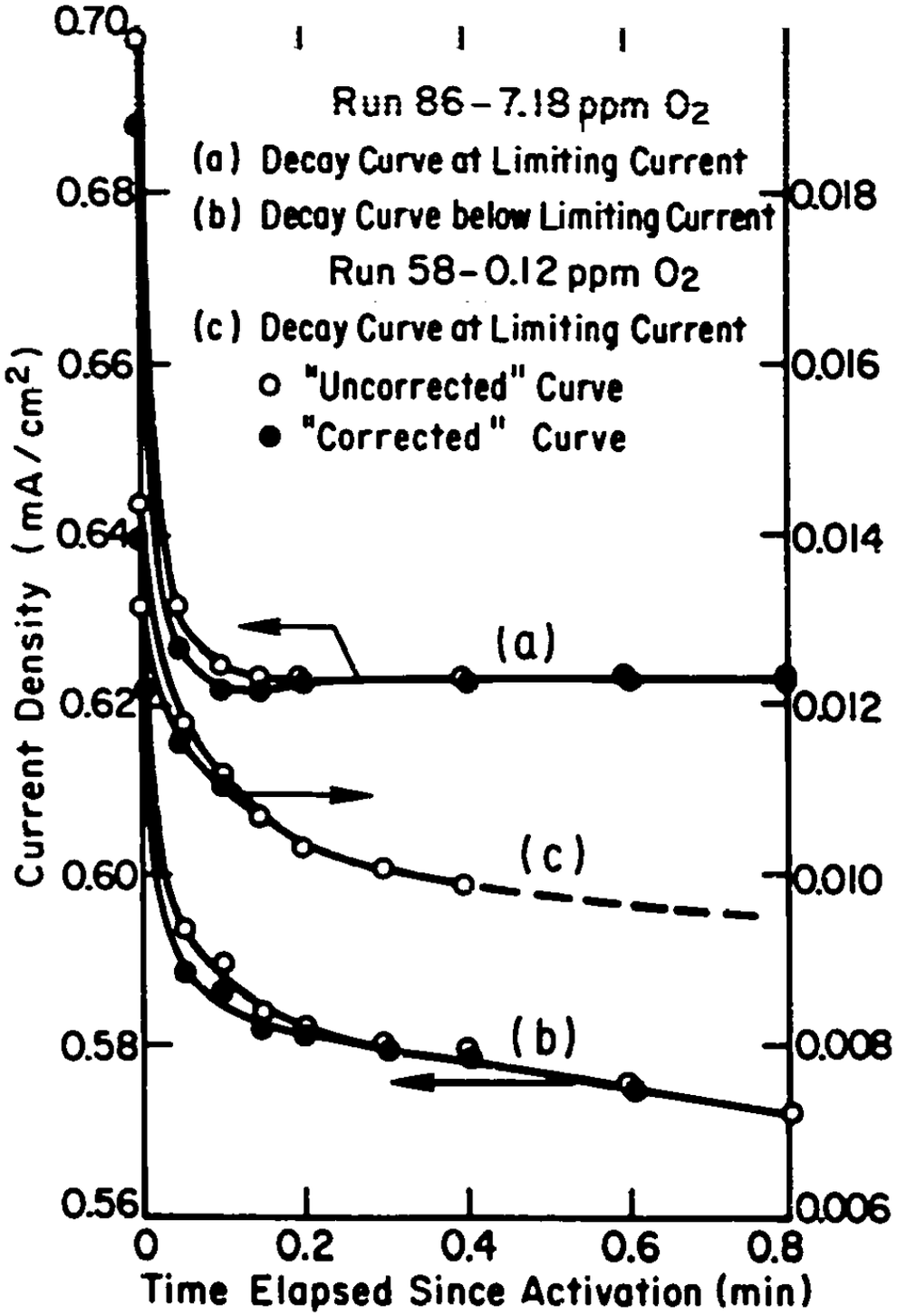

Figure 3.4. Correction of Current Decay Curves by Subtraction of Rest-Potential Decay Curve.

data obtained at a platinum RDE.

3.3. Polarization Data

3.3.1. 3.5% NaCl Solution

After a well-defined polarization curve had been consistently obtained for an air-saturated NaCl solution, as described in section 3.2., the O_2 concentration was reduced approximately fourfold. Figure 3.5 shows the polarization curve obtained at an O_2 concentration of 1.7 ppm (upper curve). The limiting current plateau was not as well defined as at the higher O_2 level. However, the current at the inflection point of the curve was within 2% of the theoretical value.

The polarization curve obtained at 0.77 ppm O_2 (Fig. 3.5 , lower curve) was similar in shape to the curve for 1.7 ppm O_2. The slope in the limiting current region of the former curve is decreased because of the compression of the vertical axis. The current at the point of inflection of this curve was again very close to the theoretical value.

At an O_2 concentration of 0.12 ppm the polarization curve (Fig. 3.6) was markedly S-shaped. This also occurred at 0.07 ppm O_2, (Fig. 3.7) the lowest concentration used in this series of experiments. In each case, however, the current at the inflection point was within a few percent of that predicted by the Levich equation. At any given O_2 concentration the

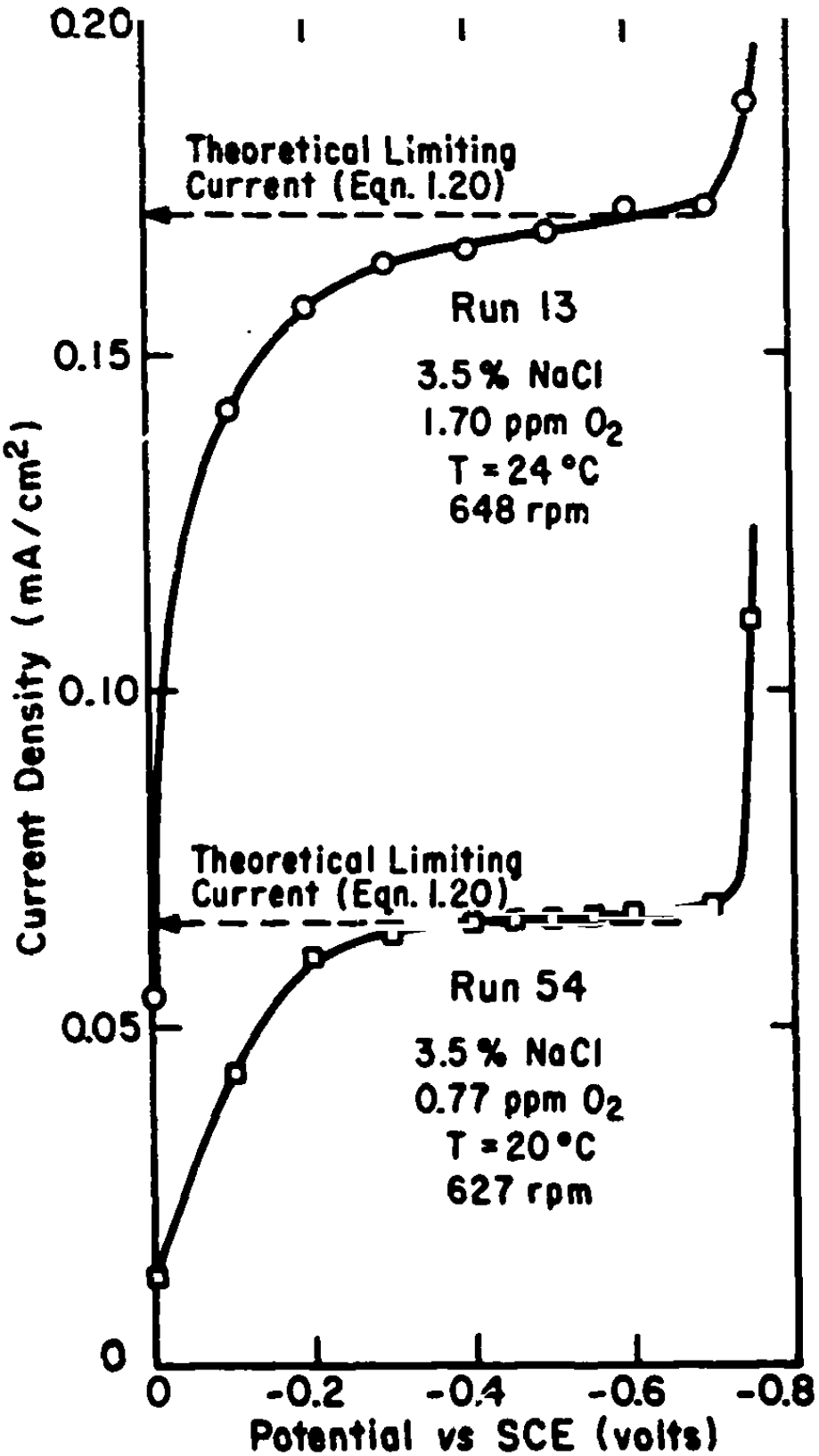

Figure 3.5. Polarization Curves for Oxygen Reduction at an Activated Platinum RDE in NaCl Solution at 1.7 ppm O_2 (upper curve) and 0.77 ppm O_2 (lower curve).

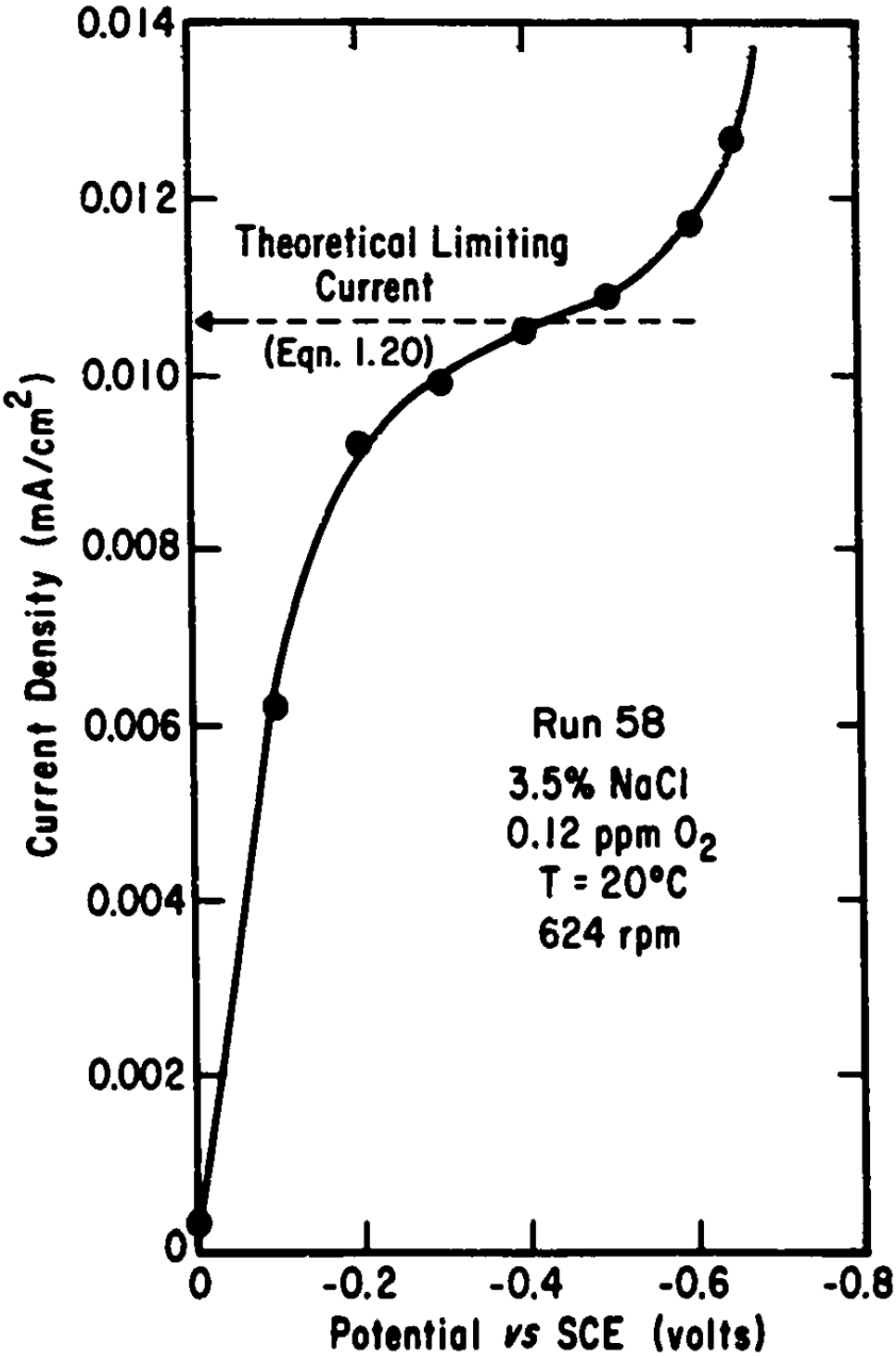

Figure 3.6. Polarization Curve for Oxygen Reduction at an Activated Platinum RDE in NaCl Solution at 0.12 ppm O_2.

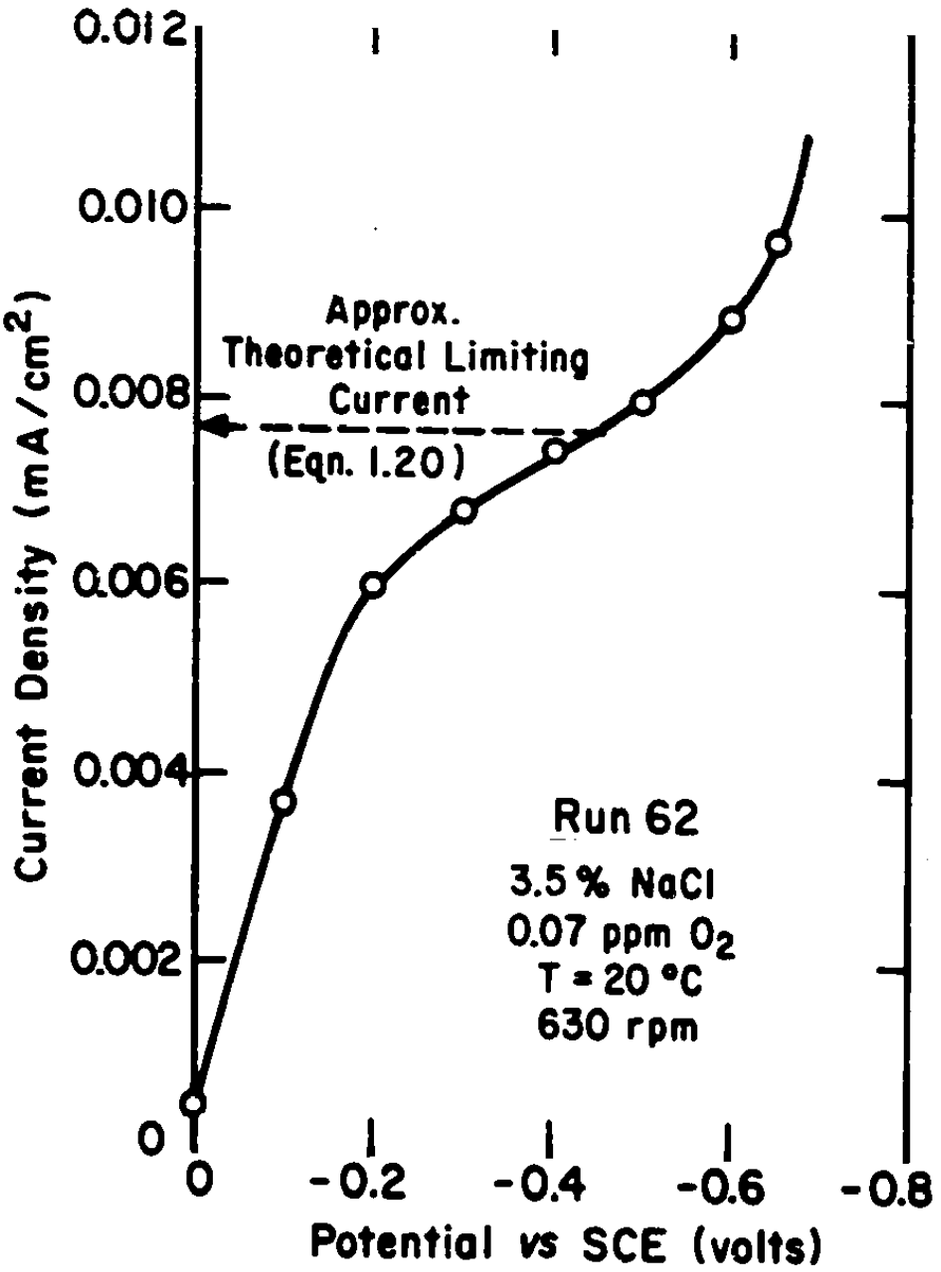

Figure 3.7. Polarization Curve for Oxygen Reduction at an Activated Platinum RDE in NaCl Solution at 0.07 ppm O_2.

inflection point always occurred within about ± 30 mV of a fixed potential. This potential was a function of O_2 concentration, as explained in Section (3.7.)

3.3.2. Seawater

In air-saturated seawater the polarization curve obtained (Fig. 3.8) was very similar to that obtained in air-saturated 3.5% NaCl solution (Fig. 3.2). The limiting current plateau was well-defined and the limiting current obtained was within 1-2% of the theoretical value. Apparently, then, at the 7.2 ppm O_2 level the many organic and inorganic constituents of seawater did not interfere with O_2 reduction at the RDE. Note, however, that H_2 evolution commenced at a more anodic potential in seawater (Run 75) than in NaCl solution (Run 66). Reasons for this are discussed in Section 3.7.

The O_2 concentration was then lowered by almost two orders of magnitude. At 0.09 ppm O_2 (Fig. 3.9) in seawater the polarization curve was again similar in shape to that obtained in 3.5% NaCl. However, the current at the point of inflection on the seawater polarization curve was consistently about 20% higher than the theoretical current.

Part of this discrepancy can be accounted for by comparing the current due to reduction of certain

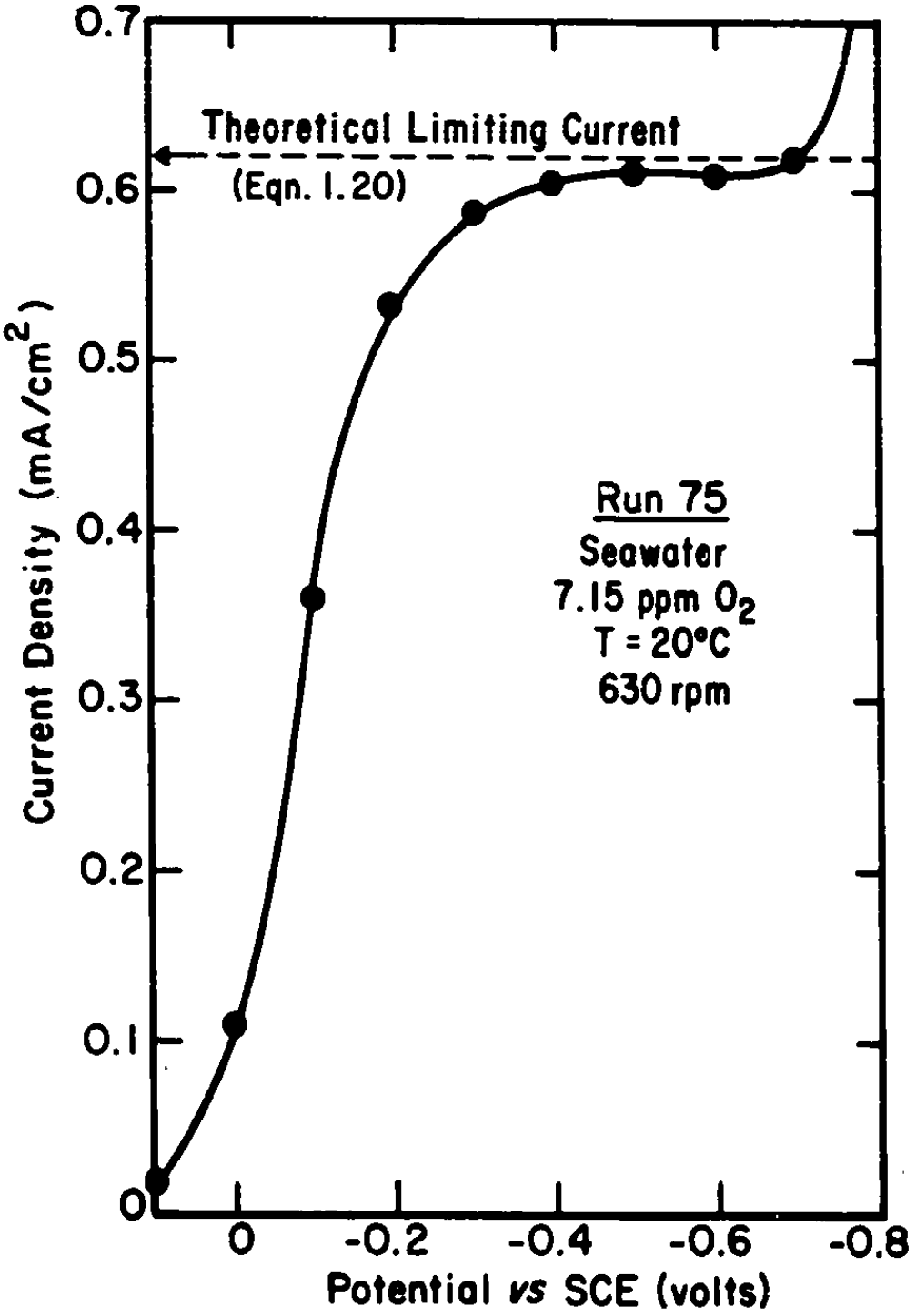

Figure 3.8. Polarization Curve for Oxygen Reduction at an Activated Platinum RDE in Air-saturated Seawater.

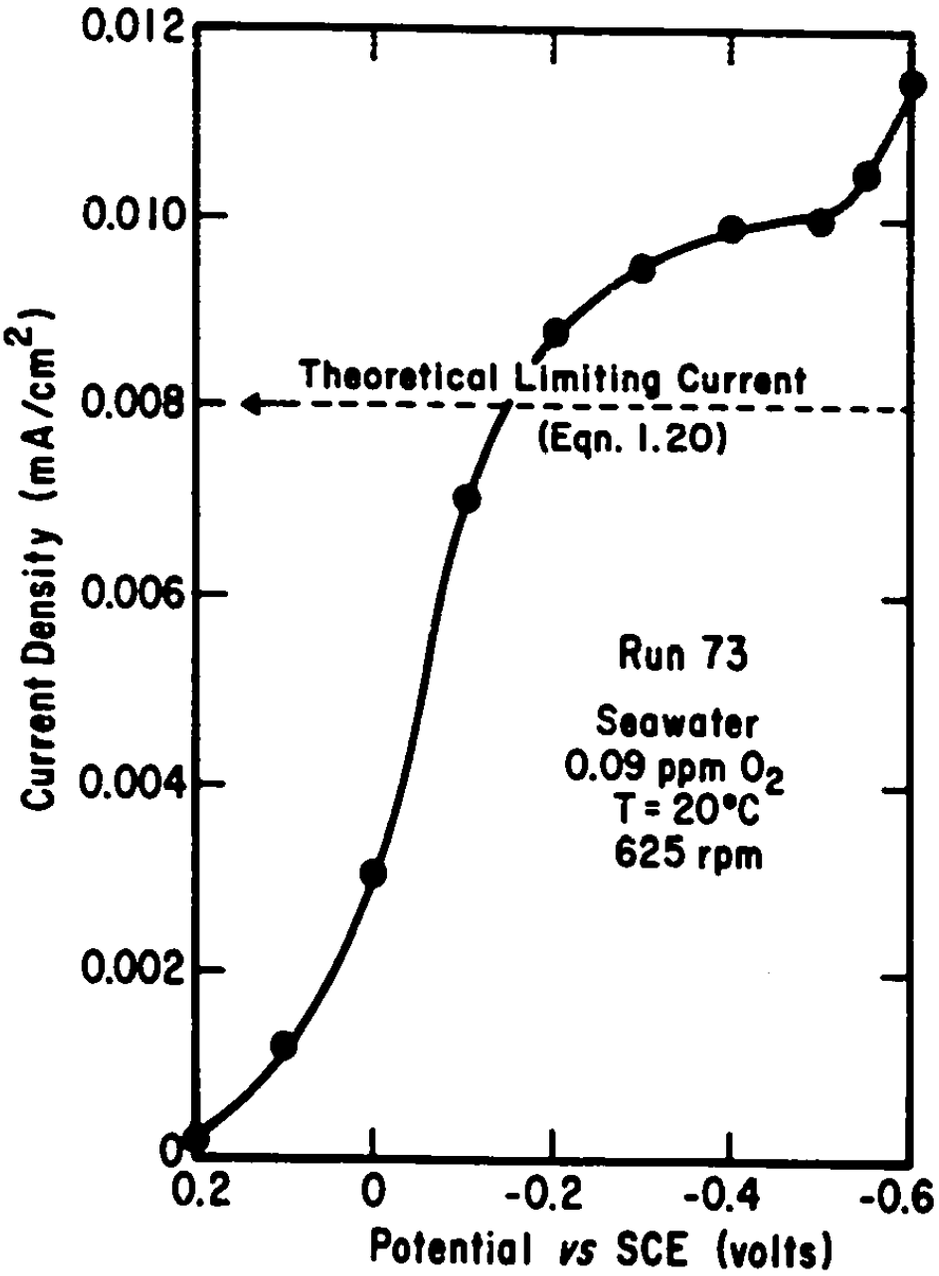

Figure 3.9. Polarization Curve for Oxygen Reduction at an Activated Platinum RDE in Seawater at 0.09 ppm O_2.

ionic species in seawater with the O_2 reduction current. The ionic species expected in seawater which are reducible in the same range of potentials as O_2 are Cu^{+2}, As^{+3}, Fe^{+3}, and Pb^{+2}. The limiting current for the reduction of any species in solution is approximately proportional to $D_i^{2/3} n_i C_i^b$. The relatively small effect of diffusivity on the other terms in the Levich equation is neglected here. Unfortunately the concentrations of these trace ionic species, in fresh seawater, vary; they may also increase in seawater which is processed in copper or steel equipment. However, the range of concentrations in which they are usually found in seawater can be used to estimate their maximum and minimum contributions to the RDE current at the 0.09 ppm O_2 level.

The calculations are summarized below in Table 3.1. The diffusivities of all the ions are assumed to be approximately equal to that of Cu^{+2}, viz, 6×10^{-6} cm^2/sec.(Selman, 1971).

TABLE 3.1.

Contribution of Reducible Ionic Species to the Limiting Current in Seawater

REDUCIBLE SPECIES	C_i^b (mg.atoms/1.) x 10^3 Min.	Max.	n_i	$D_i^{2/3}$ x 10^3	$C_i^b n_i D_i^{2/3}$ Min.	Max.
Cu^{+2}	0.02	0.20	2	0.33	0.013	0.132
As^{+3}	0.15	0.30	3	"	0.149	0.297
Fe^{+3}	0.03	0.30	1	"	0.010	0.100
Pb^{+2}	0.02	0.02	2	"	0.013	0.013
O_2	2.80		4	0.74	8.29	

By adding known amounts of Fe^{+3} and Cu^{+2} salts to NaCl solution it was confirmed experimentally that these ions are reduced in the potential range for O_2 reduction and that the value of $D_{Cu^{+2}} \sim D_{Fe^{+3}} \sim 6 \times 10^{-6}$ cm^2/sec. The maximum and minimum values of the ratio:

$$\sum_{\text{reducible ionic species}} c_i^b n_i D_i^{2/3} \Big/ \sum_{\text{reducible ionic species} + O_2} c_i^b n_i D_i^{2/3}$$

are 0.061 and 0.022 respectively. The maximum ionic contribution to the current at an O_2 conc. of 0.09 ppm is therefore about 6% which accounts for about 30% of the observed discrepancy between the experimental and theoretical currents. At least 70% and as much as 90% of this discrepancy, therefore, must be attributed to reducible organics present in the seawater, or to other causes.

3.4. Kinetic Data Obtained in Oxygen-Containing Solutions

3.4.1. Air-saturated, 3.5% NaCl Solution

A plot of limiting current vs. $\omega^{1/2}$ for a Pt RDE in air-saturated NaCl solution is shown in Fig. 3.10. All current readings were taken 0.2 minutes after activation of the RDE. As in Peters' work, this curve shows an increasing deviation from the theoretical straight line (eqn. 1.20) with increasing rotational speed. In the Introduction it was pointed out that

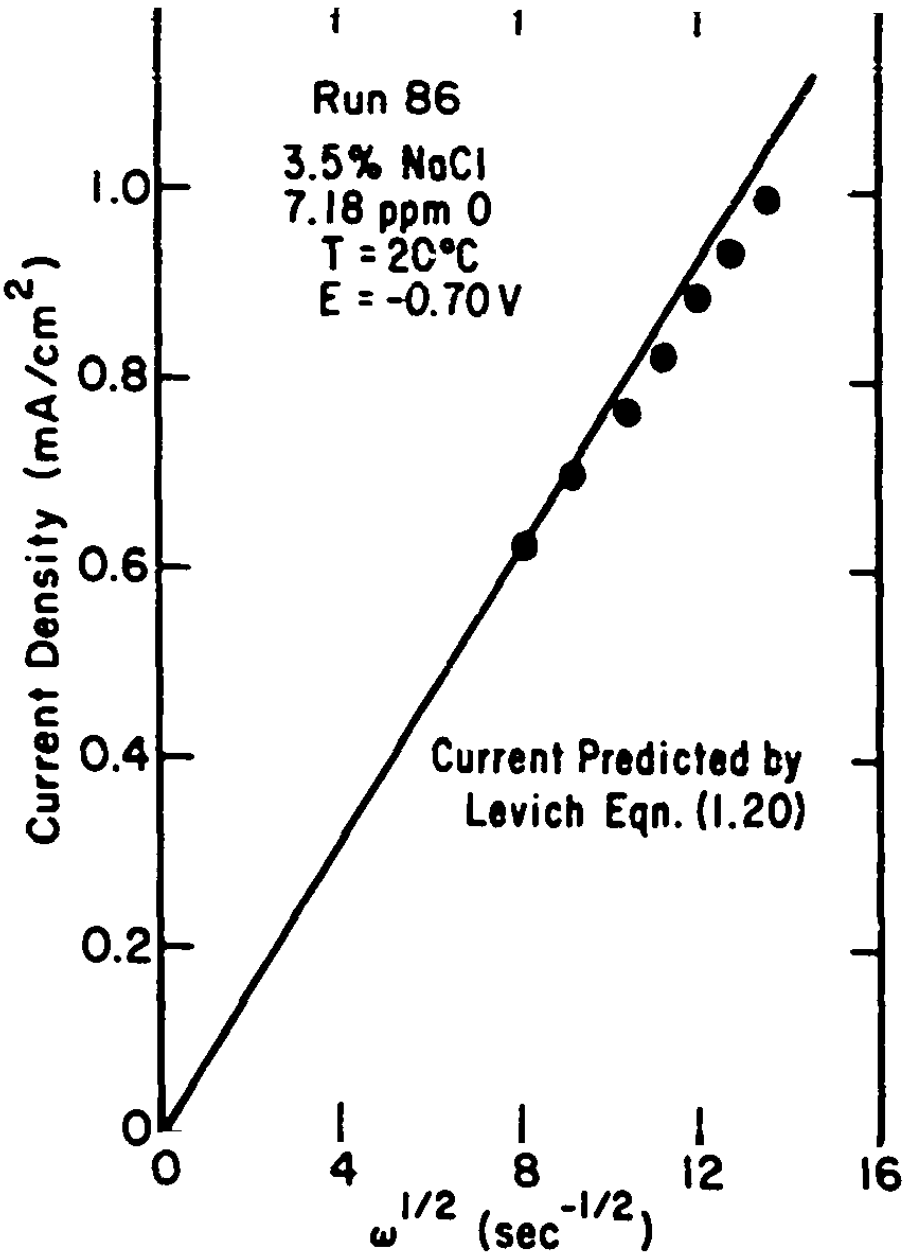

Figure 3.10. Dependence of i_{lim} on $\omega^{1/2}$ for Oxygen Reduction at an Activated Platinum RDE in Air-saturated NaCl Solution.

behavior of this type agrees well with a model in which H_2O_2 reduction is the rate-determining step in the overall reduction of O_2 to H_2O. Curves of i vs. $\omega^{1/2}$ were also measured for electrodes at which the current had reached steady state (declined electrodes) as follows: After the polarization curve had been measured for an activated electrode, as described in Section 3.1., the electrode was anodized and then held either at a potential slightly anodic to the H_2-evolution potential, in the case of air-saturated solutions, or at the inflection point potential, in the case of lower O_2 concentrations. The current was allowed to decay to a steady-state value. The rate of rotation of the RDE was then increased stepwise and the current corresponding to each rotational speed was recorded. The curves thus obtained are discussed in Section 4.3.

The reaction rate constant (k_3) for H_2O_2 reduction at an activated platinum surface was calculated using eqn. (1.23). The results are shown in Table 3.2 , in addition to those obtained in a similar experiment, and those obtained by Peters in air-saturated solution.

TABLE 3.2

Reaction Rate Constants for H_2O_2 Reduction in Air-saturated NaCl Solution

$\omega^{1/2}$ (sec.$^{-1/2}$)	k_3(cm./sec.) Run 83	Run 86	Peters(1970)
8.2			0.127
9.3	0.308*	0.192*	0.118
10.35	0.119	0.115	0.118
11.3	0.232*	0.105	
12.1	0.101	0.115	0.110
12.9	0.110	0.106	
13.65	0.112	0.103	
Mean	0.110±0.009	0.109±0.006	0.118±0.008

When calculating mean k_3 values the spurious results indicated by asterisks were rejected. This is justified in the case of the lower values of ω since at small ω the experimental current was very close to the theoretical value. Close inspection of Eqn. (1.23) will confirm that small errors in the experimental value of i_{lim} can lead to relatively large errors in the calculated value of k_3 under these conditions.

The k_3 values obtained in this study agree closely with each other, and also agree quite well with those of Peters. The value of the H_2O_2 diffusion coefficient used in calculating k_3 differed from that

used by Peters, as explained in Section 3.5.2. Peters' k_3 values were corrected for this difference in diffusion coefficient for inclusion in Table 3.2.

3.4.2. Air-saturated Seawater

A plot if i_{lim} vs. $\omega^{1/2}$ for air-saturated seawater (Fig. 3.11) is similar to that obtained with NaCl solution. Rate constants for H_2O_2 reduction were calculated and are summarized in Table 3.3. They are somewhat lower than those obtained for the NaCl solution, especially in the case of Run 65. A detailed discussion of this subject appears in Section 3.6.

3.4.3. Low O_2 Concentrations in NaCl Solution.

Figure 3.12 shows the dependence of i_{lim} on $\omega^{1/2}$ at an O_2 concentration of 0.12 ppm. This plot is similar in shape to that obtained in air-saturated solution.

Reaction rate constants evaluated at 0.77 ppm and 0.12 ppm O_2 are listed in Table 3.3. These values are significantly lower than those measured in the same medium at air-saturation. This implies that the rate constant for H_2O_2 reduction is dependent on the oxygen concentration in the bulk of the solution, a result also obtained by Peters (1970). This in turn suggests that the reaction rate constant is dependent on the H_2O_2 concentration near the RDE surface, since

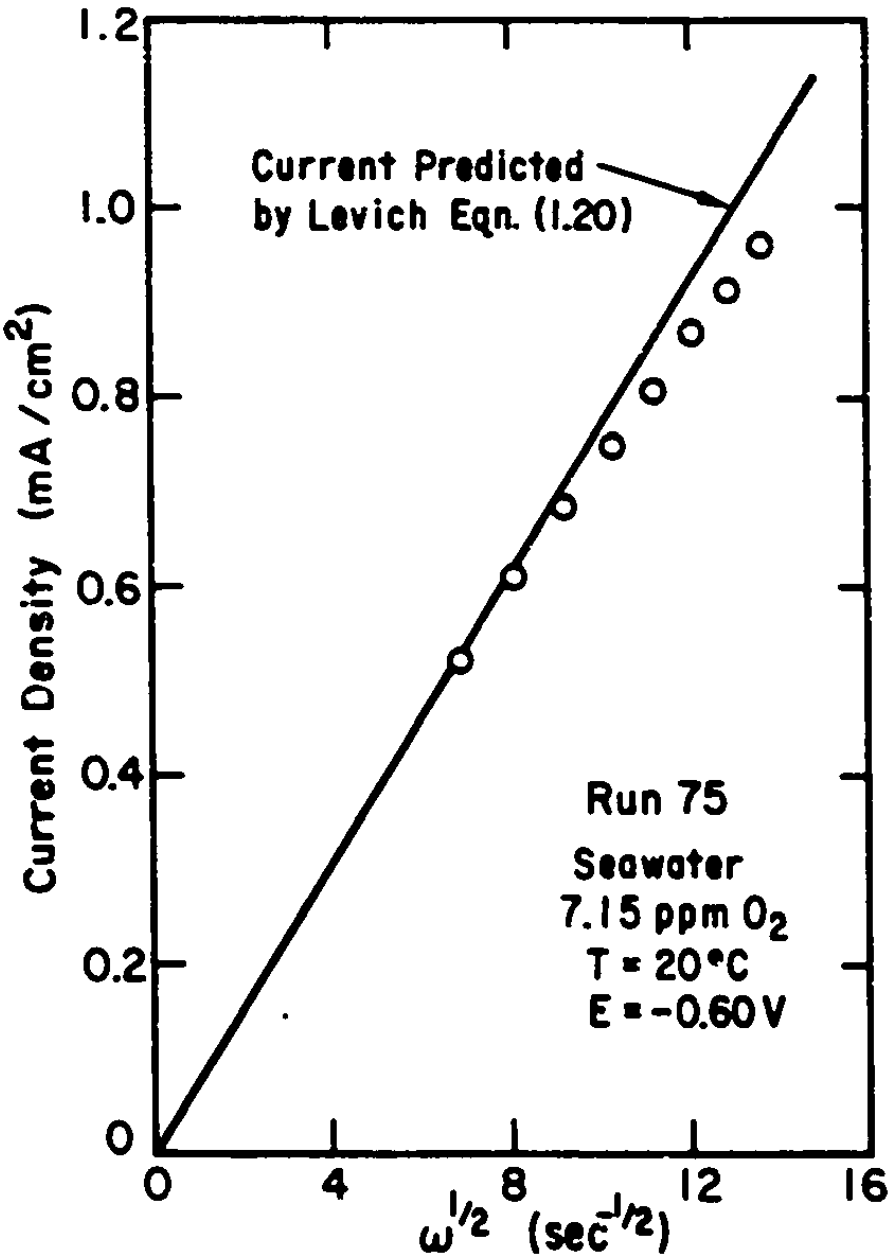

Figure 3.11. Dependence of i_{lim} on $\omega^{1/2}$ for Oxygen Reduction at an Activated Platinum RDE in Air-saturated Seawater.

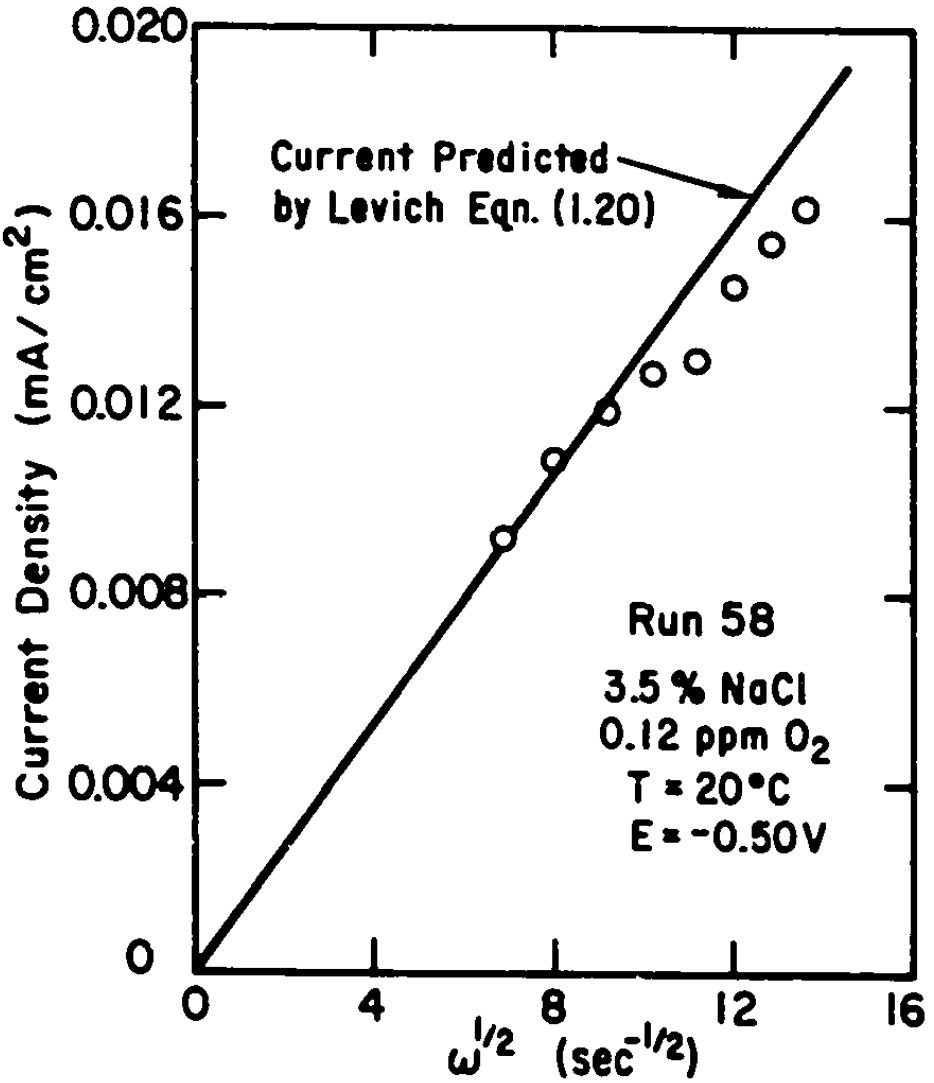

Figure 3.12. Dependence of i_{lim} on $\omega^{1/2}$ for Oxygen Reduction at an Activated Platinum RDE in NaCl Solution at 0.12 ppm O_2.

TABLE 3.3

Summary of H_2O_2 Reaction Rate Constants Measured Experimentally and Found in the Literature.

SOURCE	MEDIUM	O_2 CONCENTRATION (ppm)	k_3 (cm./sec.)	POTENTIAL (VOLTS VS. SCE UNLESS OTHERWISE STATED)
Run 83	3.5% NaCl	7.18 (Air-sat.)	0.110 ± 0.01	-0.70
Run 86	"	7.18 "	0.109 ± 0.01	-0.70
Peters (1970)	"	6.55 "	0.118 ± 0.008	-0.80
Run 65	Seawater	7.15 "	0.060 ± 0.005	-0.60
Run 75	"	7.15 "	0.073 ± 0.01	-0.60
Run 56	3.5% NaCl	0.77	0.063 ± 0.006	-0.60
Run 58	"	0.12	0.058 ± 0.01	-0.50
Run 80	3.5% NaCl	~0.03 ppm O_2 + 1.59 10^{-4}M H_2O_2	0.118 ± 0.006	-0.65
Run 81	"	~0.03 ppm O_2 + 3.08 10^{-5}M H_2O_2	0.034 ± 0.001	-0.60
Muller & Nekrasov (1965)	0.125N KOH (v. pure)	Saturated with O_2	0.036 ± 0.005 0.089 ± 0.008	+ 0.1 vs NHE + 0.5 vs NHE
Damjanovic et al. (1967b)	0.1M KOH (v. pure)	"	~0.07	0.0 vs NHE

one H_2O_2 molecule is formed at the RDE for every O_2 molecule being reduced. It thus appeared appropriate to include in this study of O_2 reduction an investigation of H_2O_2 reduction as well.

3.5. Kinetic Data Obtained in H_2O_2 Solutions

3.5.1. Choosing Appropriate H_2O_2 Concentrations

Because of the apparent dependence of the H_2O_2 reduction rate constant on H_2O_2 concentration it was thought that kinetic data measured in H_2O_2 solutions should be measured under similar conditions of H_2O_2 surface concentration to those which were present in the O_2 solutions. Every mole of O_2 reaching the RDE in an O_2 solution gives one mole of H_2O_2, if 4-electron reduction is neglected. In the H_2O_2/3.5% NaCl solutions used, therefore, O_2 was replaced by H_2O_2 on a one-to-one molar basis. This technique was only approximate. The error, caused by neglecting the fact that 4-electron reduction would reduce the amount of H_2O_2 being produced at the RDE surface in O_2 solution, is cancelled to an indeterminate extent by the fact that $D_{H_2O_2} < D_{O_2}$.

It may be of interest to point out that in Run 83, the surface H_2O_2 concentration, calculated by substituting the calculated k_3 value of 0.11 in eqn. 1.35.($f=1$, $k_4=0$) was 1.6×10^{-7}M. By contrast,

the O_2 concentration in Run 83 was 2.2×10^{-4}M, three orders of magnitude larger.

3.5.2. Polarization Data and Rate Constants for H_2O_2 Reduction in H_2O_2 Solutions

The polarization curves measured at two H_2O_2 concentrations are shown in Fig. 3.13. The H_2O_2 concentration of Run 80 was 1.89×10^{-4}M, corresponding on a molar basis to an O_2 concentration of 5.1 ppm, about 75% of air-saturation. That of Run 81 corresded to an O_2 concentration of 1 ppm.

No plateaux were observed in these curves, but points of inflection did occur. The currents at these points were assumed to be limiting currents, analogous to the situation in O_2 solutions, and were so recorded.

It was difficult to check the experimental results with the theory because the diffusivity of H_2O_2 in saline media is not well-known. Schumb (1955) quotes a range of values between 0.9 and 1.59×10^{-5} $cm.^2/sec.$ in H_2O. Myuller and Nekrasov (1964) found $D_{H_2O_2}$ in 1N H_2SO_4 to be 1.6×10^{-5} $cm.^2/sec.$ The limiting currents recorded in Runs 80 and 81 were used to estimate the diffusivity of H_2O_2 in 3.5% NaCl at 20°C. The polarization curves were corrected for trace O_2 before $D_{H_2O_2}$ was calculated, and it was assumed that the current for H_2O_2 reduction was

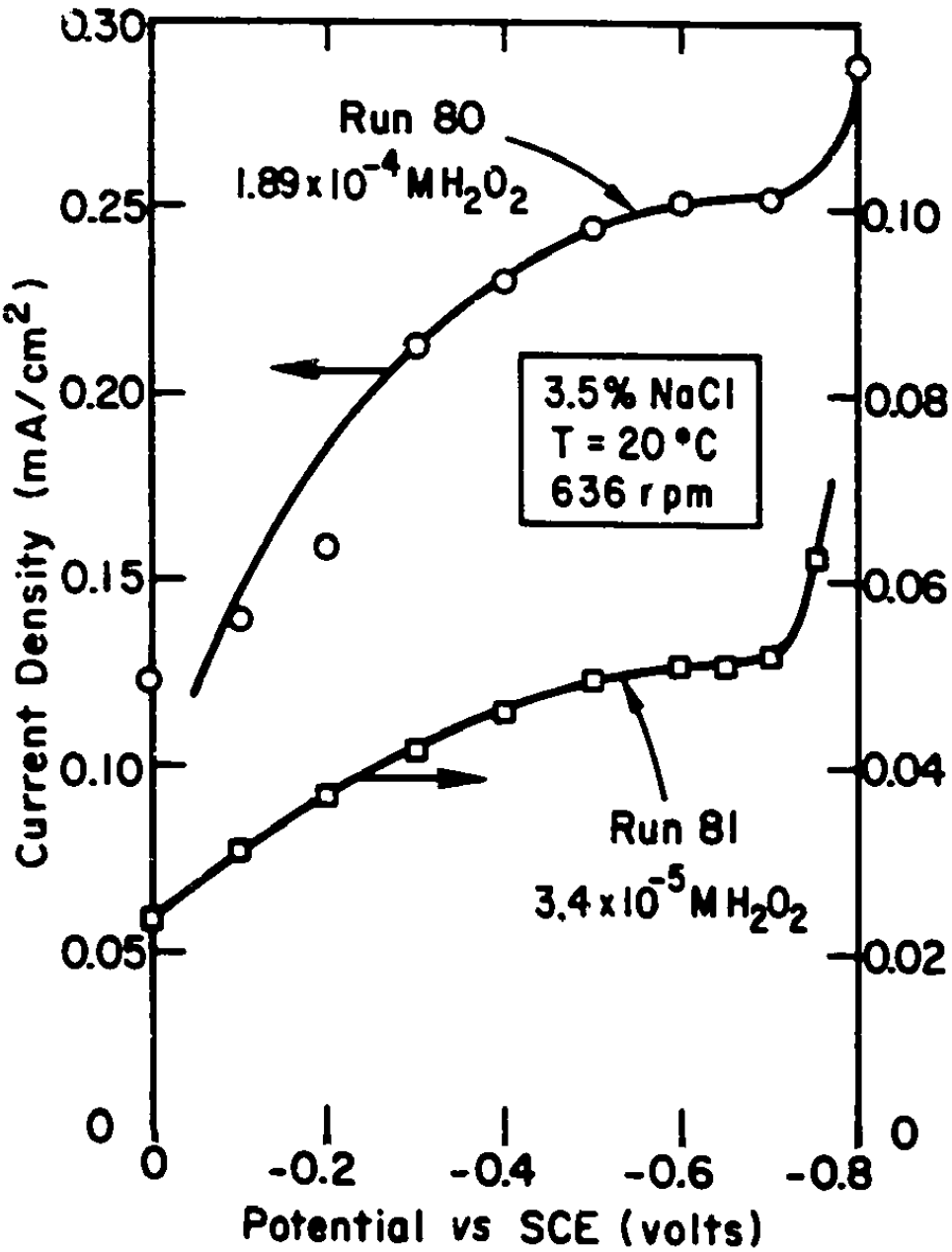

Figure 3.13. Polarization Curves for H_2O_2 Reduction at an Activated Platinum RDE in NaCl Solution; Upper Curve: 1.89×10^{-4} M H_2O_2, Lower Curve: 3.4×10^{-5} M H_2O_2.

equal to that predicted by the Levich equation. The values obtained were 1.65×10^{-5} and 1.68×10^{-5} cm.^{2}/sec., respectively. These values are higher than those quoted by Schumb, and the value of 1.3×10^{-5} used by Peters (1970), but agree well with those of Myuller and Nekrasov (1964), in 1N H_2SO_4.

It is possible that the currents measured in Runs 80 and 81 were somewhat below those corresponding to pure diffusion limitation, because of slow H_2O_2 reduction. The calculated values of $D_{H_2O_2}$ may therefore be a little low, but are probably not high. Since the 3.5% NaCl medium (0.61N in NaCl) was more similar in ionic content to 1N H_2SO_4 than the H_2O, and the temperatures were also similar, the agreement between the $D_{H_2O_2}$ values found in this study, and the value found by Myuller and Nekrasov, is reasonable to expect. Accordingly, the value $D_{H_2O_2} = 1.65 \times 10^{-5}$ cm./sec. was used when calculating k_3 from experimental data.

Curves of i_{lim} vs. $\omega^{1/2}$ for Runs 80 and 81 are shown in Fig. 3.14. They are similar in shape to those obtained in O_2 solutions. The H_2O_2 reduction rate constant was calculated from these data using eqns. 1.38 and 1.40. The results are summarized in Table 3.4., and in Table 3.3 , are listed with those obtained in O_2 solutions.

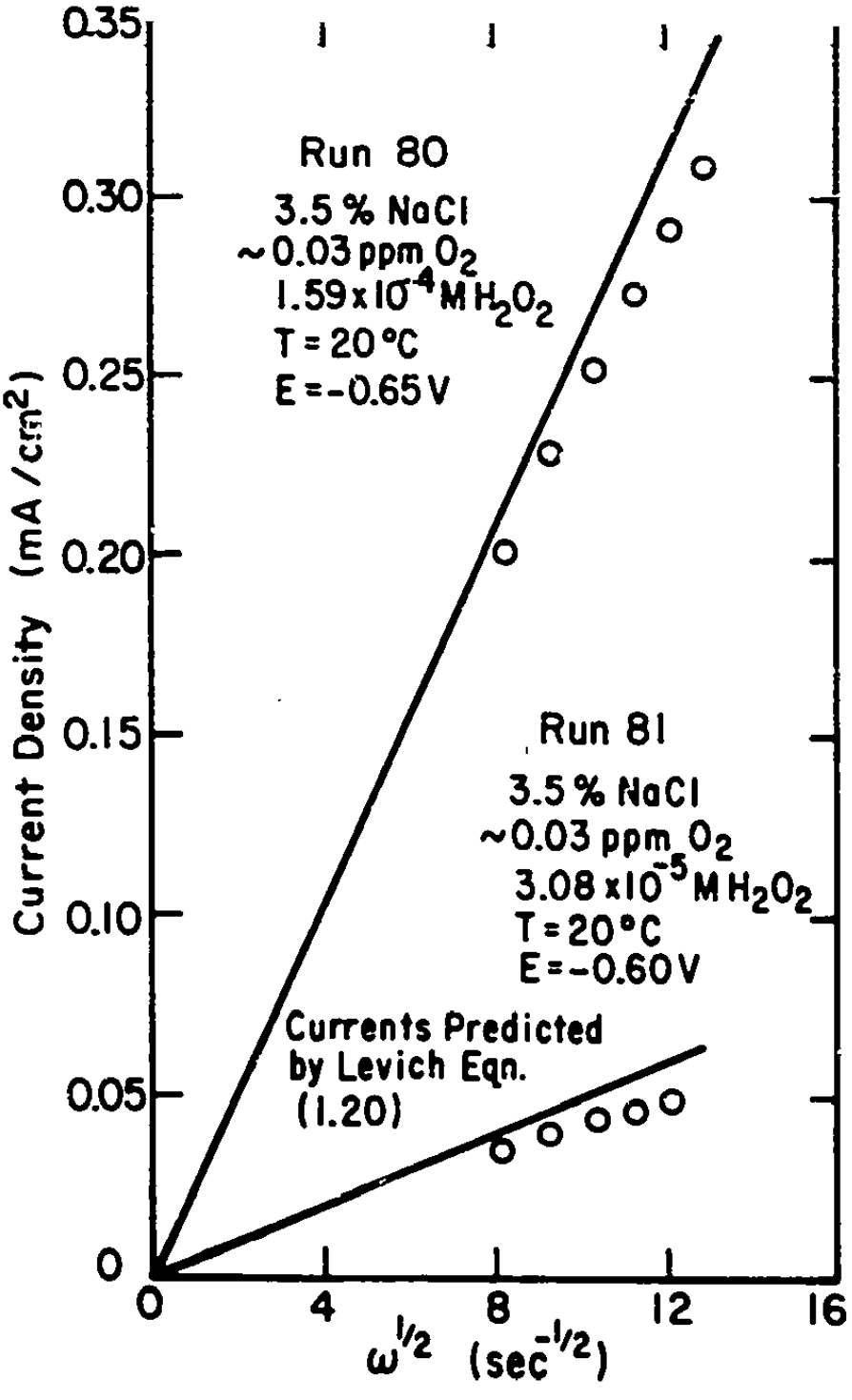

Figure 3.14. Dependence of i_{lim} on $\omega^{1/2}$ for H_2O_2 Reduction at an Activated Platinum RDE in NaCl Solution.

TABLE 3.4.

Rate Constants for H_2O_2 Reduction in H_2O_2 Solution

H_2O_2 CONCENTRATION	O_2 EQUIVALENT	k_3 (cm/sec)	SOURCE
1.59×10^{-4}M	5.1 ppm	0.118±0.006	Run 80
3.08×10^{-5}M	1.0 ppm	0.034±0.001	Run 81

The result obtained at the higher H_2O_2 concentration is very close to those obtained in air-saturated solution. This lends some support to the reaction model used in the latter case. The value obtained at the lower H_2O_2 concentration is lower than might be expected on the basis of the concentration dependence observed in O_2 solutions. This may be a consequence of neglecting 4-electron O_2 reduction and catalytic H_2O_2 decomposition, and is discussed in the next section.

3.5.3. Effect of Using an Expanded Reaction Model to Calculate the H_2O_2 Reduction Rate Constant

In this section expressions are derived for comparing the value of k_3 calculated using the simplified reaction model with the value of k_3 from the expanded reaction model, eqn. (1.22). Details of the intermediate steps in the derivations which follow are shown in Appendix B.

Two cases will be considered: that of a solution containing O_2 and a negligible amount of H_2O_2, and that of a solution containing H_2O_2 and a negligible amount of O_2. The case of a solution containing both O_2 and H_2O_2 involves some complex algebraic expressions and was not treated since it would appear to lead to intermediate results.

(a) $\underline{H_2O_2}$ Concentration Negligible Compared to $\underline{O_2}$ Concentration

The value of k_3 based on the expanded model is found by rearranging eqn. 1.41. to give

$$k_{3,exp} = \frac{\left(\frac{K_{H_2O_2}}{f}\right)^{1/2} - 1}{\frac{1}{2F_w^{1/2}K_{O_2}C_{O_2}^b} - (2-f)} - k_4\left(1-\frac{f}{2}\right) \qquad (3.1)$$

The value calculated using the simplified reaction model ($k_{3,simp}$) is found by setting f=1 and k_4=0. From 3.1

$$k_{3,simp} = \frac{\left(K_{H_2O_2}\right)^{1/2} - 1}{\frac{1}{2F_w^{1/2}K_{O_2}C_{O_2}^b} - 1} \qquad (3.2)$$

In the discussion which follows, variations in the term

$$R = \frac{k_{3,simp}}{k_{3,exp}} \qquad (3.3)$$

as a function of $\omega^{1/2}$, will be discussed in an attempt to determine which of the two alternative reaction schemes, 1.22. or 1.22.A, best describes the O_2 reduction mechanism applicable under the conditions of this study.

Let us first consider the case where f=1 but $k_4 \neq 0$. R is then given by

$$R = 1 + \frac{k_4}{2k_{3,exp}} \qquad (3.4)$$

Equation (3.4) predicts that, for a given value of k_4, the value of R is independent of ω. Experimental i_{lim}-$\omega^{1/2}$ data therefore cannot enable one to distinguish between the expanded and simplified reaction models.

Now let us assume that f<1, with the result that

$$R = \frac{1 + \frac{k_4}{k_{3,exp}}\left(1 - \frac{f}{y}\right)}{A/B} \qquad (3.5)$$

where A and B are as defined in Appendix B. Values of R have been calculated for the two cases $k_4=0$ and $k_4=k_{3,exp}$, and are listed in Table B.1. as functions of f and $\frac{2i}{i_{theor}}$. The term $\frac{2i}{i_{theor}}$ is inversely

proportional to the extent to which the measured current differed from that predicted by the Levich equation (1.20), and varied typically from about 1.95 to about 1.80 as ω increased from 64 to 160 sec^{-1}.

Considering first the case of $k_4=0$ it can be seen that R increases as $\frac{2i}{i_{theor}}$ decreases, i.e., as ω increases. The extent of this increase in R over a given range of values of $\frac{2i}{i_{theor}}$, becomes greater as f decreases. Table B.1. also shows that the effect of $k_4>0$ is to increase the value of R by a fixed proportion, but not to affect the ω-dependence of R. This can also be deduced from eqn. (1.5).

The foregoing discussion may be summarized as follows: If the value of k_3 calculated using the simplified model (eqn. 1.22.A) does not vary with increasing ω it can be concluded that 4-electron reduction occurs to a negligible extent; no conclusions can be drawn as to the rate of catalytic H_2O_2 decomposition relative to that of electrochemical H_2O_2 reduction. If the calculated value of k_3 increases as ω increases the value of f can be estimated from the extent of this increase in k_3, using Table B.1. The greater the increase, the greater the extent to which 4-electron reduction occurs. Again, no conclusions can be drawn regarding k_4.

Table 3.5. summarizes the effects of increasing ω on the values of $k_{3,simp}$ which were used to calculate the mean values listed in Table 3.3.

TABLE 3.5.

Types of ω-dependence Observed in Calculating the H_2O_2-Reduction Rate Constant

SOURCE	EFFECT OF INCREASING $\omega^{1/2}$ on $k_{3,apparent}$
Run 83	Results scattered about a mean
Run 86	"
Peters(1970)	Slight decrease
Run 65	Results scattered about a mean
Run 75	"
Run 54	Slight decrease
Run 58	"

In only one run was a systematic increase in $k_{3,simp}$ observed with increasing ω. The extent of this increase was so great that no mean value of k_3 could be calculated for inclusion in the list of $k_{3,simp}$ values (Table 3.3.). The slight decrease in $k_{3,simp}$ for two of the runs listed in Table 3.5. was probably due to experimental error. From the results tabulated one can see that 4-electron O_2 reduction

occurred to a negligible extent under the experimental conditions of this study. The extent to which catalytic H_2O_2 decomposition occurred could not be estimated.

(b) O_2 Concentration Negligible Compared to H_2O_2 Concentration

$$i = \frac{2FK_{H_2O_2}C^b_{H_2O_2}}{1 + \frac{K_{H_2O_2}^{1/2}}{k_3 + k_4(1-\frac{f}{2})}} \qquad (3.6.)$$

from which k_3 is found to be

$$k_{3,exp} = \frac{K_{H_2O_2}^{1/2}}{\frac{1}{2FK_{H_2O_2}C^b_{H_2O_2}} - 1} - k_4(1-\frac{f}{2}) \qquad (3.7.)$$

when $f=1$ and $k_4=0$,

$$k_{3,simp} = \frac{K_{H_2O_2}^{1/2}}{\frac{1}{2FK_{H_2O_2}C^b_{H_2O_2}} - 1} \qquad (3.8.)$$

Combining (3.7) and (3.8),

$$R = 1 + \frac{k_4(1-\frac{f}{2})}{k_{3,exp}} \qquad (3.9)$$

Equation (3.9) indicates that R should be independent

of both - and the H_2O_2 concentration. When $k_4=0$ eqn. (3.9) reduces to

$$\frac{k_{3,apparent}}{k_{3,actual}} = 1 \qquad (3.10)$$

and 4-electron reduction becomes unimportant. This result is to be expected since, when $k_4=0$, no O_2 is produced by catalytic H_2O_2 decomposition.

From eqn. (3.9) it can be seen that, in the case of k_3 values measured in H_2O_2 solution, the experimental results cannot be used to distinguish between reaction models.

3.6. Correlation of k_3 Values With Electrode Potential

Because H_2O_2 reduction is an electrochemical reaction the possibility exists that the rate-determining elementary step in this reaction is a potential-dependent adsorption or desorption at the RDE surface. In such a case the reaction rate constant would be potential-dependent. Damjanovic, et al. (1967b) and Muller and Nekrasov (1965) found this to be the case, although there was considerable scatter in the results of the former.

Some of the results obtained by each of the above appear in Table 1.1. It may not be appropriate to compare their results with those obtained in this

study because of the considerable differences in pH, purity, and O_2 concentration. In view of these differences it is interesting that all the k_3 values listed in Table 3.3 vary over no more than a threefold range.

Logarithms of k_3 values obtained in this study were plotted against electrode potential (Fig. 3.15). The results of Damjanovic et al. and Muller and Nekrasov are also plotted, having been corrected approximately for the different pH at which they were evaluated, by a factor of 60mV/pH unit. Although most of the results of this study are higher than those of the other researchers the slope of a line of best fit would be equal to that of Damjanovic, et al. The high values obtained in this study can be explained by the expanded-reaction-model analysis of Section 3.5.3.

It is now clear that the apparent dependence of k_3 on O_2 or H_2O_2 concentration is merely a reflection of the fact that, as the O_2 or H_2O_2 bulk concentration decreased the potential corresponding to the point of inflection on the polarization curve became more anodic. The reason for this shift in potential will be explained in Section 3.7.

The potential-dependence of k_3 can be further illustrated by calculating k_3 values at an arbitrary potential of -0.30V using polarization data from

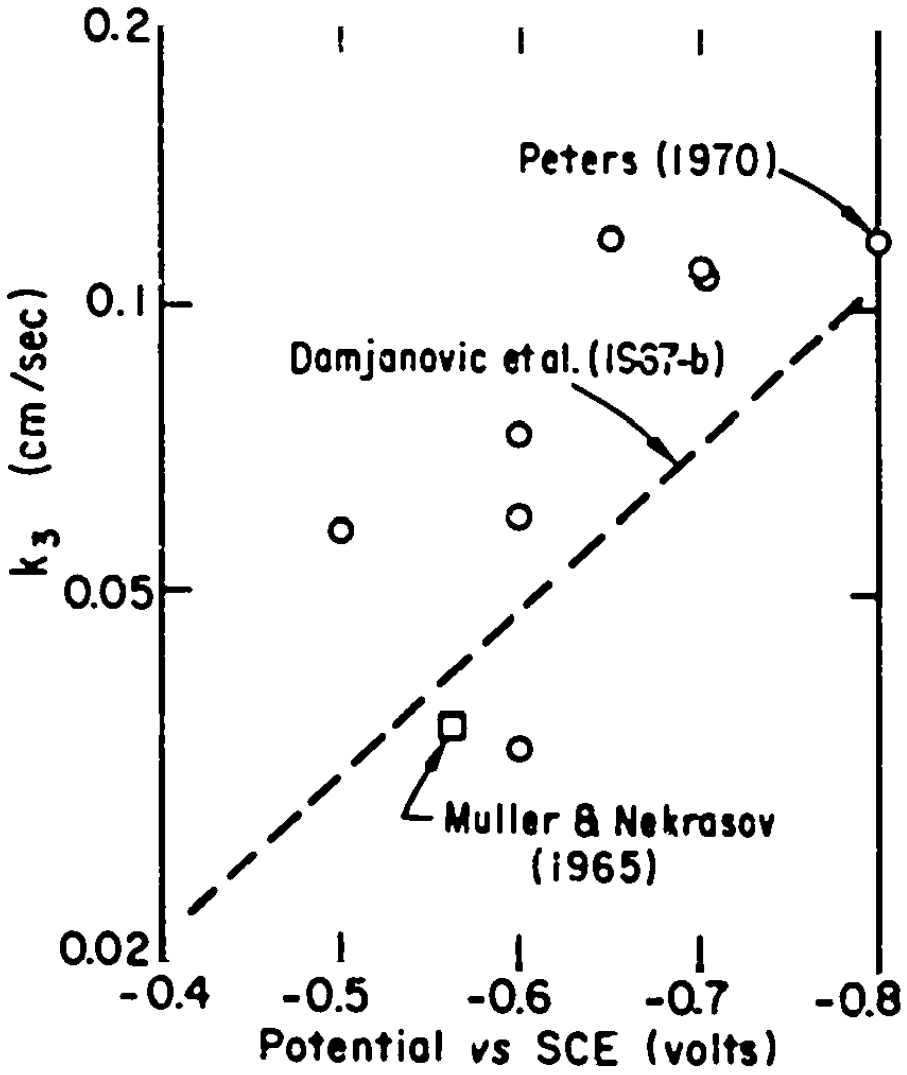

Figure 3.15. Dependence of H_2O_2 Reduction Rate Constant on Electrode Potential.

Runs 86, 54, 58, 80, and 81. All of these runs were made using 3.5% NaCl solution. The results of this calculation are listed in Table 3.6.

TABLE 3.6.

Rate Constants Calculated at an Electrode Potential of -0.30V

RUN	O_2 CONCENTRATION (ppm)	H_2O_2 CONCENTRATION	k_3 (cm./sec.)
86	7.18	0	0.079
54	0.77	0	0.037
58	0.12	0	0.045
80	~0.03	1.89×10^{-4} M	0.038
81	~0.03	3.4×10^{-5} M	0.043

These results are very susceptible to experimental error because each value was calculated using only one point on a polarization curve, rather than from five or six i-$\omega^{1/2}$ pairs, as was the case for the values listed in Table 3.3. In view of this limitation the agreement between the five calculated values is quite good.

3.7. Reasons for the Change in Shape of the Polarization Curve with Decreasing O_2 Concentration

The potential at which hydrogen evolution (reduction of H^+ ions) commences is dependent on the pH at the electrode surface. This potential is given by the Nernst equation, which can be written as

follows:

$$E^{\circ}_{H_2, a_{H^+} \neq 1} = 0 + \frac{RT}{2F} \ln a_{H^+} \qquad (3.11.)$$

Now, when O_2 is reduced at the electrode OH^- ions are produced or H^+ ions are consumed. This results in an increase in pH at the electrode surface, with respect to the pH in the bulk of the solution. At higher O_2 levels (e.g., air-saturation) hydrogen evolution occurs at a sufficiently cathodic potential so as not to obscure the limiting-current plateau for O_2 reduction. At lower O_2 concentrations less OH^- is produced at the electrode by O_2 reduction and the pH at the surface is therefore lower than in the case of, say, O_2 reduction in air-saturated solution. As eqn. (3.11.) shows, this shifts the value of $E^{\circ}_{H_2}$ to more anodic values. Eventually $E^{\circ}_{H_2}$ becomes so anodic that the limiting-current plateau is obscured. The net effect, as the H^+-reduction curve moves closer to the ascending portion of the O_2-reduction curve, is to make the measured polarization curve steeper with decreasing O_2 concentration. This explains the trend observed as one looks successively at Figs. 3.2., 3.5., 3.6., and 3.7.

It is perhaps a fortunate conincidence that the currents at the inflection points of those

polarization curves correspond to those predicted by the Levich equation. At a concentration of, say, 0.02 ppm O_2 one might find that the H^+-reduction curve overshadowed the O_2-reduction curve, leaving either no inflection point or one corresponding to a current far from the theoretical value. Moreover, had the NaCl solutions been of lower pH the shift in the H^+-reduction potential might have raised the lower limit at which the O_2 concentration was measurable using the inflection point, to a value considerably greater than the observed limit of about 0.05 ppm.

This argument suggests an explanation for the 20% error incurred when measuring O_2 concentrations in seawater using the points of inflection of polarization curves. The bicarbonate present in seawater is capable of acting as a buffer. This should result in a lower surface pH in seawater than in an NaCl solution of the same O_2 content. This difference in pH might shift the H^+-reduction curve to such an extent that the current at the inflection point includes an H^+-reduction current.

3.8. Long-term Use of a Platinum RDE as a Primary Standard for O_2 Measurement

As was mentioned earlier in this chapter a platinum RDE has the potential for use as a primary standard in measuring O_2 concentrations at the 0.1 ppm O_2 level in seawater. Rather than measuring an entire polariza-

tion curve for oxygen reduction, as was done in this study, it would be sufficient to measure the current using an activated electrode at a potential within ±50 mV of the inflection point potential, and then use eqn. (1.20) to calculate the approximate O_2 concentration. Continuous measurement of O_2 concentration would not be possible, because of the necessity for frequent reactivation of the electrode surface. However, it would be possible to make semi-continuous O_2 measurements at intervals of, say, 1 minute, using an automatic switching circuit to alternate the RDE potential to effect the activating and current-measuring processes described in Section 3.2.

Because of the low temperature sensitivity of the RDE in saline media (see Section 2.1) no correction would need to be made for temperature fluctuations over a range of about ±5°C.

The following additional work must be carried out to assess whether a platinum RDE can be used for long-term O_2 measurement in a particular location:

(i) In Section 3.3.2 of this chapter it was reported that a platinum RDE consistently gave readings which were about 20% high. It should be determined whether a similar error would occur in seawater of a different pH and composition. In addition, it is necessary to assess whether the relative error is dependent on O_2 concentration in the concentration range of interest.

(ii) In this study it was fould that the surface of a platinum RDE immersed in filtered or unfiltered seawater for up to 18 hours, retained a shiny appearance. After gentle cleaning with a cotton swab moistened with dilute HNO_3 the electrode could be left dry for a period of up to a month before re-use, upon which it would display the same behavior as before towards O_2 reduction. It would be necessary to ascertain whether microorganisms tend to grow on the active portion of an RDE immersed in seawater over an extended period, resulting in filming which would in turn alter the mass-transport or reduction kinetics of O_2 at the RDE surface. This could be determined by operating a platinum RDE on-line in a desalination plant for a prolonged period.

CHAPTER 4: ACTIVATION AND DEACTIVATION OF PLATINUM WITH RESPECT TO OXYGEN REDUCTION

4.1. Scope of this Chapter

This chapter deals with variations in the catalytic activity of platinum towards oxygen reduction as a function of electrode history, potential, and the medium in which it is immersed. A survey has been made of activation techniques mentioned in the literature, as well as theories advanced to explain their efficacy. Deactivation and poisoning mechanisms are discussed in the light of experimental results obtained in this study, as well as results obtained from the literature.

The mechanism of oxygen reduction has been shown to vary with pH (e.g. Damjanovic, et al., 1966) and purity of solution (e.g. Damjanovic, et al., 1967a). In this study experiments were performed using neutral solutions which had not been purified. Therefore, conclusions drawn in this chapter are applicable mainly to oxygen reduction in such media. This information is thus supplementary to that in the literature, which applies to purified solutions of high (12-13) or low (0-1) pH.

4.2. Time-dependence of the Oxygen Reduction Current

In this study it was found that the current due to oxygen reduction at a platinum electrode held at a constant potential between about +0.1 and -0.8 V vs

S.C.E. decreases to a non-reproducible steady-state value over a period of 30-90 minutes. A typical current-decay curve is shown in Fig. 3.1 and described in Section 3.2. Similar behavior has been observed by a number of investigators, among them being Damjanovic, et al. (1967a), Hoare (1965), Myuller and Nekrasov (1964), Oshe, et al. (1965), Tikhomirova, et al. (1967), and Yuzhanina, et al. (1970). Among the investigators who either did not observe such a time-dependence, or declined to mention it, are Ostrovidova, et al. (1970) and Nekrasov and Dubrovina (1968).

The view generally held is that the surface of the platinum changes with time, and that this affects the extent to which oxygen reduction is promoted at the surface.

Before reactivation of the surface is discussed, the changes which occur in the oxygen-reduction mechanism as the current decays, will be described.

4.3. Changes Occuring in the Reaction Mechanism, as a Function of the State of Activation of the Electrode

It is generally agreed that deactivation of the platinum surface results in inhibition of the reduction of H_2O_2, which is formed when oxygen undergoes 2-electron reduction (Hoare, 1968). For example, Tikhomirova, et al. (1967) found that at a reduced

(deactivated) platinum surface H_2O_2 was reduced at a negligible rate compared to its rate of formation. Myullier and Nekrasov (1965) found that at a deactivated platinum surface H_2O_2 was reduced at a rate an order of magnitude less than its rate of formation. At an activated surface H_2O_2 was reduced as quickly as it was formed.

The dependence of the limiting current for oxygen reduction on $\omega^{1/2}$ for a deactivated platinum RDE was measured in this study. The results of several experiments are shown in Fig. 4.1. For comparison the results obtained at an activated electrode in air-saturated 3.5% NaCl solution, and in 1.6×10^{-4} M H_2O_2 in 3.5% NaCl, are also shown, as well as the behavior predicted by the Levich equation.

From Fig. 4.1 it can be seen that the current at a deactivated electrode in air-saturated NaCl solution (Run 86) was only about 6% below that at an activated electrode. On the other hand, at a deactivated electrode in air-saturated seawater (Run 75) the drop in current was much larger. The potential at which the i-$\omega^{1/2}$ data was measured in Run 86 was -0.70V whereas in Run 75 it was -0.60V, as explained in Section 3.4.1. As Fig. 3.2 shows, the difference between the currents at an activated and a deactivated (declined) electrode increases as the potential becomes more anodic. Therefore, part of the disparity between

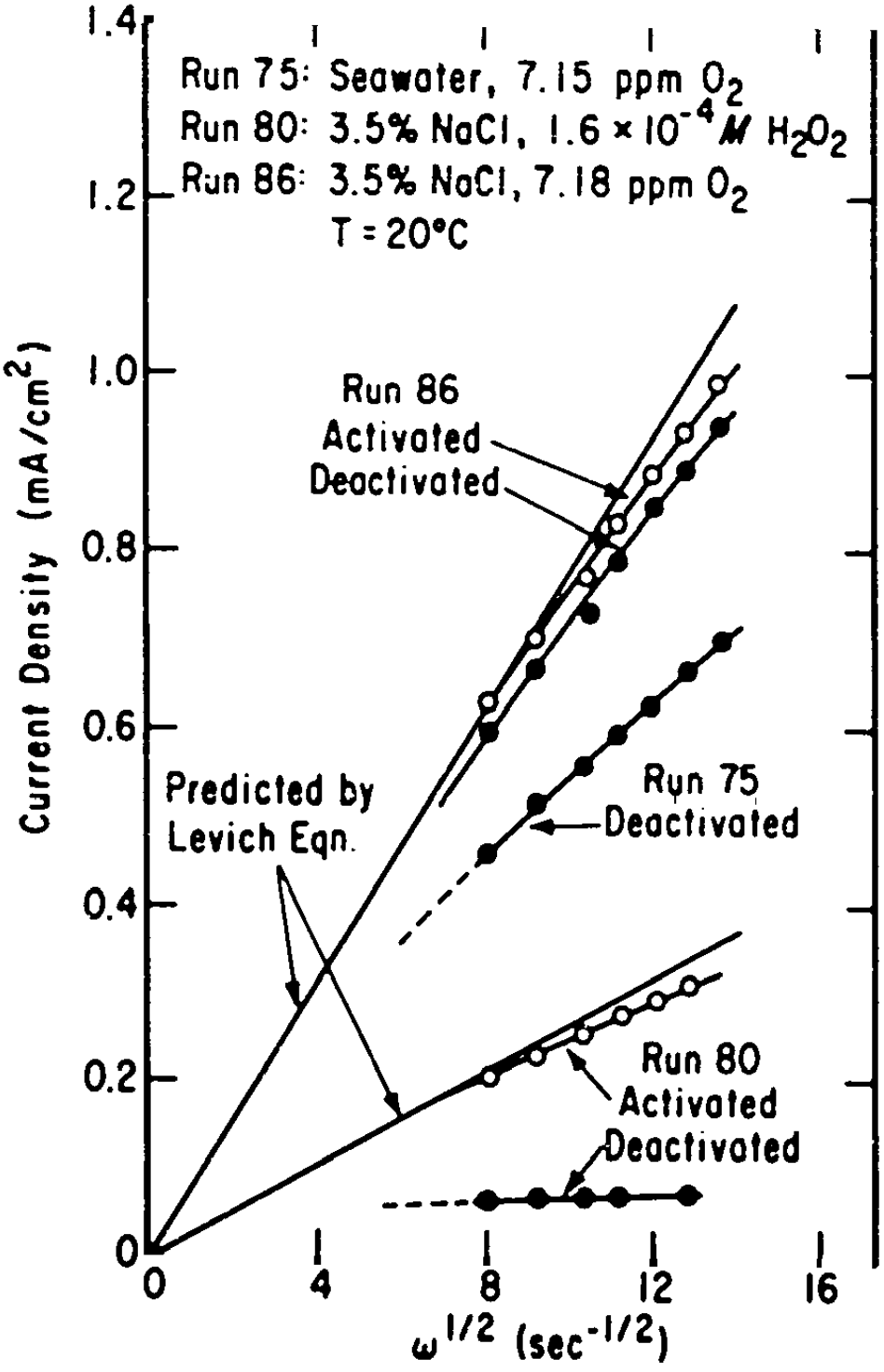

Figure 4.1. Dependence of i_{lim} on $\omega^{1/2}$ for Oxygen and H_2O_2 Reduction at Activated and Deactivated Platinum Electrodes.

Runs 75 and 86 can be attributed to this difference in electrode potentials. Other reasons for dissimilar behavior in these two media will be discussed later in this chapter.

In oxygen-free H_2O_2 solution (Run 80) the curve for a deactivated electrode fell far below that of an activated electrode. This indicates the extent to which H_2O_2 reduction is retarded at a deactivated electrode.

Analysis of the data obtained at activated and deactivated electrodes using equation (1.23) gives a quantitative measure of how much H_2O_2 reduction is inhibited at a deactivated electrode. In Table 4.1 H_2O_2 reduction rate constants are listed which were obtained under a variety of experimental conditions. Decreases in the rate constant vary from two-fold in the case of air-saturated (7.18 ppm O_2) NaCl solution to over twentyfold in the case of H_2O_2 solution. Among the factors which might have caused these differences in the extent of the fall in k_3 are differences in electrode potential and defects in the reaction model used in the calculation. These, as well as the apparent dependence of k_3 on oxygen concentration, are discussed in Chapter 3. Other factors of importance are discussed later in this chapter.

TABLE 4.1

H_2O_2 Reduction Rate Constants for Activated and Deactivated Platinum Electrodes

SOURCE	MEDIUM	O_2CONC. (ppm)	BULK H_2O_2CONC.	k_3 (cm./sec.) ACTIVATED	k_3 (cm./sec.) DEACTIVATED	ELECTRODE POTENTIAL (V.SCE)
Run 83	NaCl soln.	7.18	-0	0.110	0.045	-0.7
Run 86	"	7.18	-0	0.109	0.049	-0.7
Peters(1970)	"	6.55	-0	0.118	0.024	-0.8
Run 75	Seawater	7.15	-0	0.073	0.006	-0.6
Run 63	NaCl soln.	0.09	-0	0.043	0.0014	-0.5
Run 80	"	-0	1.6×10^{-4}M	0.118	0.0045	-0.65
Run 81	"	-0	3.1×10^{-5}M	0.034	0.0023	-0.6

4.4. Changes Occurring in the Electrode Surface During Activation and Deactivation

4.4.1 Activation

The method commonly used to activate a platinum electrode is to hold it at a potential anodic to the oxygen rest potential for a period ranging from several seconds to several minutes. There appears to be no unanimity as to the exact pretreatment to use and only recently has any work been done to systematize pretreatment. (e.g. Luk'yanycheva, et al., 1971; Tarasevich and Bogdanovskaya, 1971). Some examples of pretreatment techniques are given in Table 4.2.

In some cases where polarization curves were measured by observing the response of the current to triangular voltage pulses no pretreatment was mentioned (e.g., Nekrasov and Dubrovina, 1968). In such cases the anodic extreme of the triangular wave constituted a brief anodic pretreatment.

As can be seen from Table 4.2, the potentials and durations of pretreatment vary considerably. Moreover, none of the authors quoted justified explicitly why a specific pretreatment potential was used rather than one which was, say, 0.1V higher or lower.

One aspect common to these techniques, however, is that the potentials used were sufficient to produce a layer of adsorbed or chemically combined oxygen

TABLE 4.2

Examples of Pretreatment Techniques Used to Activate Platinum Electrodes

SOURCE	PRETREATMENT POTENTIAL (VOLTS vs. N.H.E.)	DURATION OF PRETREATMENT (min)
Blurton and McMullin (1969	None	
Damjanovic, et al. (1967)	+1.4	1.0
	then 0.0	1.0
Möller and Nekrassow (1964)	+1.8	
	then -0.2	Not stated
	then +1.3	1.0
Oshe, et al. (1965	Alternate pulses, repeated	
	+1.2	0.5
	then -0.1	0.5
Shepelev, et al.	Alternate anodic-cathodic polarization at 10mA/cm^2	
	10 cycles	1.0
Yuzhanina, et al. (1970)	+1.1	0.3
	then 0.0	0.3
This study	+0.75 - +1.25	0.1 - 1.0

at the surface (Hoare, 1968). According to Tarasevich and Bogdanovskaya (1970), oxygen is adsorbed at a platinum surface at a rate that increases approximately linearly with the anodization potential. Formation of platinum oxides commences only at potentials anodic to +1.4 to +1.6 V(NHE) in acid solution and +1.1 to +1.25 V(NHE) in alkaline solution. Damjanovic (1969) implies that oxides form at potentials anodic to +1.0 V(NHE) in acid solution.

Luk'yanycheva, et al. (1971) examined the effects of potential and duration of pretreatment on the coverage of the surface of a platinum electrode with adsorbed oxygen. They also examined the effect of the latter on the rate and mechanism of oxygen reduction. They found that the proportion of oxygen which undergoes 2-electron reduction increased with increasing coverage of the surface with oxygen during activation. Related to this observation is the fact that Tarasevich and Bogdanovskaya found that 4-electron reduction was inhibited as coverage of the platinum surface with oxygen exceeded monolayer filling.

Luk'yanycheva, et al. also found that the rate of H_2O_2 reduction increased with increased surface coverage by oxygen. This result confirms the generally-held opinion (e.g. Hoare, 1967) as to the effect of activation on H_2O_2 reduction and is in agreement with the results obtained in this study (see, for

example, Table 4.1).

4.4.2. Deactivation

In the papers quoted in the preceding section no mention was made of the possibility of poisoning of the surface of the electrode, in addition to desorption or reduction of adsorbed oxygen, when the electrode is made cathodic. This may have been so because the high purity of the solutions used in these studies made poisoning by trace organics, for example, highly unlikely.

Damjanovic, et al. (1967a) found that in impure solution the current due to oxygen reduction at a platinum RDE decreased with time at a rate one to two orders of magnitude greater than the corresponding decrease in pure solution. In impure solution 2-electron reduction of oxygen predominated over 4-electron reduction, and the rate of H_2O_2 reduction was low compared to its rate of formation. Yuzhanina, et al. (1970) also found that the proportion of 4-electron reduction decreased with decreasing purity of solution, from 90% in pure solution to 70% in impure solution. Of course these results can only be used qualitatively since, in the papers quoted, the terms "pure" and "impure" were not defined in a quantitative sense.

Hoare (1968) questioned the existence of a 4-electron reduction path. He suggested that impurities

adsorbed at the electrode inhibited catalytic decomposition of H_2O_2 formed by 2-electron oxygen reduction. This H_2O_2 could therefore be detected at the ring of an RRDE. In pure solutions, on the other hand, any H_2O_2 formed at the disk would immediately decompose catalytically if it were not reduced electrochemically, and the resulting oxygen would then be reduced quickly to H_2O_2. The apparent result would be that 4-electron reduction was occurring. This result is shown algebraically in Section 1.8. Hoare does raise a valid point, i.e., that Damjanovic, et al., erred in neglecting possible catalytic H_2O_2 decomposition at the disk when formulating their reaction model. However, the existence of a 4-electron reduction path has since been verified repeatedly by workers using the diagnostic equations which Tarasevich (1968) developed for the RRDE, and which take catalytic H_2O_2 decomposition into account.

Damjanovic, et al. (1967a) found that the rate of decay of the current for oxygen reduction in an impure solution was strongly dependent on the rate of rotation of the electrode. This implies that poisoning of the electrode was caused by diffusion of species from the bulk of the solution. No mention was made of the possibility of simultaneous removal of a layer of adsorbed oxygen from the electrode surface.

The results obtained in this study were representative of impure systems and provided an opportunity to test some hypotheses pertaining to activation and deactivation of platinum electrodes in unpurified solutions. The alternative hypotheses tested were as follows:

(i) The layer of adsorbed oxygen formed during anodic pretreatment catalyzes one or more stages in the reduction of oxygen. This layer is slowly removed when the electrode is made cathodic.

(ii) During anodic pretreatment a substance is formed which is later reduced when the electrode is made cathodic, thereby resulting in a higher current density.

(iii) During pretreatment impurities adsorbed at the platinum surface are either oxidized or desorbed. The reverse occurs during cathodic polarization.

Evidence in support of (i) above is given in Table 4.3 and illustrated graphically in Fig. 4.2. Increasing the anodization time by a factor of about 3 resulted in current increases of up to 3.5%. Similarly, as Table 4.4 shows, increasing the anodization potential produced appreciable increases in the limiting current. In each case the relative increase in current produced by a given increase in potential or duration of pretreatment was higher at low oxygen concentrations than at higher concentrations. Such an observation might be taken as support for hypothesis

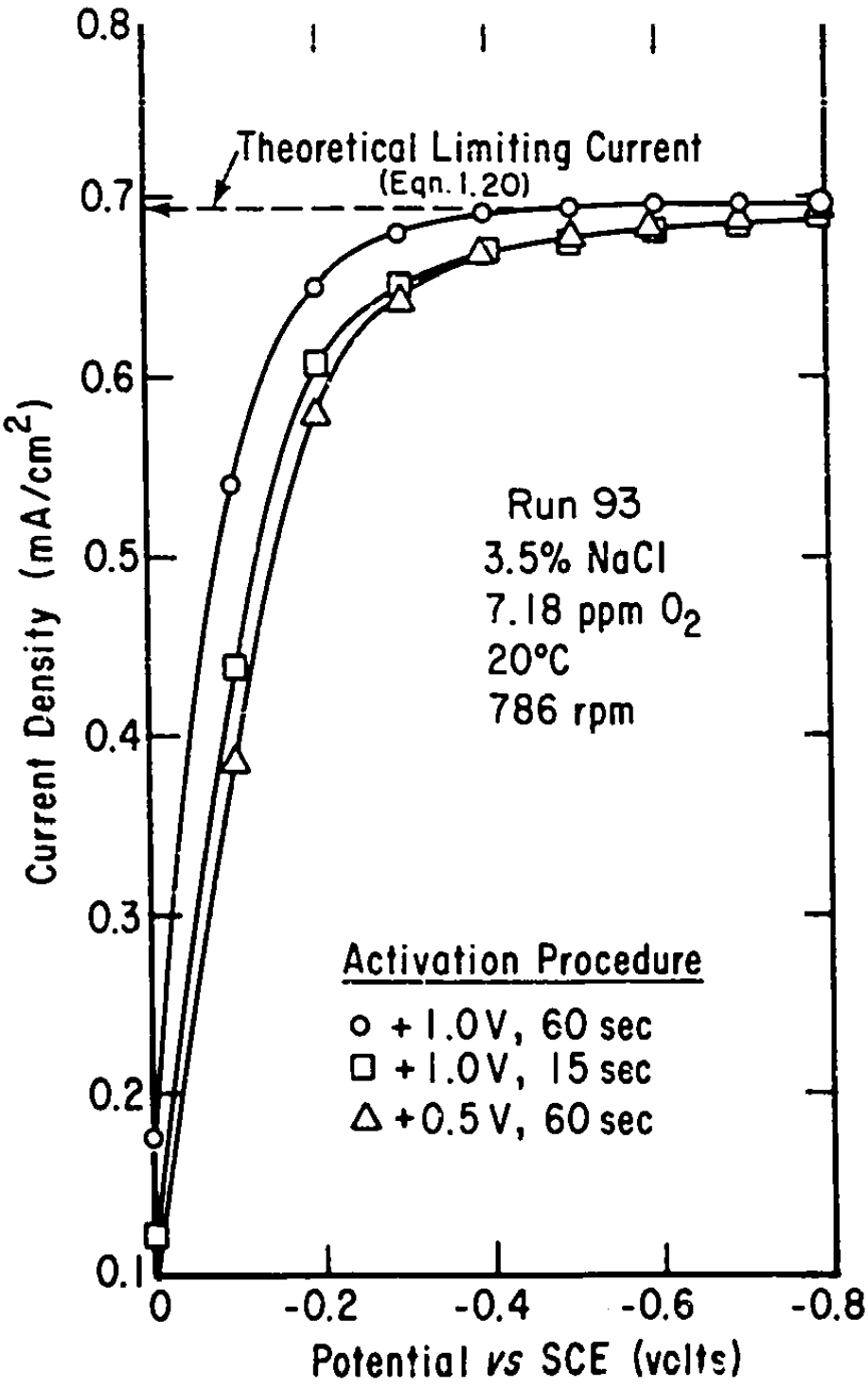

Figure 4.2. Effect of Potential and Duration of Anodization on Shape of Polarization Curve for Oxygen Reduction at an Activated Platinum RDE.

TABLE 4.3

Effect on the Limiting Current of Increases in Anodization Time

RUN	MEDIUM	O_2 CONC. (ppm)	PRETREATMENT POTENTIAL (Volts SCE)	CHANGE IN PRETREATMENT TIME	EFFECT ON LIMITING CURRENT
93	3.5% NaCl	7.18	+0.5	From 15 sec. to 60 sec.	1.5% increase
16	"	0.5	+0.5	"	3.5% increase
75	Seawater	7.15	+0.5	From 10 sec. to 60 sec.	1% increase
74	"	6.09	+0.25	From 10 sec. to 30 sec.	3.6% increase

107

TABLE 4.4

Effect on the Limiting Current of Increases in Anodization Potential

RUN	MEDIUM	O_2 CONC. (ppm)	PRETREATMENT DURATION (sec.)	CHANGE IN PRETREATMENT POTENTIAL	EFFECT ON LIMITING CURRENT
93	3.5% NaCl	7.18	15	From +0.5 to +1.0V	0.6% increase
16	"	0.5	15	From +0.5 to +1.0V	3.5% increase
			60	"	1.8% increase
75	Seawater	7.15	18	From +0.5 to +1.0V	0.6% increase
74	"	0.09	10	From +0.5 to +0.7V	3.5% increase

(ii) since the additional current due to reduction of any substance(s) formed during anodization would increase in relative magnitude with decreasing oxygen concentration. This argument is, however, easily refuted.

First, the relative increase in current produced by a given change in pretreatment at two oxygen levels was not even approximately in inverse proportion to the ratio of the oxygen concentrations, contrary to what hypothesis (ii) would predict.

Second, at a given oxygen concentration the current increase produced by an increase in activation time was much less than proportional to the additional number of coulombs passed during this period.

Third, the increased number of coulombs passed while an electrode went from the activated to the deactivated state over a period of 30-60 minutes was far greater than the number of coulombs passed during activation. This indicates that a change in catalytic activity occurs during activation, rather than the generation of a reducible species at or near the electrode surface.

Finally, an experiment was designed to test hypothesis (ii) specifically. After activation a switching arrangement (Fig. 2.2) was used to interrupt electrical contact to the RDE for a chosen length of

time between activation and cathodic polarization. For convenience this interrupted state is hereafter referred to as "standby." If a reducible, non-adsorbed substance were formed at the electrode during activation, one might expect it to diffuse away from the surface during the standby period. This would have the result that anodization would produce little or no increase in the current flowing during cathodic polarization. Some results obtained using standby are listed in Table 4.5.

In air-saturated NaCl solution and seawater containing 0.1 ppm oxygen an increase in current with increasing duration of standby mode, was observed, rather than a decrease. This rules out hypothesis (ii) as an explanation of the effects of anodization on the current.

Before reasons for the effects of standby are discussed, it is appropriate to assess the importance of poisoning of the electrode surface, as suggested in hypothesis (iii). Figure 4.3 shows some results obtained in this study on the effect of rotational speed on the rate of decay of the limiting current for oxygen reduction at a platinum RDE. It is clear that both the rate and extent of decay are proportional to the rotational speed, as Damjanovic, et al. (1967a) found. At a rotational speed of 120π sec^{-1} they observed a 30% drop in current in the first five

TABLE 4.5

Effect of Standby Mode on the Limiting Current

RUN	MEDIUM	O_2 CONC. (ppm)	TEST	EFFECT ON LIMITING CURRENT
93	3.5% NaCl	7.18	Anodize: +0.5V, 30 sec., then 30 sec. standby.	No appreciable effect
			Same pretreatment, then 5 min. standby	0.8% increase
75	Seawater	7.15	Anodize: +0.5V, 10 sec., then 60 sec. standby	No appreciable effect
74	Seawater	0.09	Anodize: +0.5V, 10 sec., then 30 sec. standby.	5% increase
			Same pretreatment, then 2 min. standby	8% increase
76	Seawater	0.10	Anodize +0.5V, 30 sec., then 60 sec. standby	5% increase

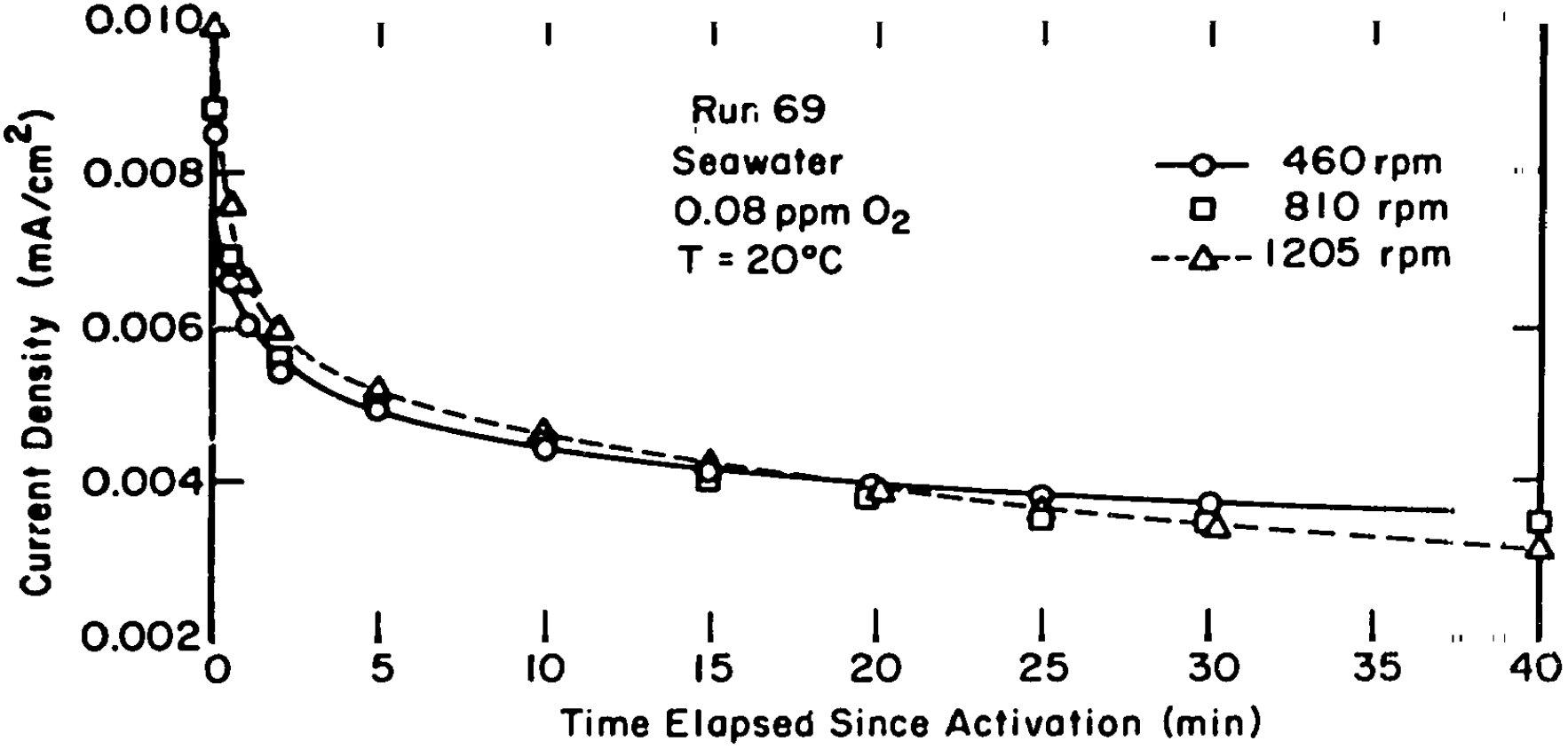

Figure 4.3. Effect of Rotational Speed on Rate of Current Decay for Oxygen Reduction at a Platinum RDE.

minutes after activation. In Run 69 of this study, at only 40π sec^{-1} (1200 rpm) a 50% drop in the current was observed in the same interval. This is not surprising since seawater was used in the latter experiment, and it probably contained more impurities than the 0.1 N H_2SO_4 used by Damjanovic, et al.

As was shown earlier in this chapter the extent of deactivation of a platinum electrode was greater in seawater than in NaCl solution. It appears, therefore, that poisoning of the electrode by impurities in solution was of considerable importance under the experimental conditions prevailing in this study. This poisoning is probably reversible; desorption of poisoning compounds takes place during anodic pretreatment. In view of the fact that investigators working with highly purified solutions have established that oxygen reduction is catalysed by the layer of adsorbed oxygen which forms at a platinum surface during anodic pretreatment, it seems likely that activation and deactivation are mixed processes involving a combination of the effects of poisoning and oxygen adsorption.

The relative effects of standby at high and low oxygen concentrations can now be explained as follows: After anodization some poisoning species may still be weakly adsorbed at the electrode. It has been proposed (Gnanamuthu and Petrocelli, 1967) that an elementary reaction step in oxygen reduction is

adsorption of molecular oxygen at the electrode. The rate of this adsorption step is probably dependent on oxygen concentration. Now, impurities adsorbed on the electrode surface may occupy sites which were active for oxygen adsorption. Thus the residual impurities might inhibit oxygen adsorption less at a high oxygen concentration than at, say, 0.1 ppm.

During standby, when the electrode is at the rest potential, the residual poisoning impurities may slowly desorb. The extent of desorption will be dependent on the duration of standby. This will have a greater relative effect on the current during subsequent cathodic polarization at lower oxygen concentrations. The same reasoning also explains the greater relative effects of duration and potential of anodization at lower oxygen concentrations.

4.5. Hysteresis

Polarization curves measured in NaCl solution and seawater exhibited hysteresis at all oxygen levels. The polarization curve measured in the direction of increasing cathodic potential (cathodic branch) lay above that measured in the opposite direction (anodic branch). This was also observed by Blurton and McMullin (1969) and Damjanovic, et al. (1967a) and was mentioned by Shumilova and Bagotzky (1968).

An example of the hysteresis observed in this study is shown in Fig. 4.4 (3.5% NaCl solution) and

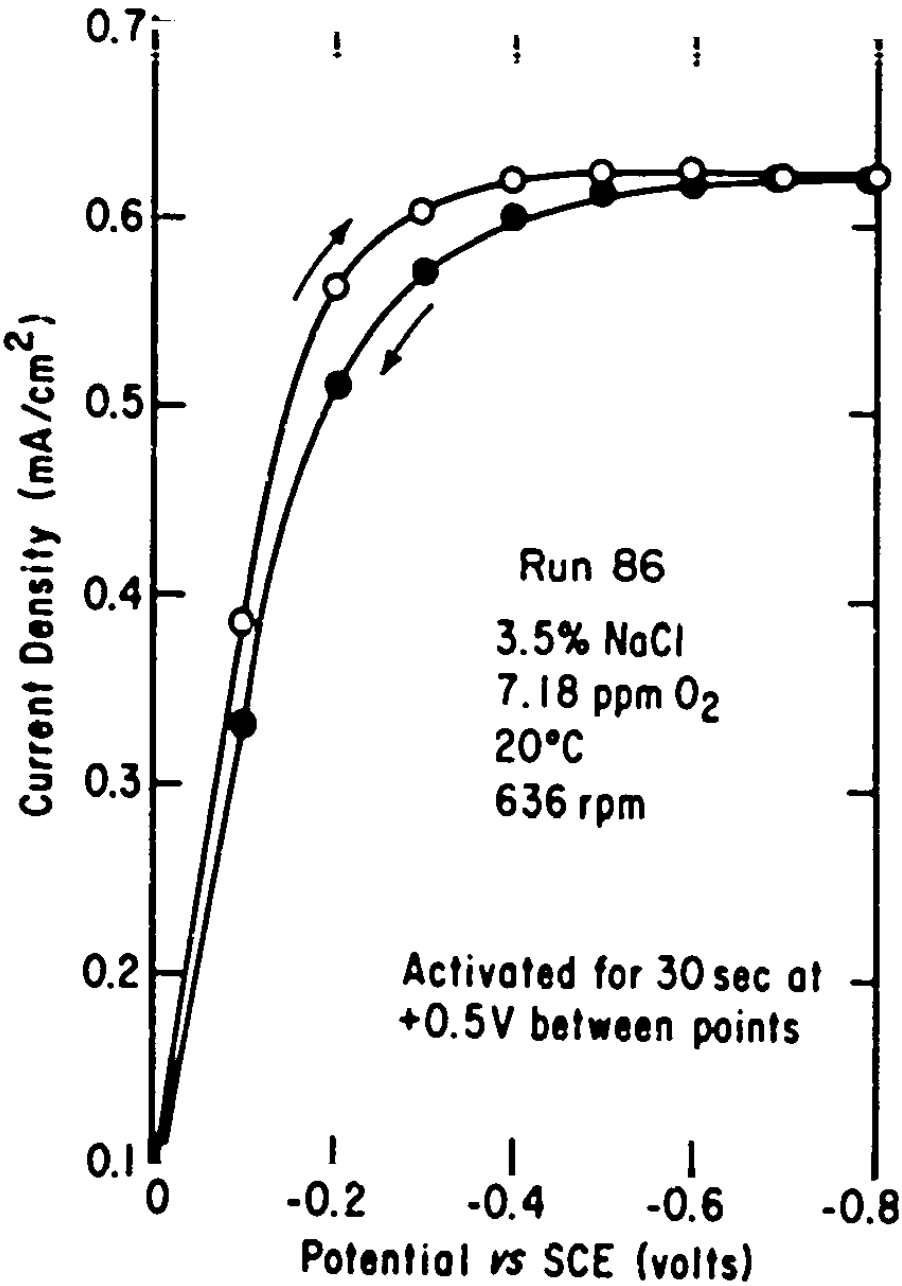

Figure 4.4. Hysteresis Curve for Oxygen Reduction at a Platinum RDE in Air-saturated NaCl Solution.

Fig. 4.5 (seawater). The same result occurred, irrespective of the order in which the branches of the polarization curve were measured. At this point it should be mentioned that all polarization curves discussed earlier in this report were cathodic branches.

Hysteresis can be explained by similar reasoning to that made in Section 4.4.2, when the effects of standby were explained. First, let us assume that the rate of adsorption of impurities at the electrode increases as the potential becomes more cathodic. Let us also assume that after anodization some residual impurities are left at the electrode surface, as suggested in the previous section.

In the course of measuring a polarization curve a number of events occur. During cathodic polarization the electrode is being poisoned, at a rate which increases as polarization proceeds towards more cathodic potentials. During anodic reactivation between points on the polarization curve the adsorbed impurities are being stripped from the electrode surface, but there will be a slight accumulation of residual impurities. By the time the anodic branch of the polarization curve is measured the concentration of impurities at the surface will be sufficient to inhibit oxygen reduction perceptibly.

As measurement of the anodic branch proceeds, less poisoning will occur during each period of

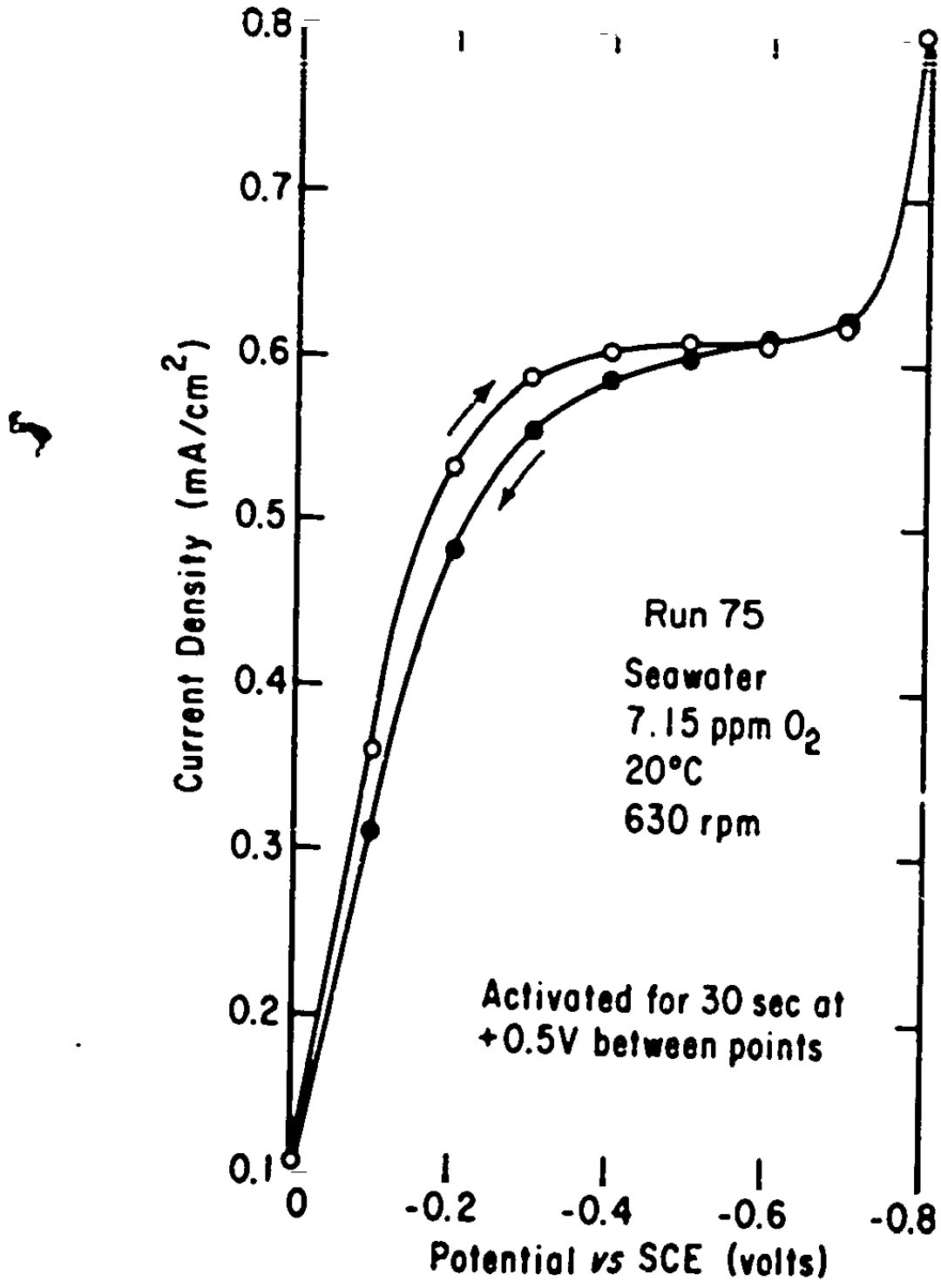

Figure 4.5. Hysteresis Curve for Oxygen Reduction at a Platinum RDE in Air-saturated Seawater.

cathodic polarization because of the decreasing cathodic potential, and some of the accumulated impurities will be removed during each anodization step. By the time the rest potential has been attained the concentration of adsorbed impurities will have reached a minimum.

This explanation also accounts for the fact that the degree of hysteresis increased with decreasing oxygen concentration, as shown in Figs. 4.5. and 4.6.

That poisoning has a strong effect on H_2O_2 reduction is illustrated in Fig. 4.7, which shows the greater extent of hysteresis in an oxygen-free solution containing H_2O_2.

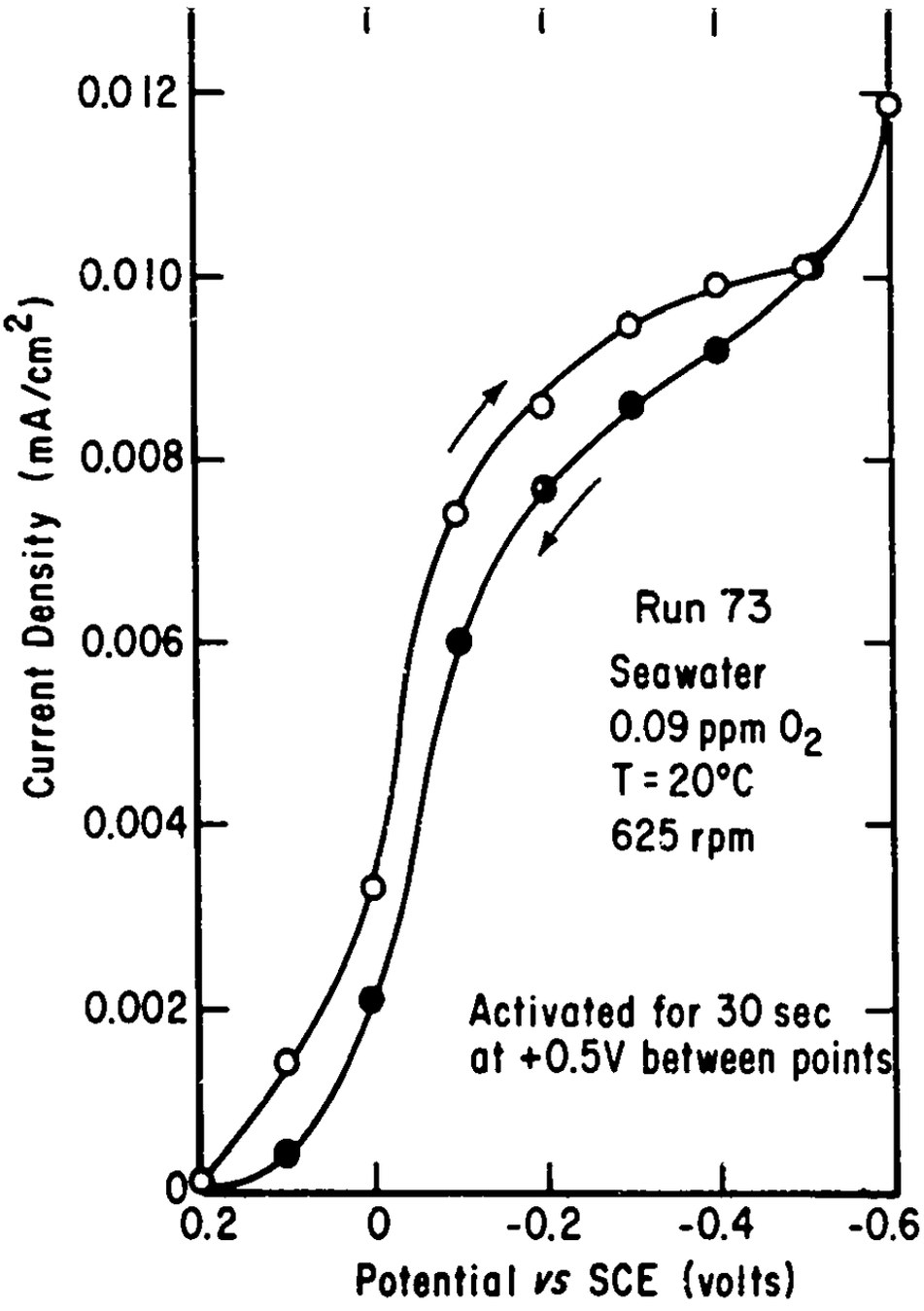

Figure 4.6. Hysteresis Curve for Oxygen Reduction at a Platinum RDE in Seawater. at 0.09 ppm O_2.

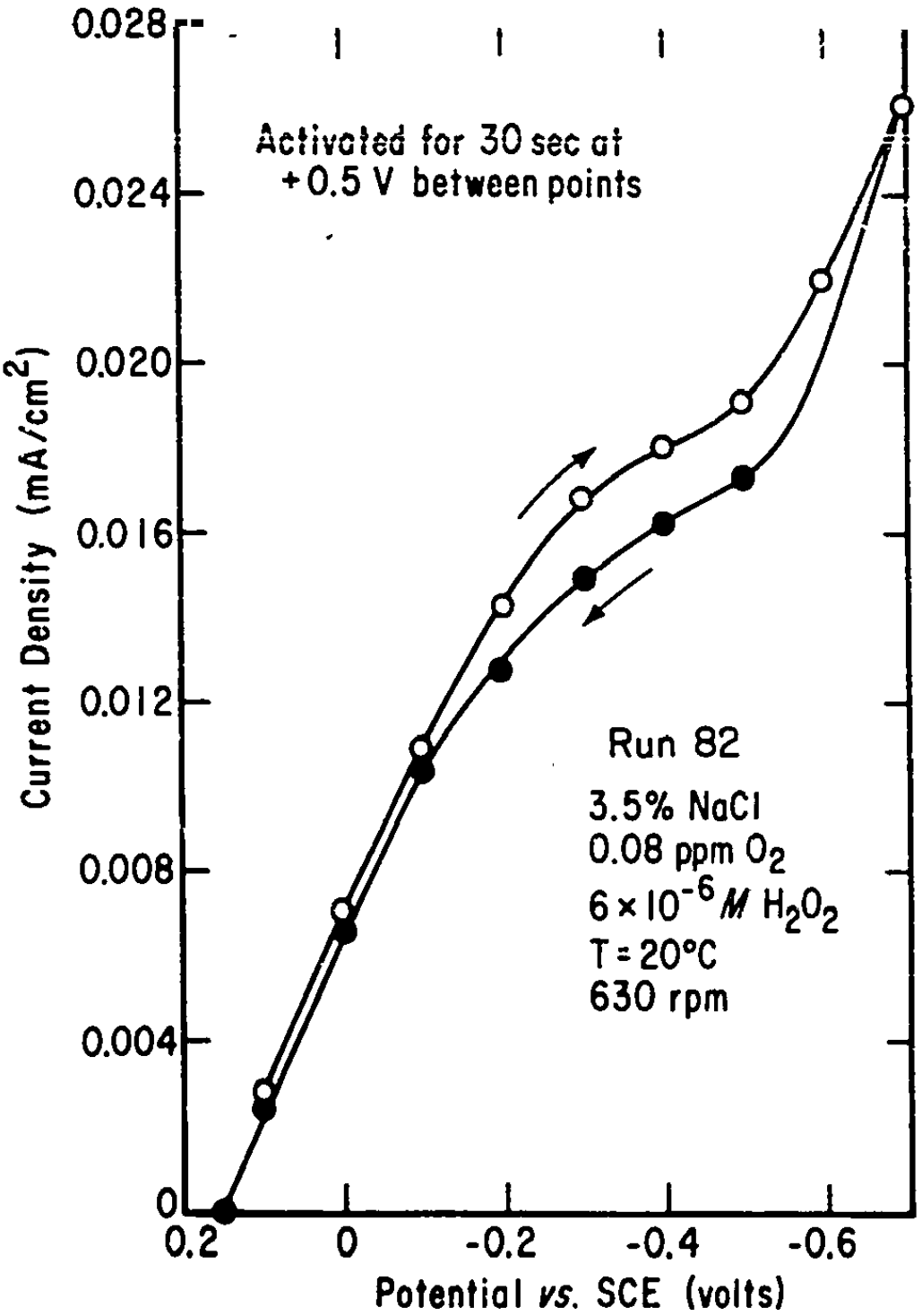

Figure 4.7. Hysteresis Curve for H_2O_2 Reduction at a Platinum RDE in an ^{2}NaCl/H_2O_2 Solution.

CHAPTER 5: STUDIES AT GOLD, SILVER, AND COPPER ELECTRODES

5.1. Scope of this Chapter

The first section contains a discussion of the transient behavior of the current for O_2 reduction at a gold electrode in air-saturated 3.5% NaCl solution. The effects of various activation techniques are compared. Polarization curves are described and conclusions are drawn using these curves, as well as $i-\omega^{1/2}$ curves, as to the probable mechanism of O_2 reduction at gold in the medium used.

Polarization data for O_2 reduction in seawater are described and compared with data obtained in NaCl solution. The lower limit of applicability of a gold RDE to the measurement of dissolved O_2 in seawater is found to be about 1 ppm.

The remainder of this chapter is devoted to brief discussions of polarization data obtained at copper and silver electrodes, both of which were found to have poor corrosion resistance compared to gold and platinum, and to give polarization data of poor reproducibility.

5.2. Polarization Data Obtained with a Gold Electrode

5.2.1. 3.5% NaCl Solution

When a gold RDE in an air-saturated NaCl solution was held at a cathodic potential the time-

dependence was similar to that of a platinum electrode. There was a fast initial transient of about five seconds' duration. The current then decreased at a somewhat lower, but more uniform, rate than that which was observed with a platinum RDE. A decay in the cathodic current on gold was also observed by Genshaw , et al. (1967). They reported that the current reached steady-state after about 1 minute, but it is more likely to have been at a quasi-steady-state.

Figure 5.1. shows the effects of various types of electrode pretreatment on the shape of the polarization curve. The technique used to measure polarization curves was as follows: The electrode was held at the pretreatment potential for several minutes. The potential was then varied stepwise, from a value close to the rest potential, to the hydrogen evolution potential. Between potential steps the electrode was, except where mentioned, held near the rest potential for a few seconds. After the electrode potential was made cathodic the current was recorded, and the current at 0.2 minutes after the potential change was plotted against the potential.

It is clear from Fig. 5.1. that cathodic pretreatment was most effective in activating the RDE surface. A quite flat limiting-current plateau resulted, the current at the plateau being within about

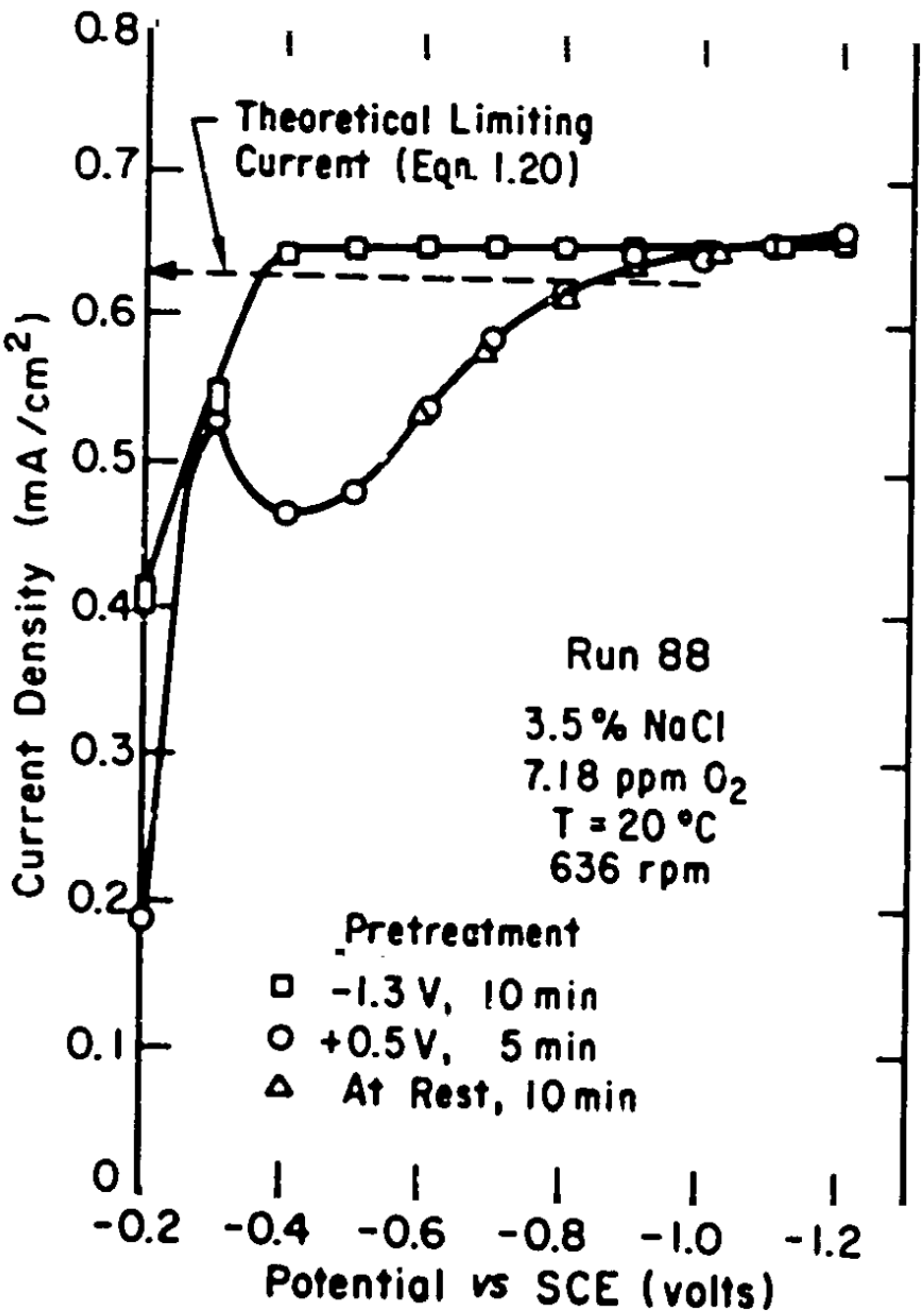

Figure 5.1. Effect of Pretreatment Technique on the Shape of the Polarization Curve for O_2 Reduction at a Gold RDE in Air-saturated NaCl Solution.

2% of that predicted by the Levich equation.

Anodization of the electrode seemed to inhibit O_2 reduction at potentials more anodic than about -0.8V. This implies that the reduction is catalyzed by an oxide-free, reduced gold surface.

When the electrode was left at the rest potential, with the potentiostat turned off, for 10 minutes, the result was the same as for an anodized electrode. It is possible that the small amount of oxidation which occurred during this period at rest was sufficient to inhibit O_2 reduction.

Tarasevich, et al. (1970) measured polarization curves for O_2 reduction at a gold electrode in oxygen-saturated alkaline solution. Their electrode was held at the rest potential for ten minutes prior to the measurement of each point on the polarization curves. No limiting-current plateaux were observed; their results thus agreed with those found in this study.

They obtained an intermediate wave, or pre-wave, whose height was equivalent to about two-thirds of the limiting-current for 4-electron reduction. In this study a small maximum occurred in the polarization curve for the anodized electrode at an equivalent potential. There were insufficient data obtained for the electrode left at the rest potential for ten

minutes in this study, to extend its polarization curve to potentials anodic to -0.6V. However, in view of the fact that the curve coincided closely with that of the anodized electrode at potentials cathodic to -0.6V, one might expect the former to exhibit at least a prewave at about -0.3V.

Using an RRDE, Tarasevich, et al. found that the amount of H_2O_2 escaping from the disk reached a maximum at the potential where the first wave occurred. Hence, at this potential the H_2O_2 formed as a result of 2-electron O_2 reduction was not electrochemically reduced to OH^- at a rate sufficient to prevent appreciable diffusion into the bulk of the solution. At more cathodic potentials the rate of H_2O_2 reduction increased rapidly.

Tarasevich, et al. concluded, as well, that 4-electron reduction took place at a negligible rate compared to 2-electron reduction. The fact that the current at the prewave was greater than that corresponding to 2-electron O_2 reduction was thought by them to be due to reduction of O_2 formed by catalytic decomposition of H_2O_2 at the disk. The maximum observed in this study might be explained by similar reasoning, coupled with the suggestion that some of the O_2 may undergo 4-electron reduction at a rate

which diminishes as the potential becomes more cathodic.

The observations made with a prereduced gold electrode in this study indicate that, at such a surface, either 4-electron O_2 reduction predominates or 2-electron reduction occurs additionally or exclusively, followed by rapid H_2O_2 reduction. This is supported by the plot of i vs. $\omega^{1/2}$ shown in Fig. 5.2. The experimental data for an activated (prereduced) electrode lie on a straight line through the origin, and slightly above the line predicted by the Levich equation. This small discrepancy may have been caused by a slight eccentricity of the electrode.

By way of contrast the plot of i vs. $\omega^{1/2}$ for an electrode left at the rest potential for ten minutes shows an increasing deviation from the theoretical line with increasing ω. This is good evidence of retardation of H_2O_2 reduction and agrees with the results of Tarasevich, et al.. The currents used to draw this plot were measured at -0.6V, a potential at which the polarization curve for this electrode lay considerably below that of a cathodically pretreated electrode.

A plot of i vs. $\omega^{1/2}$ (Fig. 5.2.) for an electrode whose activity had reached steady-state showed no evidence of inhibition of H_2O_2 reduction.

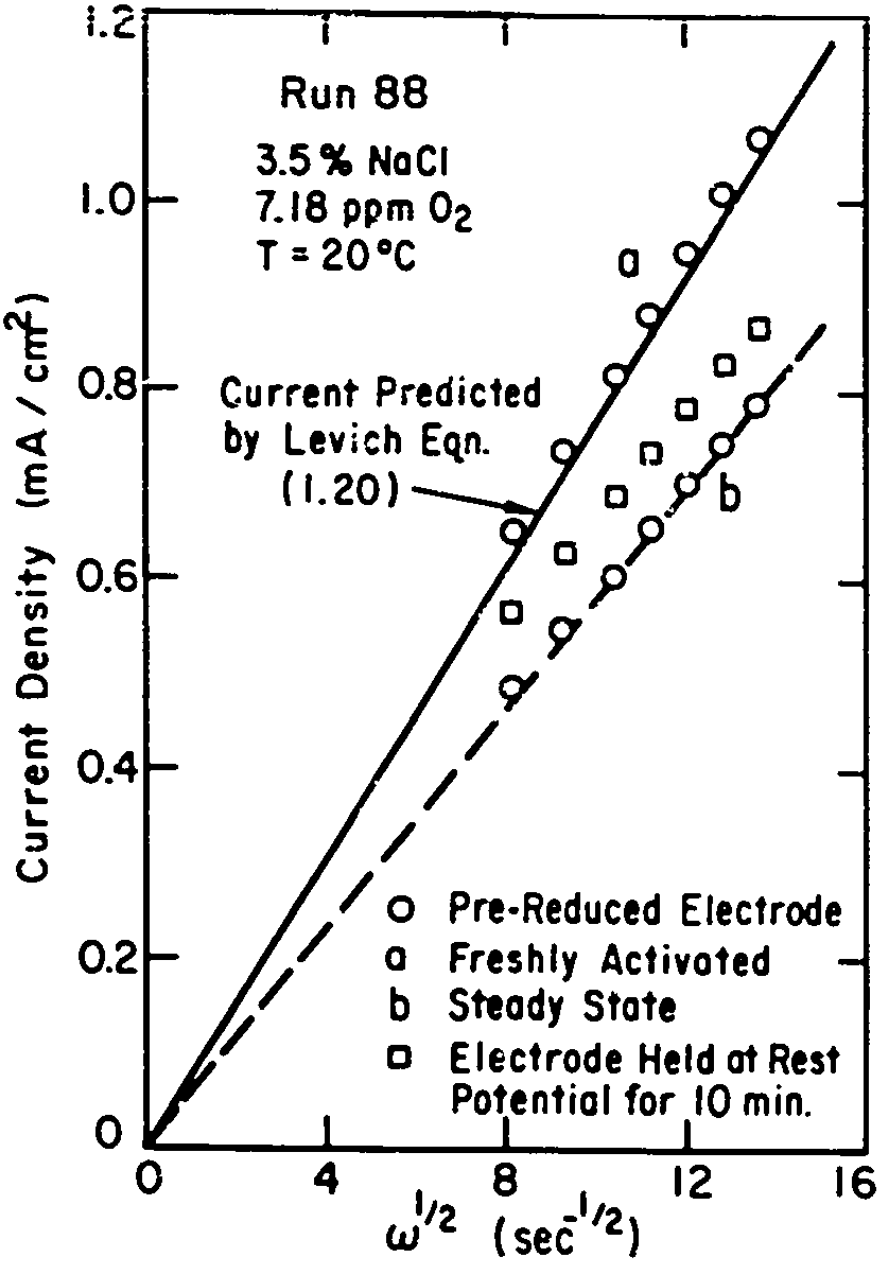

Figure 5.2. Effect of State of Electrode on Shape of i_{lim} vs $\omega^{1/2}$ Curve for Oxygen Reduction at a Gold RDE in Air-saturated NaCl Solution.

The data were scattered slightly about a straight line passing through the origin, the slope of which was about 75% of that of the line for the activated electrode. This indicates that O_2 reduction, rather than H_2O_2 reduction, is the step which is inhibited at steady state. One can conclude from these results that the reaction mechanism at a gold electrode at steady-state is different from that at both an anodized electrode and one which is held at the rest potential for some time prior to polarization.

The validity of comparison with the results of Tarasevich, et al. (obtained in pure, alkaline solution) is supported by the following: The main reaction path for O_2 reduction in 0.1N H_2SO_4 (Genshaw, et al., 1967) was found to be the same as that in 0.01-1N KOH (Damjanovic, et al., 1967c). Reduction in the limiting-current region proceeded via an H_2O_2 intermediate. The only significant difference in electrode behavior at these extremes of pH was that in the limiting-current region the H_2O_2 reduction rate constant was much higher at low pH than at high pH. In addition, Genshaw, et al. found that the mechanism of O_2 reduction in purified acid solution was identical to that in unpurified acid solution. This is not at all like the behavior of a platinum electrode, which was described in Chapter 3.

The polarization curve obtained at an O_2 concentration of 2 ppm is shown in Fig. 5.3. The electrode was activated by cathodic pretreatment, as in the case of air-saturated solution. The effect of decreasing O_2 concentration was to make the limiting-current plateau less distinct, as in the case of a platinum RDE. The current at the point of inflection of the polarization curve was within 2% of the theoretical value.

5.2.2. Seawater

Polarization curves for O_2 reduction in air-saturated seawater are shown in Fig. 5.4. Activation of the electrode in seawater was by cathodic pretreatment, as described in Section 5.1.2. No limiting-current plateau occurred, but the current at the inflection point was within about 3% of the theoretical value. The electrode had been prereduced at -1.1V for 10 minutes prior to polarization.

The absence of a limiting-current plateau was possibly due to the presence in seawater of substances which inhibit one or more stages in the reduction of oxygen on gold, irrespective of the pretreatment technique used.

As Fig. 5.7. shows, hysteresis was observed with a gold electrode. In contrast to the hysteresis observed at platinum, however, the anodic branch of

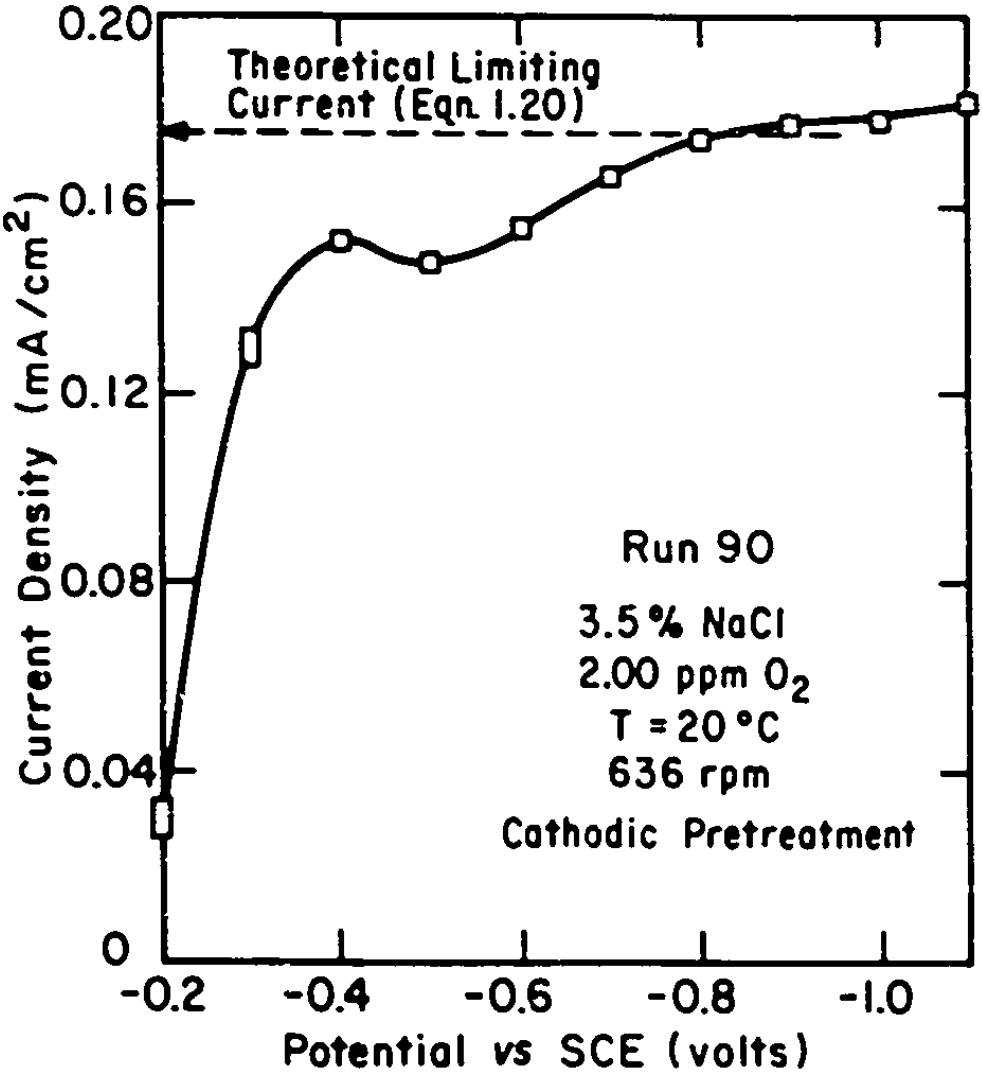

Figure 5.3. Polarization Curve for Oxygen Reduction at an Activated Gold RDE in NaCl Solution at 2.0 ppm O_2.

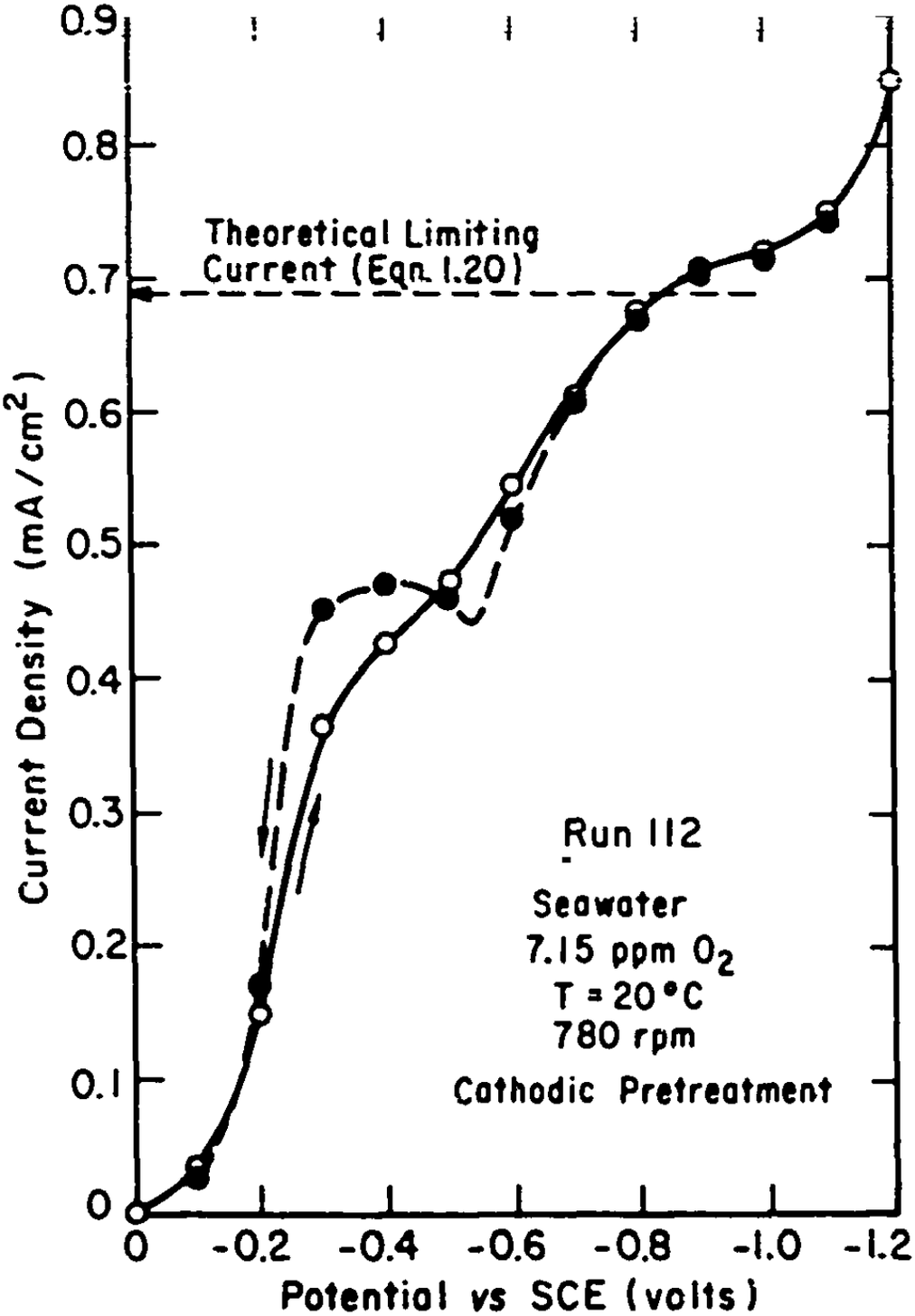

Figure 5.4. Polarization Curve for Oxygen Reduction at an Activated Gold RDE in Air-saturated Seawater.

the curve lay above the cathodic branch. This indicates that when measuring the cathodic branch of the polarization curve the exposure of the electrode to potentials anodic to -0.6V deactivated the surface. On the anodic branch the exposure to more cathodic potentials partly reactivated the electrode.

Polarization curves measured in air-saturated NaCl solution and seawater are compared in Fig. 5.5. The curve for NaCl solution was measured using an electrode which had been standing in air for some days before the experiment, and had then been prereduced at -1.3V for five minutes. It illustrates the poor reproducibility of polarization data for gold compared to that of platinum. Nevertheless the shape of the polarization curve for NaCl solution is far more characteristic of a diffusion-limited current than that of the curve for seawater.

At an O_2 concentration of 2.0 ppm the current at the inflection point of the polarization curve (Fig. 5.6.) was about 2% above the theoretical current.

At an O_2 concentration of 0.32 ppm in seawater the current at the inflection point was almost 30% greater than that predicted by the Levich equation. This discrepancy is almost 50% greater than that which was incurred using a platinum RDE at 0.1 ppm O_2.

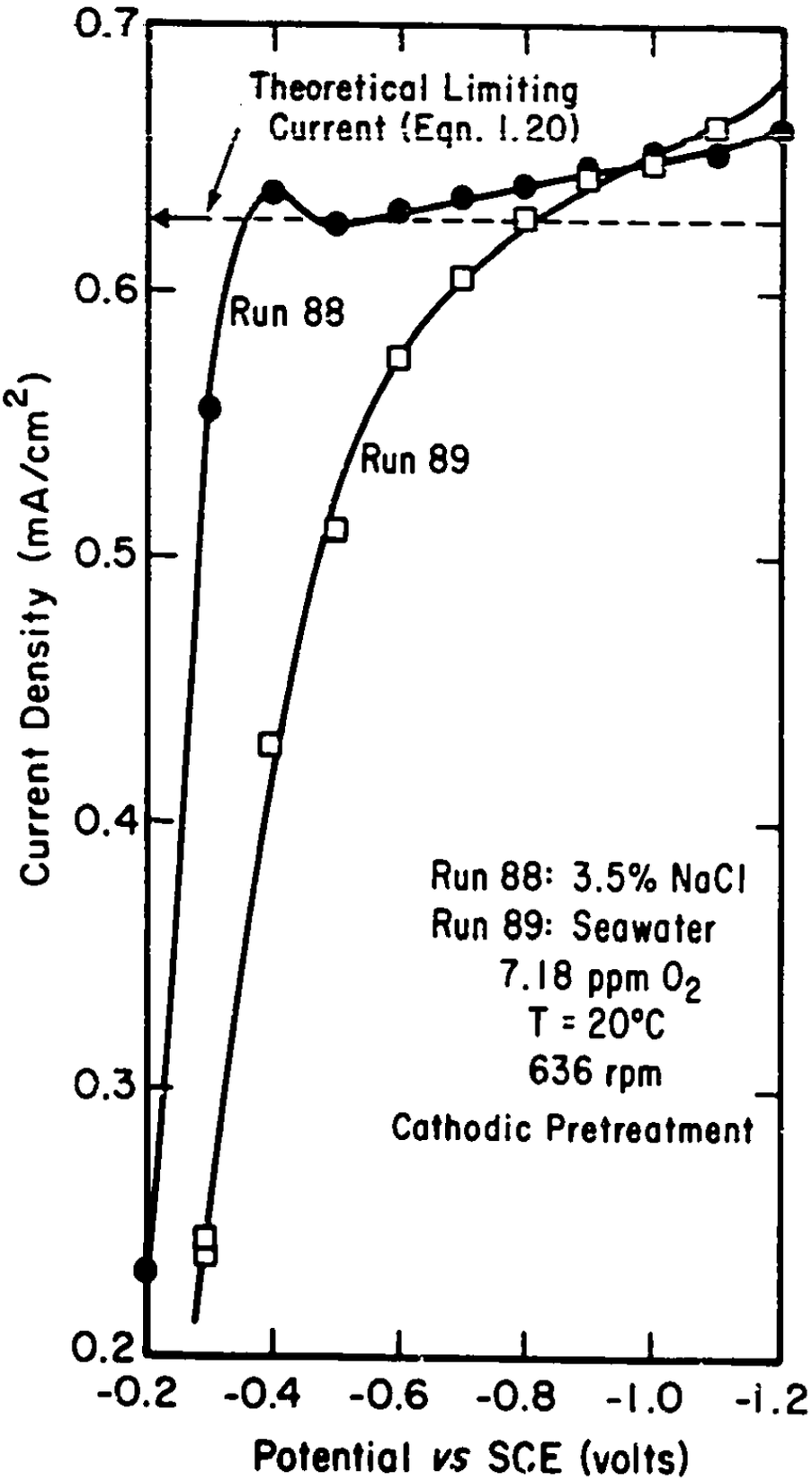

Figure 5.5. Comparison of Polarization Curves for Oxygen Reduction at an Activated Gold RDE in Air-saturated NaCl Solution and Seawater.

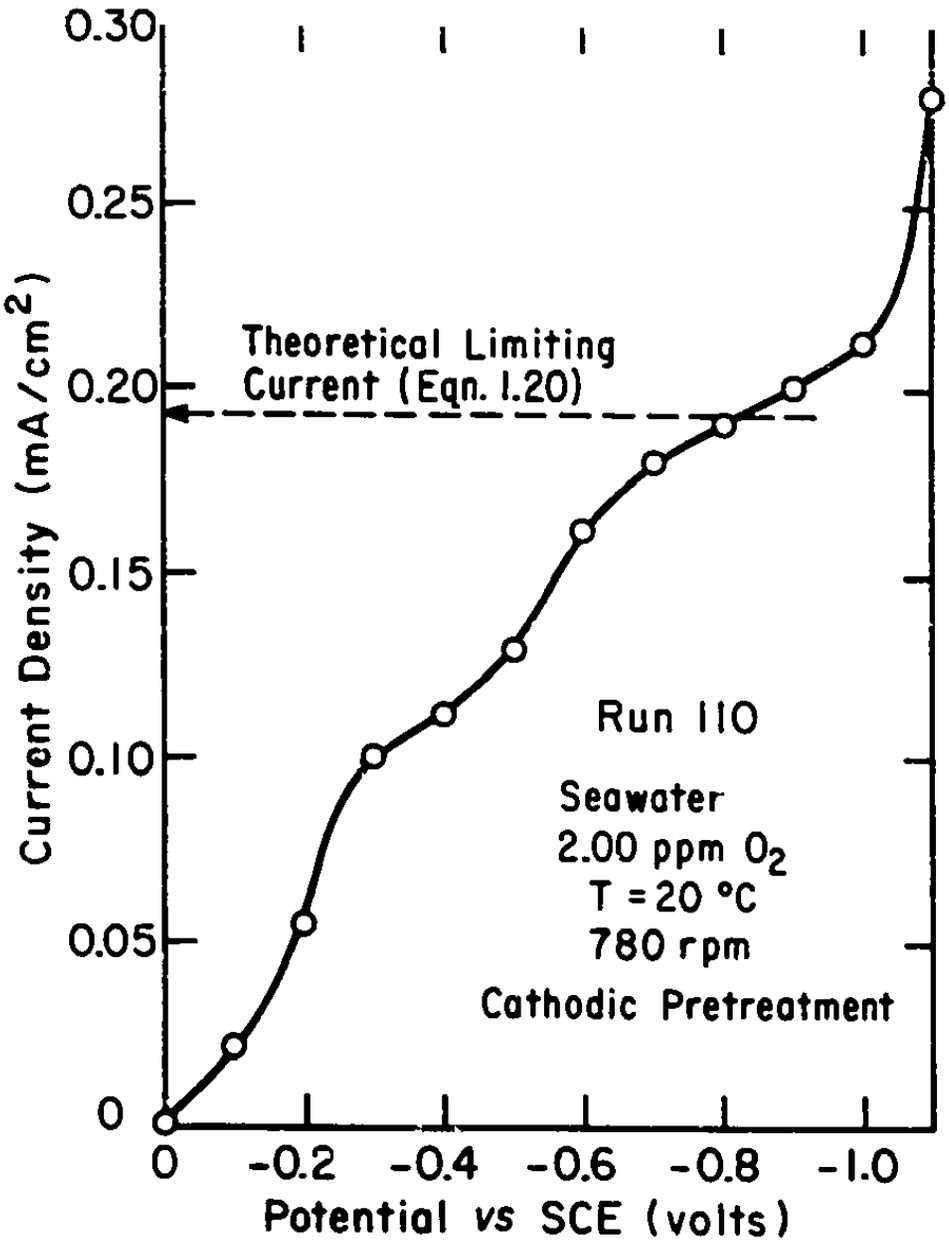

Figure 5.6. Polarization Curve for Oxygen Reduction at an Activated Gold RDE in Seawater at 2.0 ppm O_2.

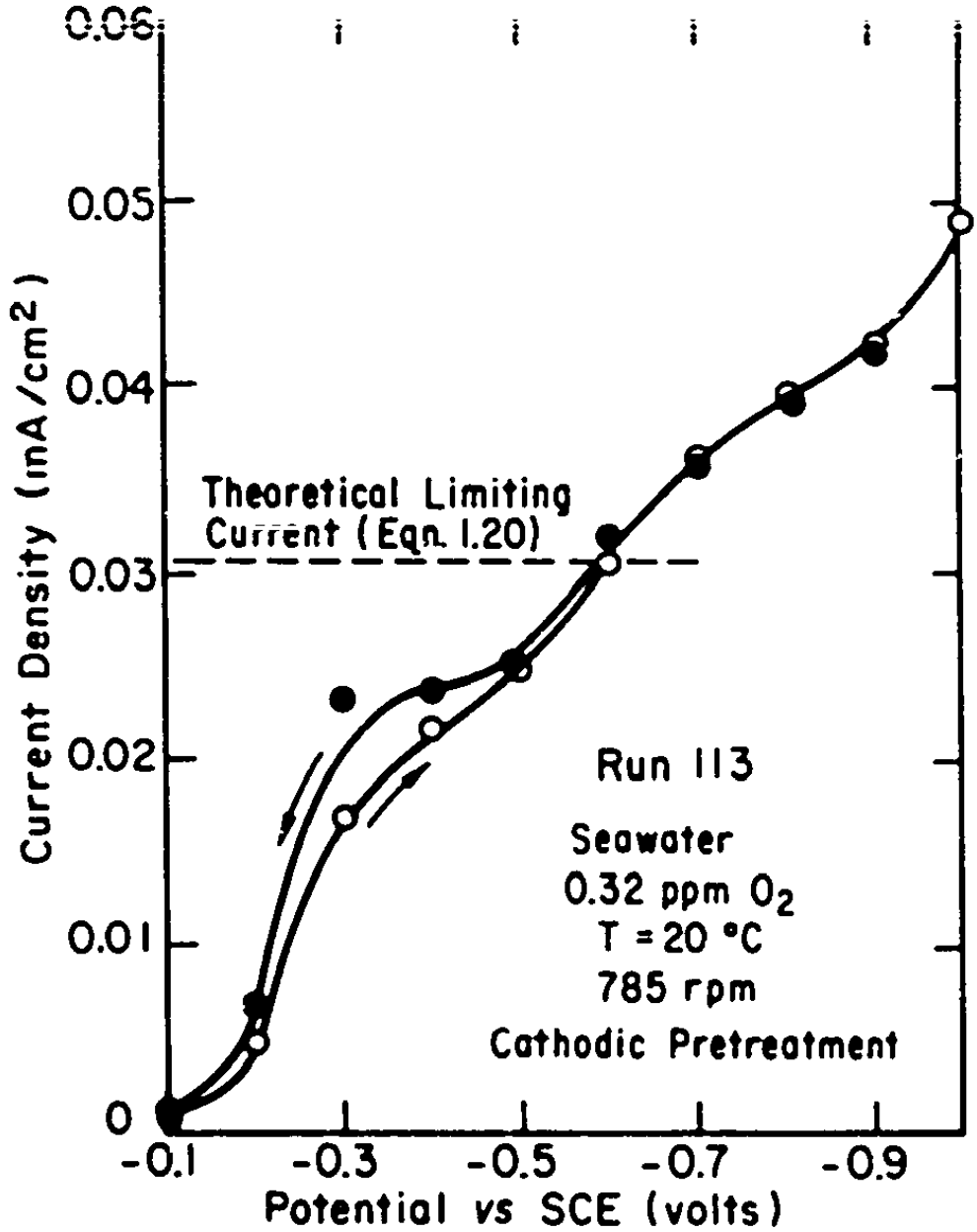

Figure 5.7. Polarization Curve for Oxygen Reduction at an Activated Gold RDE in Seawater at 0.32 ppm O_2.

This indicates that the lower limit of applicability of the gold RDE to O_2 measurement in seawater is about 1 ppm O_2.

5.3. Results Obtained with a Copper RDE

The copper RDE corroded after immersion in solution, resulting in roughening of its surface. For this reason the use of a copper RDE was not investigated further in this study.

5.4. Results Obtained with a Silver RDE

The transient nature of the current due to O_2 reduction at a freshly-polished silver RDE in air-saturated NaCl solution, was similar to that observed at a gold RDE (Section 5.2.). The technique used to measure polarization curves with the silver RDE was identical to that described in Section 5.2. for the gold RDE.

A flat limiting-current plateau was not obtained with the silver RDE, even in air-saturated solution; instead, the polarization curve sloped gently in the limiting-current potential region. The current in this region was within a few percent of that predicted by the Levich equation (1.20).

The absence of a limiting-current plateau on silver was also noted by Tarasevich, et al. (1966) and Zhutaeva, et al. (1968). The former found, however, that in the limiting-current region the measured

current corresponded to a maximum value of n, in eqn (1.20), of 3.4 instead of 4.

It is generally considered (e.g., Sepa, et al., 1970, Tarasevich, et al., 1966)that reduction of O_2 at silver is catalyzed by a reduced, oxide-free surface, and inhibited at an oxidized surface. In this study oxidation of the silver surface was found to have a deleterious effect on its O_2-reducing capability, but for different reasons, as explained below.

The electrode was anodized at +0.2V vs. SCE for 10 seconds. The polarization curve measured after anodization was of similar shape to one measured at a prereduced electrode. However, at any given potential the current underwent a nonreproducible transient of about 10 seconds' duration, and also fluctuated considerably. In seawater these effects were more exaggerated.

Examination of an anodized silver electrode showed it to be covered with a dark gray deposit. Even after prolonged cathodic treatment the electrode was a gray-brown color, and its surface could be seen by the naked eye to be pitted and rough. In addition the original behavior of the electrode could not be restored except by polishing. This evidence suggests that silver chloride readily forms at the electrode surface during brief anodization. When the electrode is made cathodic

the silver chloride is reduced back to a fine divided form of silver.

When immersed in oxygen-containing seawater, silver tends to corrode, although at a lower rate than that resulting from anodization. It might therefore be expected that a silver RDE, immersed in seawater and subjected to sporadic cathodic pulses, will eventually become so rough that it no longer fulfills the smoothness criterion for an RDE. In view of this, and taking into account the lack of a limiting-current plateau in air-saturated NaCl, solution, the silver RDE was not investigated further in this study.

CHAPTER 6. DEVELOPMENT OF A MINIATURIZED METHOD FOR THE DETERMINATION OF OXYGEN AND HYDROGEN PEROXIDE

6.1. Need for an Analytical Technique

In order to determine whether the current at the RDE agreed with that predicted by the Levich equation (1.20), it was essential that the oxygen concentration in solution be accurately known. When saturating NaCl solutions or sea water with air, the oxygen concentration in solution could be estimated from reliable tables (Green and Carritt, 1967) or correlations (Truesdale, et al., 1955). Lower oxygen concentrations were attained by saturating the test solution with oxygen-nitrogen mixtures of known composition. The O_2 concentration in solution could be estimated by applying Henry's law and assuming that the solution was in equilibrium with the gas when the RDE current reached a steady value. However, because of the possibility of leakage of O_2 into the system, which may have been of relatively high magnitude at and below the 100 ppb level, an independent means was sought for accurately measuring the O_2 concentration in solution. The analytical technique sought had to satisfy the following criteria:

(a) Not require standardization with solutions of known oxygen content,

(b) Be capable of measuring O_2 concentrations below about 50 ppb with 5% accuracy, and

(c) Compensate for interference from other substances present in solution.

In the sections which follow, two analytical techniques which do not satisfy these criteria are briefly discussed. The Winkler analysis was found to be the only technique which does satisfy these criteria. The chemistry of the Winkler titration, and the types of interference to which it is prone, are discussed.

The way in which the Winkler analysis was miniaturized for use in this study, and the degree of accuracy attained, are described in detail. The last section of this chapter concerns the modification of the miniaturized Winkler analysis for H_2O_2 determination.

6.2. Techniques Which Were Considered Unsuitable for Use in This Study

Two analytical techniques which were considered and then rejected were gasometric and colorimetric methods. The reasons for their rejection are discussed below.

A. Gasometric. It would be difficult to determine the amount of dissolved oxygen present in a liquid sample by boiling off all the dissolved gas and measuring its volume, since most of this gas would be nitrogen. The oxygen could be removed preferentially and the volume change measured, but the relative error would be large. For example, at a dissolved O_2 concentration

of 100 ppb, the gas in equilibrium with the solution contains only about 0.3% O_2, a quantity which would be extremely difficult to measure accurately. Removal of the O_2 from a sample by bubbling a stream of pure N_2 through it, and subsequent chromatographic analysis of the gas stream, would also be inadequate. From discussions with colleagues engaged in chromatographic analysis of gas mixtures, it would seem that oxygen cannot be measured accurately in a gas at concentrations below about 0.2%. The average O_2 content of an N_2 stream capable of removing all the O_2 from a 100 ppb solution would probably be an order of magnitude lower than the equilibrium value of 0.3%. Thus chromatographic analysis would not be capable of measuring O_2 at the required level.

B. Colorimetric. When an indigo carmine-potassium hydroxide reagent is added to a sample containing dissolved O_2, a color is developed which is characteristic of the O_2 concentration (ASTM, 1966). This color can be compared with a set of standards to give the O_2 concentration within 5 ppb in the 0-60 ppb range. Although this method is basically simple, it has several disadvantages:

(1) It was originally developed for use only for concentrations up to 60 ppb, and is thus not sufficiently flexible. Jones (1970) extended the range of sensitivity to 860 ppb but gave the recipes for

color standards corresponding to only five O_2 concentrations -- 0.10, 0.26, 0.40, 0.54, and 0.86 ppm.

(2) To be truly flexible, the technique would require the preparation of a very large number of color standards, some of which might be unstable to light and heat (ASTM, 1966) and would have to be constantly renewed. Moreover, preparation of standards for use above 60 ppb would necessitate standardization with O_2 solutions of known concentration, which in itself would require a reliable primary analytical technique.

(3) The technique is not amenable to instrumental analysis of the color developed because the shade, rather than the intensity of color, is the variable affected by O_2 concentration. The factor of subjectivity involved in making color comparisons was to be avoided, if possible.

(4) The technique is subject to interference from copper and ferrous ions, introducing a factor of uncertainty into analyses.

6.3. The Winkler Analysis

6.3.1. Background

This technique is generally regarded as the most reliable and reproducible one available; it was used in preparing the standard oxygen solubility tables for fresh water and seawater (e.g., Truesdale, et al., 1955), and is also used to standardize oxygen sensors and other analytical methods. Although many modifications

of the Winkler titration are used by analysts, the feature common to all of them is the conversion of oxygen to a chemically equivalent quantity of iodine, and subsequent measurement of the iodine formed by titration, usually with sodium thiosulfate. The Winkler method differentiates between dissolved oxygen and other substances capable of participating in redox reactions, by means of a blank or a system of blanks. By a judicious choice of titrant concentration, oxygen concentrations varying over a range of several orders of magnitude can be measured quite easily. Of course, this technique suffers from certain disadvantages, as do all alternative techniques, and these will be described later in this chapter. Since this method satisfies the three criteria enumerated earlier, it was chosen for use in this study.

6.3.2. Chemical Basis of the Winkler Analysis

The Winkler chemistry is as follows: A small volume of an alkaline potassium iodide solution is added to a sample whose oxygen concentration is to be measured. A similar volume of manganous sulfate solution is then added, and a finely divided precipitate of manganous hydroxide forms

$$Mn^{+2} + 2OH^{-} \rightarrow Mn(OH)_2 \qquad (6.1)$$

This precipitate reacts with dissolved O_2, as well as any oxidizing species present, to form the trivalent

manganic salt

$$2Mn(OH)_2 + \tfrac{1}{2}O_2 + H_2O \rightarrow 2Mn(OH)_3$$

or (6.2)

$$2Mn(OH)_2 + \tfrac{1}{2}O_2 \longrightarrow 2MnO(OH) + H_2O$$

Under alkaline conditions trivalent manganese is unable to oxidize I^-. When sufficient concentrated sulfuric acid is added to the sample to make it acidic, however, the I^- is oxidized to iodine.

$$2Mn(OH)_3 + 6H^+ + 3I^- \longrightarrow 2Mn^{+2} + I_3^- + 6H_2O \quad (6.3)$$

The liberated iodine can then be determined by titration directly with thiosulfate:

$$I_3^- + 2S_2O_3^{-2} \longrightarrow 3I^- + S_4O_6^{-2} \quad (6.4)$$

According to Carritt and Carpenter (1966), reactions (6.1) to (6.3) can be expected to occur to completion, so that for every molecule of oxygen reacting two molecules of I_3^- form.

A blank to compensate for oxidizing or reducing species also present in solution, is made by acidifying the sample before adding the alkaline iodide and manganous sulfate reagents. No $Mn(OH)_2$ precipitate is formed, and thus oxygen is not reduced. A negative blank, which might tend to occur in the case of a reducing sample, is avoided by adding a suitable amount of iodine to the iodide reagent. A standard correction

is applied for oxygen dissolved in the reagents.

6.3.3. End-point Detection

The course of the titration can be followed by a number of methods. The simplest is the use of a starch indicator, which turns from blue to colorless at the end-point. Of course, the lower the 0_2 concentration being measured, the lower is the intensity of color produced by the starch. Potter (1957) quotes Pieters' claim that the threshold for the use of starch as an indicator is 2.1×10^{-6} N I_2. This is equivalent to a dissolved 0_2 content of 17 ppb and defines the accuracy of titrations performed with a starch indicator. Edgington and Roberts (1969) found that when titrating with $Na_2 S_2 0_3$ solutions more dilute than 0.005 N the starch end-point became somewhat indistinct. In this study it was found necessary to use concentrations as low as 0.00025 N, a factor of 20 lower, in order to afford sufficient accuracy in reading titrant volumes. Thus it was thought appropriate to use a non-subjective means of detecting the end point. The slightly arbitrary choice of potentiometric, rather than amperometric, titration was adopted. The titration technique will be fully described further on. A detailed description of reagent compositions and standard analytical procedure is given in the ASTM handbook (1966).

6.3.4. Interferences to the Winkler Analysis

The Winkler analysis is subject to the following interferences:

(a) Contamination of the sample with atmospheric oxygen during sampling.

(b) Errors in the volumes of reagents added, especially that of the iodized KI solution, which contains a relatively large concentration of species capable of participating in redox reactions.

(c) Air-oxidation of I^- in the sample during and after transfer to the vessel in which the titration is performed.

(d) Volatilization of the iodine in the fixed sample.

These factors have been studied by a number of authors (Carritt and Carpenter, 1966; Potter, 1957; Edgington and Roberts, 1969). Potter (1957) designed a modified version of the ASTM-recommended sample vessel to eliminate factor (b), and also devised titration vessels for iodometric titration under a bubbling N_2 stream, so as to eliminate factor (c).

Edgington and Roberts (1969) preferred to adapt a 300 ml. BOD bottle to oxygen-free sample collection by building a container which could accomodate the bottle and be purged with N_2. Titrations were performed in an open beaker inside an N_2-filled vessel. Care was taken to avoid using a moving N_2 stream, which might encourage the volatilization of I_2 from

the fixed sample.

6.4. Development of the Analytical Technique Used in This Study

6.4.1. The Need for a Small Sample Volume

The sample volume recommended by ASTM (1966) varies from 300 ml. to 500 ml.; the sample vessel is to be flushed with at least 10 changes of test solution. Edgington and Roberts recommended at least 5 changes of solution when taking a 300 ml. sample. Thus, the minimum volume necessary to take one sample is 1500 ml. This posed a problem as far as the RDE cell system was concerned, since the total volume of the system was only about 1 liter, of which 400 ml. was available for sampling, the rest being needed to fill the cell and permit recirculation of solution. Some type of miniaturized titration was therefore required, involving samples no larger than about 30 ml., and needing no flushing. Jones (1970) described a technique in which a 100-ml. round-bottom boiling flask was evacuated, after which the sample was drawn in, almost completely filling the vessel. An indigo-carmine reagent was added to the flask before evacuation. This technique was not used in the present study for several reasons. First, it was found to be very difficult to add reagents to a full vessel; the hypodermic syringe used tended to refill. Second, transfer of the fixed sample to a titration vessel

would have been very difficult, and the amount of solution remaining on the walls of the vessel may not have been constant. Finally, thorough cleaning of the sample vessels would have been troublesome.

Miniaturization of the technique used by Edgington and Roberts, using 35 ml. BOD bottles, was investigated, and found to be cumbersome. Transfer of the fixed sample to the titration vessel seemed to contain the same inherent disadvantages as in Jones' method.

6.4.2. Description of the Miniature Sample Vessel

A new miniaturized titration vessel was designed, which was particularly well-suited to the RDE system, and which was thought to incorporate all of the improvements made by the above-mentioned researchers. Especially convenient was the fact that sample fixing and titration could be carried out in the same vessel. This vessel consisted of a 40 ml. weighing bottle, onto which connections were blown, as shown in Fig. 6.1. Four such vessels could be coupled to a gas manifold by means of ball joints, so that four samples could be treated simultaneously. Each vessel could be evacuated by means of a vacuum pump capable of less than 0.5 mm Hg. absolute pressure, then quickly filled with oxygen-free nitrogen. The ground glass 34/12 joint of each sample vessel was lapped with carborundum powder, to prevent jamming during evacuation.

Each injection tube was sealed with a Bittner

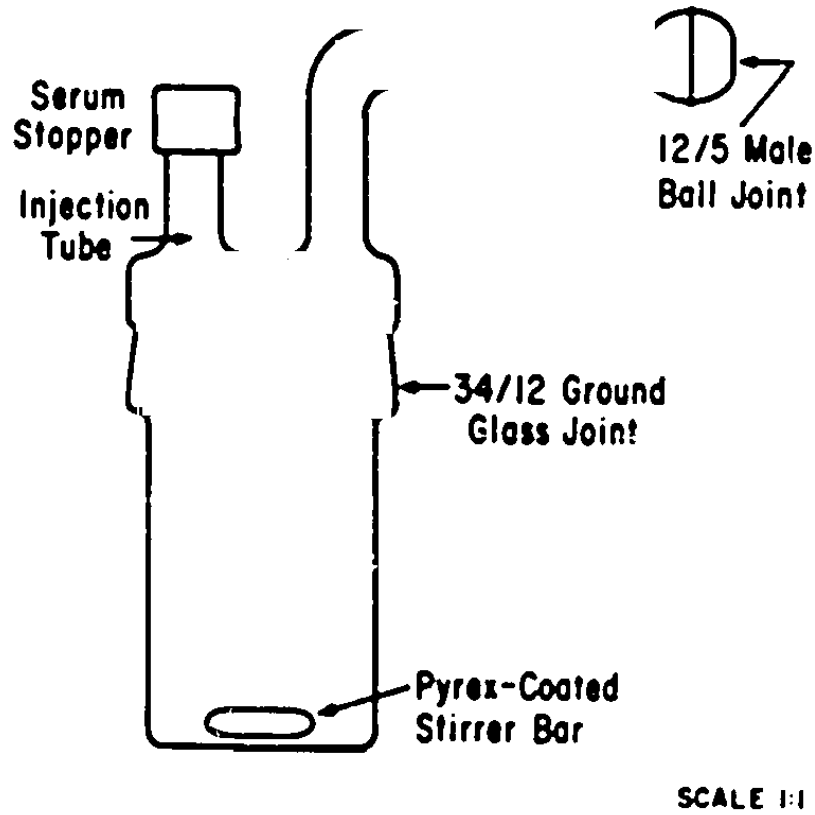

Figure 6.1. Miniature Sample Vessel for Winkler Analysis.

1083 Series, #10 rubber serum stopper, through which the sample and reagents were injected. Stirring of the samples after the addition of each reagent, was effected by Pyrex-coated 1/2-in. magnetic stirrer bars, which were placed in each vessel prior to evacuation. Pyrex-coated stirrers were used because Edgington and Roberts (1969) found that Teflon-and Tygon-coated stirrers absorbed O_2 to an extend which was not negligible at the 100 ppb O_2 level, and which moreover was not constant. Pyrex, on the other hand, was found to absorb a negligible amount of O_2.

6.4.3. Sampling Procedure

In this study a special sampling technique was used, which facilitated an accurate correction for oxygen dissolved in the reagents. By contrast the standard Winkler analysis assumes a constant correction for this quantity.

Edgington and Roberts (1969) claim the credit for developing this technique, although it was first suggested by Schwartz and Gurney in 1934 (Potter, 1957). Its basis is as follows:

When a liquid sample is treated according to the Winkler technique and titrated, the titer represents the sum of four quantities. This can be stated conveniently as

$$S = S_{O_2} + S_{red} + R_{O_2} + R_{red} \qquad (6.5)$$

where S is the titer volume (ml.)

S_{O_2}, S_{red} are the portions of the titer due to oxygen, and reducing or oxidizing species in the sample, respectively,

R_{O_2} and R_{red} are the portions of the titer due to oxygen, and reducing or oxidizing species in the reagents, respectively.

S_{red} and R_{red} are positive if the sample and blank are oxidizing, and negative if they are reducing. Note that these quantities are expressed in terms of an equivalent amount of oxygen. Since the blank does not respond to dissolved oxygen its titer can be written:

$$B = S_{red} + R_{red} \tag{6.6}$$

If twice the normal volume of each reagent is added to a new sample-blank set, the titers thus obtained can be expressed as

$$DS = S_{O_2} + S_{red} + 2R_{O_2} + 2R_{red} \tag{6.7}$$

and

$$DB = S_{red} + 2R_{red} \tag{6.8}$$

By rearranging eqns. (6.5)-(6.8) it can be shown that (Edgington and Roberts, 1969)

$$S_{O_2} = 2S - DS - (2B - DB) \tag{6.9}$$

$$R_{O_2} = DS - S - B \tag{6.10}$$

$$S_{red} = 2B - DB \qquad (6.11)$$

and

$$R_{red} = DB - B \qquad (6.12)$$

It can be seen that this technique requires twice as many samples as does the standard Winkler technique. It does, however, permit improved precision at and below the 50 ppb O_2 level, where the relative error due to uncertainties in the O_2 content of the reagents, may be considerable.

That fluctuations can occur in the O_2 content of the Winkler reagents, was demonstrated by Edgington and Roberts (1969), who investigated various ways of deoxygenating the iodide and $MnSO_4$ solutions, and were able to reduce their O_2 content by about 75%. However, without the use of special handling equipment it was found impossible to maintain a constant O_2 concentration. Also, air-saturation of the reagents still did not result in a constant, reproducible concentration. Nevertheless, it should be pointed out that the deviations were only of the order of about 2 ppb O_2, an error which is of little significance except when analyzing solutions of O_2 content below, say, 50 ppb. In all other cases a standard correction for O_2 in the reagents might suffice.

Some typical titration results are shown in Table 6.1. The titers are expressed as meq. of I_2,

and the quantities S_{O_2}, R_{O_2}, S_{red}, and R_{red} are expressed in terms of the oxygen equivalent, in ppm.

TABLE 6.1

Examples of Winkler Titration Results

RUN	O_2 LEVEL	S	R	nS	nR	S_{O_2}	R_{O_2}	S_{red}	R_{red}
			(meq. $\Delta_2 \times 10^3$)				(ppm O_2)		
52	-6.8	16.96	0.09	17.03	0.19	6.76	-0	-0	0.04
58	-0.1	0.44	0.08	0.59	0.18	0.12	0.02	-0	0.04

Note that S_{red} and R_{red} are independent of O_2 concentration. This is to be expected since the medium and reagents were the same for each run.

Before samples were collected the ball joint and main (34/12) joint of each sample vessel were lightly greased. The area greased was clear of the highest liquid level attained in each sample vessel, so that contamination of the samples with grease was not possible. The gas manifold was thoroughly flushed with nitrogen. The sample vessels were connected to the manifold and evacuated, and then filled with N_2 ("Hi-pure", approx. 10 ppm O_2, or "O_2-free", 2-4 ppm O_2). This procedure was usually carried out three times before a sample was injected into the sample vessel. A slight N_2 overpressure was maintained in the

manifold/sample vessel system by means of a bubbler.

Samples were withdrawn from the saturator by means of a 20 ml., glass B-D Yale hypodermic syringe with a 20-gage stainless steel 'Luer-Lok' needle, which was inserted into the saturator via a silicone rubber septum. Initially a Hamilton gas-tight syringe with a teflon-tipped plunger was used, but it was very difficult to dislodge gas bubbles from the surface of the teflon. This syringe finally broke while being tapped to dislodge a tenacious gas bubble; the B-D syringe with glass plunger was then used, and proved to be easier to handle.

Prior to taking each sample, the syringe was flushed by filling and emptying it a few times while it was inserted through the septum. A sample was then withdrawn, and injected into a sample vessel.

Reagents were handled in 0.5 cc B-D Tuberculin syringes fitted with 23 gage stainless steel needles. During a set of titrations a small quantity of each reagent was kept in a test tube open to the air. It was assumed that the reagents were substantially saturated with air, and that their O_2 content was constant during an experiment. Since the volume of each sample was only 20 ml., instead of the usual 300-500 ml., the reagent volumes were reduced accordingly.

Titration of a fixed sample was effected by

quickly removing the serum stopper from the injection tube and inserting the specially-constructed titration apparatus. Since N_2 was able to flow into the sample vessel and out of the injection tube during this step, there was little opportunity for air to enter the vessel and affect the I^-/I_3^- balance.

Volatilitization of I_2 from fixed samples during titration, was minimized by keeping the samples cool:

The electrical stirrer used to stir the samples tended to heat up during analyses, and warm the samples. Using an air-powered stirrer was considered inconvenient because of the poor speed control available with such a device. So a small cooling device, consisting of a copper tube through which air flowed, with holes drilled in it, and shaped to fit the top of the stirrer, was built and performed well.

After use, each sample vessel was degreased with hexane. Vessels and stirrer bars were soaked for at least 18 hours in chromic-acid cleanser, after which the cleanser was rinsed off and the vessels soaked for one day in a mild detergent solution. They were then scrubbed, rinsed with tap water, then distilled water, and dried in an oven.

6.4.4. Miniature Titration Apparatus

The titration apparatus is shown in Fig. 6.2. The portion which was inserted into the fixed sample consisted of a burette tip, a platinum wire electrode,

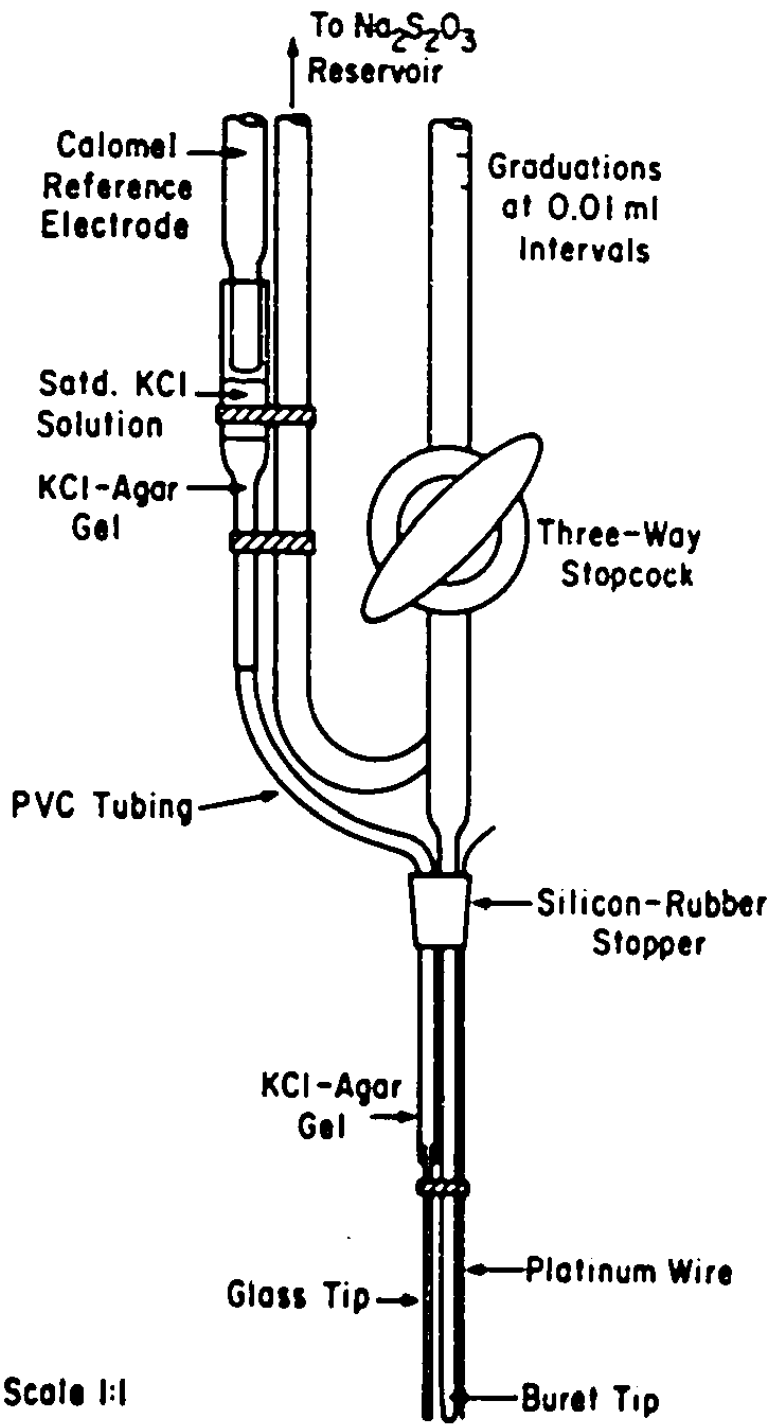

Figure 6.2. Miniature Titration Apparatus for Winkler Analysis.

and a KCI-agar salt bridge. The whole assembly was of 6 mm. diameter at the stopper. The salt bridge terminated at the upper end in a narrow cell into which a calomel reference electrode was inserted. The burette was of 2 ml. capacity, calibrated in hundredths of a ml., and filled from a reservoir via a 3-way tap.

The potential due to the I_3^-/I^- redox couple at the platinum electrode, relative to the calomel electrode, was indicated by a Beckman Model 76 pH meter. A curve was plotted of potential *vs.* volume of $Na_2S_2O_3$ titrant added, giving an S-shaped curve. The end-point was indicated by the point of inflection of this curve. For a given sampling mode (e.g., S or DS) and solution being analysed the inflection point usually occurred at a fixed potential. The oxygen content of the sample was calculated using eqn. (6.9).

6.5. Reproducibility of Oxygen Measurements Made Using the Miniaturized Analytical Technique

When analyzing solutions for O_2 content two sets of samples were usually taken. Each four-sample set was analysed by the single/double reagent addition technique described in Section 6.4.3. Each titer value used in calculating the O_2 concentration by means of eqn. (6.9), was therefore the mean of two values. Extra samples were taken to compensate for spurious titers, but the small volume of the RDE system limited the number of possible samples to about 12.

Table 6.2 summarizes the reproducibility obtained in sample and blank titers at two O_2 levels. The reproducibility of blank titers was always better than about 4%, and often as good as 1%, irrespective of O_2 concentration. Although good reproducibility of sample titers could be obtained at O_2 concentrations as low as 70 ppb, in some experiments at the 100 ppb - O_2 level the sample titers tended to fluctuate wildly. This was attributed to shortcomings inherent in the use of a syringe for sampling, and will be more fully discussed in the next section.

It should be noted that although some of the % errors listed in Table 6.2 for blanks are higher than those listed for samples, the former are equivalent to far smaller absolute quantities of oxygen.

6.6. Sources of Error Inherent in the Analytical Technique Used in This Study

The largest fluctuations in titer occurred with samples of low oxygen content. This indicated that oxygen was leaking into the samples during sampling and/or fixing. Four possible sources of error were proposed and tested. They were: (i) Leakage of O_2 into the sample syringe during sampling,

(ii) Leakage of O_2 through holes in the serum stoppers on the injection tubes,

(iii) Contamination of samples by manganic oxide pushed into the samples by the acid reagent syringe, and

TABLE 6.2

Typical Sample and Blank Titers Obtained at High and Low O_2 Levels

O_2 CONCENTRATION (ppm)	TYPE OF TITER	TITER VOLUMES (ml)	DEVIATION FROM MEAN
7.2	Sample	4.25 4.34 4.28 4.36	± 1.0%
7.2	Blank	0.199 0.199 0.182 0.182	± 4%
0.1	Sample	1.621 1.569 1.399 1.468	± 7%
0.1	Blank	0.709 0.720 0.716 0.732 0.731 0.733	± 1.4%

(iv) Errors resulting from the 0_2 content of the N_2 blanket above the samples in the sample vessels.

(i) One shortcoming of the analytical procedure is the inability of the sample syringe to be flushed thoroughly before a sample is taken. A film of liquid is always present between the barrel and plunger of the syringe when the syringe contains no sample. This film may have a relatively high 0_2 content, since it will tend to equilibrate with atmospheric 0_2 each time the syringe is opened. The weight of such a film was found to be about 0.06 gm. If this film was relatively saturated with air it could contain about 5 ppm 0_2 at 25°C, i.e., a total of 0.3×10^{-6} gm. 0_2. In a 20 ml. sample containing 100 ppb 0_2 there are 2.0×10^{-6} gm. 0_2. Hence the error incurred when the film is mixed with a fresh sample, may be as much as 15%.

This proposal was tested in two ways. In the first test several samples were taken in the normal manner, i.e., by simply withdrawing the plunger of the syringe. Samples were then taken by withdrawing the plunger and depressing it three times before actually removing the sample. It was thought that the latter technique would exaggerate the extent of contamination by air dissolved in the film on the plunger. The samples were fixed and titrated. The results of this test were inconclusive, since the titers fluctuated in each case.

In the second test sampling of an NaCl solution containing about 60 ppb O_2, was carried out inside an N_2-filled glove bag. The resulting titers exhibited much less fluctuation than those obtained previously. This confirmed that the sampling technique was a source of error.

(ii) By the time the sample and reagents have been injected through the serum stopper into a sample vessel, the stopper has been punctured three times. It was found that the punctures did not always reseal. Whether O_2 was leaking through puncture holes and contaminating samples during fixing, was tested as follows: Of eight sample vessels in which samples were being fixed, the stoppers of four were sealed with grease. After fixing and titration, it was found that both sets of samples exhibited the same random fluctuations in titer, so that leakage of O_2 through serum stoppers could not be considered a source of error.

(iii) When the reagent syringes were inserted through a stopper and emptied, a drop of reagent sometimes remained on the needle tip. When the needle was withdrawn, this liquid could be wiped off onto the inside of the serum stopper. Thus the alkaline iodide and the manganous sulfate could have combined to form an oxygen-fixing manganous hydroxide deposit on the inside of the stopper, adjacent to the puncture holes. Air diffusing through these holes could have

oxidized the deposit during the approximately ten minutes of fixing. When the H_2SO_4 syringe was inserted it might have carried some of the oxidized deposit down into the solution, thus increasing the amount of manganic ion in solution, and leading to a high titer. This proposal was tested by injecting KI and $MnSO_4$ reagents through serum stoppers placed on N_2-filled sample vessles. These were allowed to stand for 1 hour, after which the serum stoppers were transferred to vessels containing 20 ml. of NaCl solution and 0.2 ml. of iodide reagent. 0.2 ml. of H_2SO_4 was injected through the serum stoppers into the samples, which were titrated. These 'contaminated' titers were compared with those of samples to which 0.2 ml. each of HI and H_2SO_4 reagents had been added. The results, shown in Table 6.3, are so similar that they cannot account for any of the scatter normally present in titers, and so the possibility of this type of error can be eliminated completely.

TABLE 6.3

Effect of Deposit on Serum Stopper

SAMPLE	TYPE	TITER (mℓ)	AVERAGE (mℓ)
1	"Contaminated"	0.245	0.247 ± 0.011
2		0.258	
3		0.237	
4	"Normal"	0.232	0.229 ± 0.003
5		0.226	

(iv) One of the major shortcomings of the sample vessels is the presence of a gas blanket above the sample during O_2 fixing, a situation which does not normally occur in Winkler analyses. It is essential that no oxygen be present in this gas, because of the possibility of its diffusing into the sample during fixing. Using the solution for the analogous problem of heat transfer through a slab (Perry, et al., 1963) it was calculated that 95% of the O_2 present in the N_2 gas blanket can diffuse to the gas-liquid interface and react in about one minute. This is far less than the recommended fixing time of 5-15 minutes (ASTM, 1966).

The N_2 gas originally used in this study was Liquid Carbonic "hi-pure," with an average O_2 content of 10 ppm by volume. It was calculated that the O_2 present in a blanket of this gas could result in a 15% error when measuring an O_2 concentration of 100 ppb. This error was reduced to less than 5%, when measuring low O_2 concentrations, by the use of Matheson "O_2-free" N_2, which was certified to contain less than 5 ppm O_2, and averaged 3 ppm O_2.

Since diffusion and dissolution of the O_2 in the gas blanket are so rapid, one might expect all samples to be affected by this O_2 to the same extent. The trace O_2 in the gas blanket cannot, therefore, account for fluctuations in titer.

In this study the titration results were not

corrected for O_2 present in the N_2. It is recommended that where higher precision is required at and below 100 ppb, a deoxygenation train be used to remove trace O_2 from the N_2, to below the 1 ppm level.

6.7. Modification of the Analytical Technique for Use in H_2O_2 Analysis

In the experiments where H_2O_2 was reduced at an RDE, an independent measure of H_2O_2 concentration was required to check whether the Levich equation was obeyed. Since H_2O_2 was consumed at the working electrode but not replaced at the counter-electrode, frequent H_2O_2 analyses had to be made. The limitation of sample volume described in Section 6.4.1 applied, so it was appropriate to use the analytical equipment which had been developed for the Winkler titrations.

Conveniently, an iodometric method for H_2O_2 analysis is available (Scott, 1939). H_2O_2 is reduced by I^- in acid solution as follows:

$$H_2O_2 + 2I^- + 2H^+ \rightleftharpoons I_2 + 2H_2O \qquad (6.13)$$

This reaction takes about 30 minutes to occur to completion, but the addition of several drops of 1M. ammonium molybdate renders the reaction instantaneous.

Since the blank in a Winkler titration involves an acid solution, it seemed logical to treat a sample for H_2O_2 analysis as if it were a Winkler blank, and then add a few drops of ammonium molybdate solution.

Samples were protected from air-oxidation during fixing and titration by an N_2 blanket. Since the H_2O_2 concentrations being measured were about four orders of magnitude lower than those for which the analytical procedure described in the literature had been designed, reagent concentrations could be reduced accordingly. The reagents, and volumes thereof, used in analyses, were identical to those used for O_2 analyses. Before the addition of H_2O_2 (injected as "1-volume" solution) to the RDE system, a blank analysis was performed on the circulating solution. The titer obtained was then used as a blank for the samples containing H_2O_2.

The reproducibility of the H_2O_2 titers was generally better than 2%; the largest scatter observed in titers was 5.3%.

Albery, W. J. and S. Bruckenstein, "Ring-Disk Electrodes. Part 2-Theoretical and Experimental Collection Efficiencies", Trans. Faraday Soc., 62, 1920 (1966).

American Society for Testing and Materials, "Manual on Industrial Water and Industrial Wastewater", 2nd edition. 313, STP No. 148-I, ASTM., Philadelphia (1966).

Bagotskii, V. S., Filinovskii, V. Yu., and N. A. Shumilova, "Kinetics of Individual Stages of the Oxygen Reduction Reaction. Derivation of Basic Equations", Elektrokhimiya, 4, 1247 (1968).

Bardin, M. B. and A. I. Dikusar, "Effect of the Eccentricity of a Rotating Disk Electrode on the Limiting Diffusion Current", Elektrokhimiya, 6, 1147 (1970).

Behrens, H. C., "Improved ppb Oxygen Analyzer for Sea-Water", Report on Research Carried out by Texas Contract Research Division of Dow Chemical Co., under Contract No. 1832 (1969) for the Office of Saline Water, Materials Division, Washington, D. C. (1970).

Blurton, K. F. and E. McMullin, "The Cathodic Reduction of Oxygen on Platinum in Alkaline Solutions", J. Electrochem. Soc., 116, 1476 (1969).

Bonnemay, M., Bernard, C., Magner, G., and M. Savy, "Étude expérimentale en fonction du pH de la réduction de l'oxygène sur l'or", C. R. Acad. Sc. Paris, 270, 1556 (1970).

Carritt, D. E.and J. H. Carpenter, "Comparison and Evaluation of Currently Employed Modifications of the Winkler Method for Determining Dissolved Oxygen in Seawater", J. Marine Res., 24, 286 (1966).

Damjanovic, A., Genshaw, M. A., and J. O'M. Bockris, "Distinction Between Intermediates Produced in Main and Side Electrode Reactions", J. Chem. Phys., 45, 4057 (1966a).

Damjanovic, A., Genshaw, M. A., and J. O'M. Bockris, "The Role of Hydrogen Peroxide in the Reduction of Oxygen at Platinum Electrodes", J. Phys. Chem., 70, 3761 (1966b).

Damjanovic, A. and V. Brusic , "Oxygen Reduction at Pt-Au and Pd-Au Alloy Electrodes in Acid Solution", Electrochimica Acta, 12, 1171 (1967).

Damjanovic, A., Genshaw, M. A., and J. O'M Bockris, "The Role of Hydrogen Peroxide in Oxygen Reduction at Platinum in H_2SO_4 Solution", J. Electrochem. Soc., 114, 466 (1967a).

Damjanovic, A., Genshaw, M. A., and J. O'M Bockris, "The Mechanism of Oxygen Reduction at Platinum in Alkaline Solutions with Special Reference to H_2O_2", J. Electrochem. Soc., 114, 1107 (1967b).

Damjanovic, A., Genshaw, M. A., and J. O'M. Bockris, "Hydrogen Peroxide Formation in Oxygen Reduction at Gold Electrodes", J. Electroanal. Chem., 15, 173 (1967c).

Damjanovic, A., in "Modern Aspects of Electrochemistry", Vol. 5, J. O'M. Bockris and B. E. Conway, eds., Plenum Press, New York, pg. 369 (1969).

Edgington, H. C. and R. M. Roberts, "Development of a Calibration Module for Trace Oxygen Analyzers", Aerojet-General Corporation Report No. 1289-F, prepared under Contract D.I. 14-01-0001-2127 for the Office of Saline Water, Materials Division, Washington, D.C. (1969).

Genshaw, M. A., Damjanovic, A., and J. O'M. Bockris, "Hydrogen Peroxide Formation in Oxygen Reduction at Gold Electrodes", J. Electroanal. Chem., 15, 163 (1967a).

Genshaw, M. A., Damjanovic, A., and J. O'M. Bockris, "The Role of Hydrogen Peroxide in Oxygen Reduction at Rhodium Electrodes", J. Phys. Chem.,, 71, 3722 (1967b).

Giner, J. Parry, J. M., and L. Swette, Oxygen Reduction on Gold Alloys in Alkaline Electrolyte", "Fuel Systems-Part II", in Advan. Chem. Ser. 90, 102 (1969).

Gnanamuthu, D. S., and J. V. Petrocelli, "A Generalized Expression for the Tafel Slope and the Kinetics of Oxygen Reduction on Noble Metals and Alloys", J. Electrochem. Soc., 114, 1036 (1967).

Green, E. J. and Carritt, D. E., "New Tables for Oxygen Saturation of Seawater", J. Marine Res., 25, (1967).

Hoare, J. P., "Oxygen Overvoltage Measurements on Bright Platinum in Acid Solutions; Part I: Bright Platinum", J. Electrochem. Soc., 112, 602 (1965).

Hoare, J. P., "Oxygen Overvoltage on Bright Gold-1", Electrochimica Acta, 11, 311 (1966).

Hoare, J. P., "The Electrochemistry of Oxygen", Wiley & Sons, Inc., New York (1968).

Jones, D. A., "Determining the Dissolved Oxygen in Small Quantities of Water", Corrosion-N.A.C.E., 26, 151 (1970).

Khomutov, N. E. and Zakhodyakina, N. A., "Dependence of Polarization Potentials on the Nature of the Electrode Material for Cathodic Reduction of Oxygen", Izvestiia Vyssh. Ucheb. Zaved., Khim. Khim. Tekhnol., 13, 1184 (1970).

Khrushcheva, E. I., Nekrasov, L. N., Shumilova, N. A., and M. R. Tarasevich, Electrochemical Behavior of Oxygen and Hydrogen Peroxide on a Smooth Rhodium Electrode in Acid Solutions", Elektrokhimiya, 3, 831 (1967).

Luk'yanycheva, V. I., Yuzhanina, A. V., Lentsner, B. I., Knots, L. L., Shumilova, N. A., and V. S. Bagotskii, "The State of the Adsorbed Oxygen and its Effect on the Mechanism of Molecular Oxygen Reduction at a Platinum Electrode in an Alkali Solution", Elektrokhimiya, 7, 1287 (1971).

Morcos, I., and E. Yeager, "Kinetic Studies of the Oxygen-Peroxide Couple on Pyrolytic Graphite", Electrochimica Acta, 15, 953 (1970).

Müller, L., and L. Nekrassow, "Untersuchung des Elekrochemischen Reduktionsprozesses von Sauerstoff an Platin mit Hilfe der Rotierenden Scheibenelektrode mit Ring", Electrochimica Acta, 9, 1015 (1964).

Müller, L., and L. N. Nekrasov, "Zum Mechanisms der Kathodischen Reduktion von Sauerstoff an Einer Glatten, Aktiven Platinelektrode in Alkalischer Lösung", J. Electroanal. Chem., 9, 282 (1965).

Nekrasov, L. N., Krushcheva, E. I., Shumilova, N. A., and M. R. Tarasevich, "An Investigation of the Electrochemical Reduction of Oxygen on a Rhodium Electrode in Alkaline Solution", Elektrokhimiya, 2, 363 (1966).

Nekrasov, L. N., and E. I. Khrushcheva, "Influence of the State of the Electrode Surface on the Kinetics of the Cathodic Reduction of Oxygen on Ruthenium in Alkaline Solutions", Elektrokhimiya, 3, 166 (1967).

Nekrasov, L. N., and N. I. Dubrovina, "Investigation of the Influence of the Adsorption of Certain Cations and Anions upon the Kinetics of the Reduction of Oxygen on Platinum", Elektrokhimiya, 4, 362 (1968).

Newman, J., "Schmidt Number Correction for the Rotating Disk", J. Phys. Chem., 70, 1327 (1966).

Oshe, A. I., Tikhomirova, V. I., and V. S. Bagotskii, "Ionization of Oxygen at an Oxidized Platinum Electrode in Acid Solutions", Elektrokhimiya, 1, 688 (1965).

Perry, R. H., Chilton, C. H., and S. D. Kirkpatrick, eds., "Chemical Engineers' Handbook", 4th Edition, McGraw-Hill, New York, 14.13 (1963).

Peters, A. R., "Cathodic Reduction of Oxygen on a Platinum Rotating Disk Electrode in a Saline Solution", M. S. Thesis, University of California, Berkeley (1970).

Potter, E. C., "The Microdetermination of Dissolved Oxygen in Water", J. Appl. Chem., 7, Part I-p. 285, Part II-p. 297, Part IV-p. 317 (1957).

Prater, K. B. and R. N. Adams, "A Critical Evaluation of Practical Rotated Disk Electrodes", Anal. Chem., 38, 153 (1966).

Radyushkina, K. A., Tarasevich, M. R., and R. Kh. Burshtein, "Parallel Series Stages in the Reactions of Oxygen and Hydrogen Peroxide-III. Reactionof Oxygen and Hydrogen Peroxide at a Rhodium Electrode", Elektrokhimiya, 6, 1352 (1970).

Riddiford, A. C., "The Rotating Disk System", in "Advances in Electrochemistry and Electrochemical, Engineering", Vol. 4, C. Tobias, Ed., Interscience Publishers, New York (1966).

Sabirov, F. Z., and M. R. Tarasevich, "Kinetics of Oxygen Ionization on Polygraphite and Vitreocarbon Electrodes in Acid and Alkaline Solutions", Elektrokhimiya, 5, 608 (1969).

Sabirov, F. Z., Tarasevich, M. R., and R. Kh. Burshtein, "Mechanism of Oxygen Reduction on Pyrographite in Acidic Solutions", Elektrokhimiya, 6, 1130 (1970).

Schumb, W. C., Satterfield, C. N., and R. L. Wentworth, "Hydrogen Peroxide", Reinhold Publishing Corp., New York (1955).

Scott, W. W., ed., "Standard Methods of Chemical Analysis", Vol. 2, 5th Edition, D. Van Nostrand Co., Inc., Princeton, N. J., (1939).

Selman, J. R., "Measurement and Interpretation of Limiting Currents". Ph.D. Thesis, University of California, Berkeley (1971).

Šepa, D., Vojnovic, M., and A. Damjanovic, "Oxygen Reduction at Silver Electrodes in Alkaline Solutions", Electrochimica Acta, 15, 1355 (1970).

Shepelev, V. Ya., Tarasevich, M. R., and Burshtein, R. Kh., "Influence of Pressure on Oxygen Ionization at a Platinum Electrode, Part I", Élektrokhimiya, 7, 999 (1971).

Shumilova, N. A. and V. S. Bagotzky, "Oxygen Ionization on Nickel in Alkaline Solutions", Electrochim. Acta, 13, 285 (1968).

Smyrl, W. H. and J. Newman, "Ring-Disk and Sectioned Disk Electrodes", J. Electrochem. Soc., 119, 212 (1972).

Tarasevich, M. R., Shumilova, N. A., and R. Kh. Burshtein, "Investigation of the Adsorption and Ionization of Oxygen by the Method of Triangular Voltage Pulses", Izvestiya Akademii Nauk SSSR, Seriya Khimicheskaya, 1, 32 (1966).

Tarasevich, M. R., "Determining the Kinetic Parameters of the Electrochemical Reactions of Oxygen and Hydrogen Peroxide", Élektrokhimiya, 4, 210 (1968).

Tarasevich, M. R., Sabirov, F. Z., Mertsalova, A. P., and R. Kh. Burshtein, "Ionization of Oxygen on Pyrographite in Alkaline Solutions", Élektrokhimiya, 4, 432 (1968).

Tarasevich, M. R., Radyushkina, K. A., Filinovskii, V. Yu., and R. Kh. Burshtein, "Parallel-Series Stages in the Reactions of Oxygen and Hydrogen Peroxide-IV. Reaction of Oxygen and Hydrogen Peroxide at a Gold Electrode", Élektrokhimiya, 6, 1522 (1970).

Tikhomirova, V. I., Luk'yanycheva, V. I., and V. S. Bagotskii, "Use of a Rotating Platinum Disk Electrode with Preliminary Vacuum Pretreatment of the Surface for Study of the Ionization of Molecular Oxygen in an Alkali", Élektrokhimiya, 3, 762 (1967).

Truesdale, G. A., Downing, A. L., and G. F. Lowden, "The Solubility of Oxygen in Pure Water and Seawater", J. Appl. Chem., 5, 53 (1955).

Yeager, E., Krouse, P., and K. V. Rao, "The Kinetics of the Oxygen-Peroxide Couple on Carbon", Electrochimica Acta, 9, 1057 (1964).

Kuznanina, A. V., Luk'yanycheva, V. I., Shumilova, N. A., and V. S. Bagotskii, "Investigation of the Mechanism of the Cathodic Reduction of Oxygen on Smooth Anodically-Cathodically Treated Platinum in Alkaline Solution", Elektrokhimiya, 6, 1054 (1970).

Zhutaeva, G. V., Merkulova, N. D., Shumilova, N. A., and V. S. Bagotskii, "The Kinetics of Individual Stages in the Reduction of Oxygen II. Reduction of Oxygen on Silver in Alkaline Solution", Elektrokhimiya, 4, 1253 (1968).

NOMENCLATURE

c	concentration
D	diffusivity
E	potential
f	fraction of O_2 undergoing 2-electron reduction
F	the Faraday number
$\bar{g}$	gravitational force
i	current density
I	current
J	mass flux
k	reaction rate constant
K	$= \frac{0.6205\ Sc^{-2/3}\ \nu^{1/2}}{1 + 0.298\ Sc^{-1/3} + 0.14514\ Sc^{-2/3}}$, the convective rate constant, eqn(1.20)
n	number of electrons transferred per mole of reactant
N	mass flux
NHE	normal hydrogen electrode
p	pressure
r	radius, radial coordinate
R	$= \frac{k_{3,simp}}{k_{3,exp}}$, ratio of rate constants, see section 3.5.3

Re	$= r_o^2 \omega/\nu$, Reynolds number
Sc	$= \nu/D$, Schmidt number
SCE	saturated calomel electrode
t	time
$\bar{v}$	velocity vector
y	vertical coordinate

Greek Symbols

δ	boundary layer thickness
ν	kinematic viscosity
ρ	density
ϕ	azimuthal coordinate
ω	rate of rotation

Subscripts

D	disk
exp	expanded reaction model
H	hydrodynamic
i	species "i"
lim	diffusion-limited
M	mass transport
o	outer
r	radial direction
R	ring
simp	simplified reaction model
theor	theoretically predicted

y	vertical direction
ϕ	azimuthal direction

Superscripts

b	bulk of solution
s	surface of the electrode

APPENDIX A

Summary of Experiments Mentioned in Text

RUN	ELECTRODE MATERIAL	MEDIUM	O_2 CONC. (ppm)	H_2O_2 CONC.	EFFECT INVESTIGATED	LOCATION IN TEXT
13	Pt	3.5%NaCl	1.7	--	Polarization curve.	Sec 3.3.1 & Fig 3.5
16	"	"	0.5	--	Effect of potential and duration of anodization on i_{lim}.	Sec 4.4.2
25	"	"	6.71	--	Current decay.	Secs 3.2,4.2 & Fig. 3.1
54	"	"	0.77	--	Polarization curve.	Sec. 3.3.1 & Fig 3.5
58	"	"	0.12	--	Polarization curve.	Sec 3.3.1 & Fig 3.6
					i_{lim} vs. $\omega^{1/2}$, k_3	Sec 3.4.3 & Fig 3.12
62	"	"	0.07	--	Current decay.	Secs 3.2,4.2 & Fig. 3.1
					Polarization curve.	Sec 3.3.1 & Fig 3.7
63	"	"	0.09	--	Effect of electrode deactivation on k_3.	Sec 4.3
65	"	Seawater	7.15	--	k_3	Sec 3.4.2

RUN	ELECTRODE MATERIAL	MEDIUM	O_2 CONC. (ppm)	H_2O_2 CONC.	EFFECT INVESTIGATED	LOCATION IN TEXT
69	Pt	3.5%NaCl	0.08	--	Effect of ω on rate of current decay.	Sec 4.4.2 & Fig 4.3
73	"	"	0.09	--	Polarization curve.	Sec 3.3.2 & Fig 3.9
					Hysteresis.	Sec 4.5 & Fig 4.6
74	"	"	0.09	--	Effect of Standby, and potential and duration of anodization, on i_{lim}.	Sec. 4.4.2
75	"	"	7.15	--	Current decay.	Secs 3.2,4.2 & Fig 3.1
					Polarization curve.	Sec 3.3.2 & Fig 3.8
					i_{lim} vs $\omega^{1/2}$, activated Pt.	Sec 3.4.2 & Fig 3.11
					k_3 c.f. NaCl soln.	Sec 3.4.2
					i_{lim} vs $\omega^{1/2}$, deactivated Pt.	Sec 4.3 & Fig 4.1
					Effect of electrode deactivation on k_3	Sec 4.3
					Effect of Standby, and potential and duration of anodization, on i_{lim}.	Sec 4.4.2
					Hysteresis.	Sec 4.5 & Fig 4.5

RUN	ELECTRODE MATERIAL	MEDIUM	O_2 CONC. (ppm)	H_2O_2 CONC.	EFFECT INVESTIGATED	LOCATION IN TEXT
76	Pt	3.5%NaCl	0.10	--	Effect of Standby on i_{lim}.	Sec 4.4.2
80	"	"	~0.03	$1.6 \cdot 10^{-4}$M	Polarization curve and estimation of $D_{H_2O_2}$.	Sec 3.5.2 & Fig 3.13
					i_{lim} vs $\omega^{1/2}$, activated Pt.	Sec 3.5.2 & Fig 3.14
					k_3, activated Pt.	Sec 3.5.2
					i_{lim} vs $\omega^{1/2}$, deactivated Pt.	Sec 4.3 & Fig 4.1
					Effect of electrode deactivation on k_3.	Sec 4.3
81	"	"	~0.03	$3.1 \cdot 10^{-5}$M	Polarization curve and estimation of $D_{H_2O_2}$.	Sec 3.5.2 & Fig 3.13
					i_{lim} vs $\omega^{1/2}$, activated Pt.	Sec 3.5.2 & Fig 3.14
					k_3, activated Pt.	Sec 3.5.2
					Effect of electrode deactivation on k_3	Sec 4.3
82	"	"	0.08	$6 \cdot 10^{-6}$M	Hysteresis.	Sec 4.5 & Fig 4.7

RUN	ELECTRODE MATERIAL	MEDIUM	O_2 CONC. (ppm)	H_2O_2 CONC	EFFECT INVESTIGATED	LOCATION IN TEXT
83	Pt	3.5%NaCl	7.18	--	k_3, activated Pt.	Sec. ..4.1
					Effect of electrode deactivation on k_3.	Sec 4.3
86	"	"	7.18	--	Polarization curve.	Sec 3.2 & Fig 3.2
					Optimum time to measure current after activation of electrode.	Sec 3.2 & Fig 3.3
					Correction of current decay curve.	Sec 3.2 & Fig 3.4
					i vs $\omega^{1/2}$, activated Pt.	Sec 3.4 & Fig 3.10
					k_3, activated Pt.	Sec 3.4
					i vs $\omega^{1/2}$, deactivated Pt.	Sec 4.3 & Fig 4.1
					Effect of electrode deactivation on k_3.	Sec 4.3
					Hysteresis.	Sec 4.5 & Fig 4.4
88	Au	"	7.18	--	Effect of pretreatment technique on shape of polarization curve.	Sec 5.2.1 & Fig 5.1
					Effect of state of electrode surface on shape of i vs $\omega^{1/2}$ curve.	Sec 5.2.1 & Fig 5.2

RUN	ELECTRODE MATERIAL	MEDIUM	O_2 CONC. (ppm)	H_2O_2 CONC.	EFFECT INVESTIGATED	LOCATION IN TEXT
89	Au	Seawater	7.15	--	Polarization curve.	Sec 5.5.2 & Fig 5.5
90	"	3.5%NaCl	2.0	--	Polarization curve.	Sec 5.2.1 & Fig 5.1
93	Pt	"	7.18	--	Effect of potential and duration of anodization on shape of polarization curve.	Sec 4.4.2 & Fig 4.2
					Effect of Standby, and potential and duration of anodization, on i_{lim}.	Sec 4.4.2
110	Au	Seawater	2.0	--	Polarization curve.	Sec 5.2.2 & Fig 5.6
112	"	"	7.15	--	Polarization curve.	Sec 5.2.2 & Fig 5.4
113	"	"	0.32	--	Polarization curve.	Sec 5.2.2 & Fig 5.7
					Hysteresis.	Sec 5.2.2 & Fig 5.7

Appendix B

Part 1: Derivation of Expanded-Model Equation used in Section 3.5.3

(a) H_2O_2 concentration negligible compared to O_2 concentration. Equation (1.37) becomes

$$i = 2F\pi^{1/2}K_{O_2}c_{O_2}^{b}\left[(2-f) + \frac{f}{1+\frac{K_{H_2O_2}\pi^{1/2}}{k_3+k_4(1-\frac{f}{2})}}\right] \qquad (B.1)$$

which leads to the result

$$k_3 = \frac{K_{H_2O_2}\pi^{1/2}}{\left(\frac{f}{\frac{i}{2F\pi^{1/2}K_{O_2}c_{O_2}^{b}}-(2-f)}\right)^{-1}} - k_4(1-\frac{f}{2}) \qquad (B.2)$$

This value of k_3 will be referred to hereafter as $k_{3,exp}$. Note that in eqn. (B.2) the term $\frac{i}{2F\pi^{1/2}K_{O_2}c_{O_2}^{b}}$ is equal to $\frac{2i}{i_{theor}}$ where $i_{theor} = 4F\pi^{1/2}K_{O_2}c_{O_2}^{b}$, the current predicted by the Levich equation (1.20) for 4-electron reduction of O_2.

The simplified reaction model assumes $f = 1$ and $k_4 = 0$. Under these conditions eqn. (B.2) reduces to

$$k_3 = \frac{K_{H_2O_2}^{1/2}}{\frac{1}{\frac{2i}{i_{theor}} - 1} - 1} = k_{3,simp} \qquad (B.3)$$

Let $R = \frac{k_{3,simp}}{k_{3,exp}}$. Then

$$R = \frac{\frac{K_{H_2O_2}^{1/2}}{\frac{1}{\frac{2i}{i_{theor}} - 1} - 1}}{\frac{K_{H_2O_2}^{1/2}}{\frac{f}{\frac{2i}{i_{theor}} - (2-f)} - 1} - k_4(1-\frac{f}{2})} \qquad (B.4)$$

Dividing numerator and denominator of eqn (B.4) by the expression for $k_{3,simp}$, one obtains

$$R = \frac{\frac{1}{\frac{1}{\frac{2i}{i_{theor}} - 1} - 1}}{\frac{f}{\frac{2i}{i_{theor}} - (2-f)} - 1 - \frac{k_4(1-\frac{f}{2})}{k_{3,simp}}} \qquad (B.5)$$

Equation (B.5) can be rewritten in a more convenient form.

Let $A = \frac{1}{\frac{2i}{i_{theor}} - 1} - 1$; $B = -\frac{f}{\frac{2i}{i_{theor}} - (2-f)} - 1$

One then obtains,

$$R = \frac{1}{\frac{A}{B} - k_{3,simp}\,(1-\frac{f}{2})} \qquad (B.6)$$

Eqn (B.6) can be written as

$$R = \frac{1}{\frac{A}{B} - \frac{k_4}{k_{3,exp}}\,\frac{(1-\frac{f}{2})}{R}} \qquad (B.7)$$

which leads to the result

$$R = \frac{k_4}{1 + k_{3,exp}\,\frac{(1-\frac{f}{2})}{A/B}} \qquad (B.8)$$

When $k_4 = 0$ and $f < 1$ eqn (B.8) simplifies to

$$R = \frac{1}{A/B} \qquad (B.9)$$

When $f = 1$ and $k_4 > 0$ eqn (B.8) becomes

$$R = 1 + \frac{k_4}{2k_{3,exp}} \qquad (B.10)$$

(a) O_2 concentration negligible compared to H_2O_2 concentration. Equation (1.37) becomes

$$i = \frac{2FK_{H_2O_2}c^b_{H_2O_2}\omega^{1/2}}{1 + \frac{K_{H_2O_2}\omega^{1/2}}{k_3+k_4(1-\frac{f}{2})}} \qquad (B.11)$$

k_3 is then given by

$$k_{3,exp} = \frac{K_{H_2O_2}\omega^{1/2}}{\frac{i}{2FK_{H_2O_2}c^b_{H_2O_2}\omega^{1/2}} - 1} - k_4(1-\frac{f}{2}) \qquad (B.12)$$

When $f = 1$ and $k_4 = 0$, in accordance with the simplified reaction model, eqn (B.12) reduces to

$$k_{3,simp} = \frac{K_{H_2O_2}\omega^{1/2}}{\frac{i}{2FK_{H_2O_2}c^b_{H_2O_2}\omega^{1/2}} - 1} \qquad (3.13)$$

Combining eqns (B.12) and (B.13) one can show that

$$R = \frac{k_{3,simp}}{k_{3,exp}} = 1 + \frac{k_4(1-\frac{f}{2})}{k_{3,exp}} \qquad (B.14)$$

When $f = 1$ eqn (B.14) becomes

$$R = 1 + \frac{k_4}{2k_{3,exp}} \qquad (B.15)$$

Part 2: Calculation of k_3 Ratios Predicted by Eqns. (B.8) and (B.9)

The term $2i/i_{theor}$ typically varied from a value of 1.95 at low $\omega^{1/2}$(~8 sec.$^{-1/2}$) to 1.80 at high $\omega^{1/2}$(~13 sec.$^{-1/2}$). Values of R for the cases $k_4 = 0$ and $k_4 = k_{3,exp}$ have been calculated and are listed in Table B.1.

TABLE B.1

Effect of ω, f and k_4 on the k_3 Ratio, R

f	i^{2i}_{theor}	A	B	$R(=k_{3,simp}/k_{3,exp})$ $k_4=0$	$k_4=k_{3,exp}$
0.95	1.95	0.0526	0.0555	1.0555	1.6097
	1.90	0.1111	0.1176	1.0588	1.6148
	1.85	0.1765	0.1875	1.0625	1.6203
	1.80	0.2500	0.2667	1.0667	1.6267
0.90	1.95	0.0526	0.0588	1.1176	1.7324
	1.90	0.1111	0.1250	1.1250	1.7437
	1.85	0.1765	0.2000	1.1333	1.7566
	1.80	0.2500	0.2857	1.1429	1.7714
0.80	1.95	0.0526	0.0667	1.2667	2.0266
	1.80	0.2500	0.3333	1.3333	2.1333
0.70	1.95	0.0526	0.0769	1.4615	2.4116
	1.80	0.2500	0.4000	1.6000	2.6400
0.50	1.95	0.0526	0.1111	2.1111	3.6943
	1.80	0.2500	0.6667	2.6667	4.6667